NUREG/CR-4219
ORNL/TM-9593/V8&N2
Vol. 8, No. 2

# Heavy-Section Steel Technology Program

## Semiannual Progress Report for April–September 1991

Prepared by
W. E. Pennell

Oak Ridge National Laboratory

Prepared for
U.S. Nuclear Regulatory Commission

NUREG/CR-4219
ORNL/TM-9593/V8&N2
Vol. 8, No. 2
RF

# Heavy-Section Steel Technology Program

Semiannual Progress Report for April–September 1991

Manuscript Completed: March 1992
Date Published: April 1992

Prepared by
W. E. Pennell

Oak Ridge National Laboratory
Operated by Martin Marietta Energy Systems, Inc.

Oak Ridge National Laboratory
Oak Ridge, TN 37831-6285

**Prepared for**
**Division of Engineering**
**Office of Nuclear Regulatory Research**
**U.S. Nuclear Regulatory Commission**
**Washington, DC 20555**
**NRC FIN B0119**
**Under Contract No. DE-AC05-84OR21400**

# Abstract

The Heavy-Section Steel Technology (HSST) Program is conducted for the Nuclear Regulatory Commission (NRC) by Oak Ridge National Laboratory (ORNL). The program focus is on the development and validation of technology for the assessment of fracture-prevention margins in commercial nuclear reactor pressure vessels. The HSST Program is organized in 10 tasks: (1) program management, (2) fracture methodology and analysis, (3) material characterization and properties, (4) special technical assistance, (5) fracture analysis computer programs, (6) cleavage-crack initiation, (7) cladding evaluations, (8) pressurized-thermal-shock technology, (9) analysis methods validation, and (10) fracture evaluation tests. The program tasks have been structured to place emphasis on the resolution fracture issues with near-term licensing significance. Resources to execute the research tasks are drawn from ORNL with subcontract support from universities and other research laboratories. Close contact is maintained with the sister Heavy-Section Steel Irradiation (HSSI) Program at ORNL and with related research programs both in the United States and abroad. This report provides an overview of principal developments in each of the ten program tasks from April 1, 1991, to September 30, 1991.

# Contents


| | Page |
|---|---|
| Abstract | iii |
| List of Figures | ix |
| List of Tables | xi |
| Preface | xiii |
| Executive Summary | xv |
| 1 Program Management | 1 |
| References | 3 |
| 2 Fracture Methodology and Analysis | 7 |
| 2.1 Introduction | 7 |
| 2.2 Applicability of Plane-Strain Fracture Toughness Toward the Evaluation of Circumferential Surface Cracks | 7 |
| 2.2.1 Fracture Analysis of a Compact-Tension Specimen Subjected to Generalized Plane-Strain Loading | 7 |
| 2.2.2 Modified-Boundary Model of Near-Crack-Tip Region | 10 |
| 2.2.3 Analysis in Support of the Proposed ORNL Biaxial Test | 11 |
| 2.2.4 Constraint Effects for Circumferential Flaws | 11 |
| 2.2.4.1 Introduction | 11 |
| 2.2.4.2 Yield Zone Extent | 12 |
| 2.2.4.3 Hydrostatic Constraint Factor | 13 |
| 2.2.4.4 Quantitative Effects of Constraint for A 533 B Steel | 14 |
| 2.3 Dynamic Fracture Analysis of Pressure Vessels | 15 |
| 2.3.1 Introduction | 15 |
| 2.3.2 Fracture Analyses | 16 |
| 2.3.2.1 Finite-Element Model | 16 |
| 2.3.2.2 Finite-Element Analyses | 16 |
| 2.4 Elastic-Plastic Fracture Mechanics in Inhomogeneous Materials and Structures | 19 |
| 2.4.1 Experimental WG Workscope | 19 |
| 2.4.2 Theoretical WG Workscope | 20 |
| 2.4.3 Estimation Scheme WG Workscope | 20 |
| 2.4.4 Residual Stress Measurements | 20 |
| 2.4.5 Proposed General Review Meeting | 20 |
| References | 21 |

3 Material Characterization and Properties ..... 23

3.1 Characterization of HSST Plate 013B in the L-S Orientation ..... 23
3.2 Thermal Aging of Stainless Steel Cladding ..... 23
3.3 ASTM Fracture-Toughness Testing Standards Development ..... 26
3.4 Study of Low-Toughness Zones ..... 26

3.4.1 ORNL Studies ..... 26
3.4.2 University of Maryland Studies ..... 28

3.4.2.1 Initiation from Cleavage Cracks ..... 28

3.4.3 Battelle Memorial Institute ..... 28

3.4.3.1 Failure Analysis ..... 28
3.4.3.2 Effect of Crack-Tip Morphology on Cleavage Crack Extension ..... 28

References ..... 28

4 Special Technical Assistance ..... 29

4.1 Yankee Rowe PTS Probabilistic Fracture-Mechanics Sensitivity Analysis ..... 29

4.1.1 Background Information ..... 29
4.1.2 Scope of the Sensitivity Analysis ..... 29
4.1.3 Methods of Analysis ..... 29

4.1.3.1 Overview ..... 29
4.1.3.2 Fracture Analysis Methods—Basic Methodology ..... 30
4.1.3.3 Types of Flaws ..... 30
4.1.3.4 Fracture Analysis Method for Surface Flaws ..... 30
4.1.3.5 Fracture Analysis Method for Subclad Flaws ..... 32
4.1.3.6 Fracture Analysis Method for Embedded Flaws ..... 32

4.1.4 Results ..... 32

4.2 Review of Inglis' Analysis for the Cases of Equibiaxial and Uniaxial Loading of a Through Crack in a Wide Plate ..... 37

4.2.1 Introduction ..... 37
4.2.2 Equibiaxial Loading ..... 38
4.2.3 Uniaxial Loading ..... 39

References ..... 39

5 Fracture Analysis Computer Programs ..... 41

5.1 Background Information ..... 41
5.2 Enhancements ..... 41

6 Cleavage-Crack Initiation ..... 43

6.1 Shallow-Crack Fracture-Toughness Testing ..... 43

6.1.1 Rotation Factor Development ..... 43
6.1.2 Development Phase ..... 44
6.1.3 Production Phase ..... 46
6.1.4 Future Work ..... 47

6.2 Lower-Bound Initiation Toughness ..... 47
6.3 Gradient Effects on Fracture ..... 48
6.4 Thickness Influence on Toughness ..... 49

References ..... 49

7 Cladding Evaluations ..... 51

7.1 Objective ..... 51
7.2 Study of the Effect of Cladding on Reactor Vessel Integrity ..... 51
7.3 Effect of Irradiated Cladding on the Behavior of Shallow Flaws ..... 52
7.4 Discussions of EPI Program and PTS Experiments in Japan ..... 52

7.4.1 Introduction ..... 52
7.4.2 Department of Nuclear Engineering, University of Tokyo ..... 52
7.4.3 Komae Research Laboratory, Central Research Institute of Electric Power Industry ..... 54
7.4.4 Department of Mechanical Engineering Sciences, Tokyo Institute of Technology ..... 54
7.4.5 Takasago R&D Center, Mitsubishi Heavy Industries ..... 54
7.4.6 Department of Ocean Mechanical Engineering, Kobe University of Mercantile Marine ..... 55
7.4.7 Department of Energy Engineering, Toyohashi Institute of Technology ..... 56

References ..... 56

8 Pressurized-Thermal-Shock Technology ..... 59

8.1 Background Information ..... 59
8.2 Analytical Solution to Thermal-Streaming Problem ..... 59
8.3 Anticipated Activities ..... 59
References ..... 59

9 Analysis Methods Validation ..... 61

9.1 Background Information ..... 61
9.2 CSNI/FAG Final Report on Project FALSIRE Workshop ..... 61
9.3 Joint IAEA and OECD/NEA Meeting on Fracture Mechanics Verification by Large-Scale Testing ..... 62
9.4 CSNI/FAG Phase II Project ..... 62
9.5 Spinning-Cylinder Experiments ..... 62
Reference ..... 63

10 Fracture Evaluation Tests ..... 65

10.1 Introduction ..... 65
10.2 Shallow-Crack Fracture-Toughness Testing Program ..... 65

10.2.1 Specimen Fabrication and Testing ..... 65
10.2.2 Thickness Effects on Toughness (Six Additional Beam Tests) ..... 65
10.2.3 Shallow-Crack Testing Production Phase ..... 66
10.2.4 Test Reports ..... 68

10.3 Full-Thickness, Shallow-Crack, Clad Beam Tests ..... 68
10.4 Out-of-Plane Biaxial Loading Fracture-Toughness Tests ..... 69
References ..... 69
Appendix 10.1: Shallow-Crack Fracture Toughness Testing ..... 71

Conversion Factors ..... 77
Prior Heavy-Section Steel Technology Reports ..... 79

# List of Figures


| Figure | | Page |
|---|---|---|
| 1.1 | Summary of principal HSST program research tasks | 1 |
| 1.2 | Level 1 breakdown structure for HSST Program | 2 |
| 1.3 | Resources applied to HSST Program R&D tasks | 3 |
| 2.1 | Applied J vs area A within maximum principal stress contour of $\sigma_{pl}$ = 1375 MPa for IT-CT specimen subjected to four cases of out-of-plane strain | 9 |
| 2.2 | Applied J vs area A within maximum principal stress contour of $\sigma_{pl}$ = 1400 MPa for IT-CT specimen subjected to five cases of out-of-plane strain | 9 |
| 2.3 | Applied J vs area A within maximum principal stress contour of $\sigma_{pl}$ = 1425 MPa for IT-CT specimen subjected to four cases of out-of-plane strain | 9 |
| 2.4 | Region of plasticity in GPS model of IT-CT specimen corresponding to maximum pin load of 35 kN and three values of out-of-plane strain | 10 |
| 2.5 | Yield zone area as function of load level | 12 |
| 2.6 | Contours of hydrostatic constraint factor, $\sigma_m/\sigma_{eff}$, in crack-tip region for plane-strain configuration under axial loading | 13 |
| 2.7 | Contours of hydrostatic constraint factor, $\sigma_m/\sigma_{eff}$, in crack-tip region for axisymmetric configuration under axial loading | 13 |
| 2.8 | Contours of hydrostatic constraint factor, $\sigma_m/\sigma_{eff}$, in crack-tip region for axisymmetric configuration under combined loading | 14 |
| 2.9 | $K_c$ as function of constraint measure Q as inferred from experimental data by Theiss and Bryson for SENB specimens of A 533 B steel | 14 |
| 2.10 | Finite-element model of RPV | 16 |
| 2.11 | K vs a/W for application-mode dynamic analysis using initiation-toughness curve | 17 |
| 2.12 | Comparison of K vs a/W for static and generation mode dynamic analyses | 18 |
| 2.13 | Comparison of K vs a/W for static and application-mode dynamic analyses | 19 |
| 3.1 | Results of CVN testing in L-S orientation for characterization block 13BA/5 postweld heat treated at 621°C (1150°F) for 40 h | 24 |
| 3.2 | Results of CVN testing in T-L orientation for characterization block 13BA/5 postweld heat treated at 621°C (1150°F) for 40 h | 24 |
| 3.3 | Effects of neutron irradiation and thermal aging at 288°C on initiation fracture toughness, $J_{Ic}$, of three-wire type 308 stainless steel cladding at various test temperatures | 27 |

3.4 Effects of neutron irradiation and thermal aging at 288°C on deformation J-integral tearing modulus of three-wire type 308 stainless steel cladding at various test temperatures ..... 27

4.1 Probabilistic fracture-mechanics methodology for surface flaws ..... 31

4.2 Probabilistic fracture-mechanics methodology for subclad flaws ..... 33

4.3 Probabilistic fracture-mechanics methodology for embedded flaws ..... 35

4.4 Comparison of Inglis' complete solution for crack-tip stresses in uniaxially loaded center cracked plate with one-term LEFM approximation ..... 37

4.5 Coordinate definition for Inglis' analysis ..... 38

6.1 Preliminary $K_c$ vs temperature toughness data ..... 47

6.2 Unorthodox quenching procedure being used in gradient study ..... 48

10.1 Photograph of production beam with instrumentation ..... 67

10.2 Photograph of representative shallow- and deep-crack [HSST beams 25 (left) and 26] ..... 67

# List of Tables


| Table | | Page |
|---|---|---|
| 2.1 | Out-of-plane strain conditions imposed on GPS model of IT-CT specimen | 8 |
| 3.1 | Summary of CVN tests in the L-S and T-L orientations on material from characterization block 13BA/5 [flame-cut from HSST Plate 013B and postweld heat treated at 621°C (1150°F) for 40 h] | 25 |
| 3.2 | Unloading compliance J-R test results of 12.7-mm-thick three-wire stainless steel cladding fracture-toughness specimens (10% side-grooved on each side) | 25 |
| 6.1 | Rotation factor data | 44 |
| 6.2 | HSST development beam data with CTOD toughness | 45 |
| 6.3 | J-integral toughness and constant parameter, m, determination | 46 |
| 6.4 | Actual and "predicted" toughness values using modified Irwin $\beta_c$ correlation | 46 |
| 10.1 | Test matrix for the six additional beams | 65 |
| 10.2 | Test matrix for the production beams tested to date | 66 |
| 10.3 | Crack-depth measurements for a representative deep- and shallow-crack beam | 68 |

# Preface

The Heavy-Section Steel Technology (HSST) Program, which is sponsored by the Nuclear Regulatory Commission, is an engineering research activity devoted to extending and developing the technology for assessing the margin of safety against fracture of the thick-walled steel pressure vessels used in light-water-cooled nuclear power reactors. The program is being carried out in close cooperation with the nuclear power industry. This report covers HSST work performed in April–September 1991. The work performed by the Oak Ridge National Laboratory (ORNL) and by subcontractors is managed by the Engineering Technology Division (ETD) of ORNL. Major tasks at ORNL are carried out by the ETD and the Metals and Ceramics Division. The following is a list of prior progress reports on this program:

ORNL-4176
ORNL-4315
ORNL-4377
ORNL-4463
ORNL-4512
ORNL-4590
ORNL-4653
ORNL-4681
ORNL-4764
ORNL-4816
ORNL-4855
ORNL-4918
ORNL-497[illegible]
ORNL/TM-4655 (Vol. II)
ORNL/TM-4729 (Vol. II)
ORNL/TM-4805 (Vol. II)
ORNL/TM-4914 (Vol. II)
ORNL/TM-5021 (Vol. II)
ORNL/TM-5170 (Vol. II)
ORNL/NUREG/TM-3
ORNL/NUREG/TM-28
ORNL/NUREG/TM-49
ORNL/NUREG/TM-64
ORNL/NUREG/TM-94
ORNL/NUREG/TM-120
ORNL/NUREG/TM-147
ORNL/NUREG/TM-166
ORNL/NUREG/TM-194
ORNL/NUREG/TM-209
ORNL/NUREG/TM-239
NUREG/CR-0476 (ORNL/NUREG/TM-275)
NUREG/CR-0656 (ORNL/NUREG/TM-298)
NUREG/CR-0818 (ORNL/NUREG/TM-324)
NUREG/CR-0980 (ORNL/NUREG/TM-347)
NUREG/CR-1197 (ORNL/NUREG/TM-370)
NUREG/CR-1305 (ORNL/NUREG/TM-380)
NUREG/CR-1477 (ORNL/NUREG/TM-393)
NUREG/CR-1627 (ORNL/NUREG/TM-401)
NUREG/CR-1806 (ORNL/NUREG/TM-419)
NUREG/CR-1941 (ORNL/NUREG/TM-437)
NUREG/CR-2141, Vol. 1 (ORNL/TM-7822)
NUREG/CR-2141, Vol. 2 (ORNL/TM-7955)
NUREG/CR-2141, Vol. 3 (ORNL/TM-8145)
NUREG/CR-2141, Vol. 4 (ORNL/TM-8252)
NUREG/CR-2751, Vol. 1 (ORNL/TM-8369/V1)
NUREG/CR-2751, Vol. 2 (ORNL/TM-8369/V2)
NUREG/CR-2751, Vol. 3 (ORNL/TM-8369/V3)
NUREG/CR-2751, Vol. 4 (ORNL/TM-8369/V4)
NUREG/CR-3334, Vol. 1 (ORNL/TM-8787/V1)
NUREG/CR-3334, Vol. 2 (ORNL/TM-8787/V2)
NUREG/CR-3334, Vol. 3, (ORNL/TM-8787/V3)
NUREG/CR-3744, Vol. 1 (ORNL/TM-9154/V1)
NUREG/CR-3744, Vol. 2 (ORNL/TM-9154/V2)
NUREG/CR-4219, Vol. 1 (ORNL/TM-9593/V1)
NUREG/CR-4219, Vol. 2 (ORNL/TM-9593/V2)
NUREG/CR-4219, Vol. 3, No. 1 (ORNL/TM-9593/V3&N1)
NUREG/CR-4219, Vol. 3, No. 2 (ORNL/TM-9593/V3&N2)
NUREG/CR-4219, Vol. 4, No. 1 (ORNL/TM-9593/V4&N1)
NUREG/CR-4219, Vol. 4, No. 2 (ORNL/TM-9593/V4&N2)
NUREG/CR-4219, Vol. 5, No. 1 (ORNL/TM-9593/V5&N1)
NUREG/CR-4219, Vol. 5, No. 2 (ORNL/TM-9593/V5&N2)
NUREG/CR-4219, Vol. 6, No. 1 (ORNL/TM-9593/V6&N1)
NUREG/CR-4219, Vol. 6, No. 2 (ORNL/TM-9593/V6&N2)
NUREG/CR-4219, Vol. 7, No. 1 (ORNL/TM-9593/V7&N1)
NUREG/CR-4219, Vol. 7, No. 2 (ORNL/TM-9593/V7&N2)
NUREG/CR-4219, Vol. 8, No. 1 (ORNL/TM-9593/V8&N1)

# Executive Summary

W. E. Pennell

The Heavy-Section Steel Technology (HSST) Program is conducted for the Nuclear Regulatory Commission (NRC) by Oak Ridge National Laboratory (ORNL). The program focus is on the development and validation of a fracture-mechanics-based technology for the evaluation of fracture-prevention margins in nuclear reactor pressure vessels (RPVs). Prior phases of the program generated the required technology, which was then transferred to national consensus Codes and Standards. Subsequent large-scale fracture tests have revealed the need for further development and refinement of the technology. Irradiation effects research programs and reactor vessel surveillance programs have identified further areas where extension of the fracture technology is required. Recent experience with licensing application of the technology has also identified areas in which additional development is required. Current HSST program activities are structured to provide the necessary fracture technology developments and to support NRC in the licensing application of that technology.

## 1 Program Management

The HSST Program is organized in ten interrelated Tasks, each with its own Level 2 work-breakdown-structure (WBS) and milestone schedule. The individual Task WBS elements and milestone schedules are combined into the HSST Program Level 1 WBS and milestone schedule. This is used in conjunction with a cost-schedule control system to track performance against objectives down to the individual Task milestone level and guide the implementation of necessary corrective actions. During the current reporting period the overall program cost and schedule variances were –0.6% and –12.0%, respectively. The –12.0% schedule variance was due to an NRC-directed change in the program to provide support to an ongoing nuclear plant reactor vessel integrity evaluation. The scope of this evaluation was greater than had been originally anticipated and was not fully reflected in the program WBS and milestone schedule at the close of the current reporting period.

The program is staffed with personnel from the Engineering Technology, Metals and Ceramics, and Computing and Telecommunications Divisions at ORNL, with additional support from extensive university, consultant, and research laboratory subcontracts. During the current reporting period, HSST Program personnel published 7 reports and 12 papers and made numerous technical presentations.

The HSST Program management joined with personnel from Framatome to organize sessions on Reactor Vessel Integrity at the ASME PV&P Division Conference held in San Diego, California, in June 1991. The volume of papers from these sessions was assembled and edited at ORNL before its publication by ASME in a volume entitled "Pressure Vessel Integrity—1991," ASME-Vol. 213 (MPC-Vol. 32).

A program management review of the potential effect of out-of-plane (OOP) stresses on crack-tip constraint and fracture toughness was completed. The review objective was to determine if the potential effects of OOP stresses on fracture toughness justified experimental investigation of this loading condition. The primary conclusion from the review was that the predicted effect of OOP stresses on fracture toughness was dependent on the model used to make the prediction. It was concluded that biaxial fracture tests would be required to resolve this issue.

## 2 Fracture Methodology and Analysis

Principal fracture issues investigated in this task during the current reporting period were (1) the effect of out-of-plane stresses and strains on material fracture toughness, (2) the effect of reactor vessel inertia on crack-arrest behavior during a pressurized-thermal-shock (PTS) event, and (3) the development of an engineering scheme for the application of fracture mechanics principles to the analysis of inhomogeneous materials. Investigation of the latter issue was by means of support provided by the HSST Program to the Japanese Program for Elastic-Plastic Fracture Mechanics in Inhomogeneous Materials and Structures (EPI).

A dual parameter J-$A_{CR}$ fracture correlation, developed by J. Keeney-Walker, is being applied to the investigation of out-of-plane strain effects on fracture toughness. A three-dimensional (3-D) elastic-plastic, finite-element analysis model with the capability of providing a detailed definition of the crack-tip stress and strain fields is used in

this investigation. The generalized plane-strain boundary condition incorporated into this model provides a capability for imposing a range of out-of-plane strains. In the current reporting period the sensitivity of the J-$A_{CR}$ curves to the stress selected to define the $A_{CR}$ boundary was investigated. Results show the influence of imposed out-of-plane strains on $A_{CR}$ to decrease significantly as the value of the boundary condition stress increases. Selection of the correct value for this stress is clearly essential for the further development of this model. Matching the model predictions to the available fracture-toughness data in the plane stress to plane strain constraint domain provides a basis for making this selection.

A parallel investigation of the effect of transverse strains on fracture toughness is focussing on techniques to refine the analysis of crack-tip stress-strain fields using crack-tip models with boundary conditions derived from single-parameter fracture-mechanics technology. Prior work in this area used a slip-line-based analytical model in conjunction with a stress-state-dependent, fracture-strain failure criterion. In the current reporting period, a new finite-element-based boundary layer model has been developed. A stress-based failure criterion has been substituted in place of the strain-based criterion used in the previous model. To date neither model predicts any significant effect of either positive or negative out-of-plane strain on fracture toughness. Calibration of these models using available fracture-toughness data from the plane stress to plane strain domain is scheduled for the next phase of the program. This calibration could influence the model predictions.

Studies of circumferential crack constraint effects continued at the University of Maryland using an axisymmetric elastic-plastic, finite-element model of a reactor vessel with a continuous uniform depth crack. In the current reporting period the crack-tip mesh geometry was modified to overcome plastic-zone definition problems encountered with the previous model. Results obtained with the revised model show little effect of out-of-plane stresses on the plastic zone area but a marked effect of these stresses on the hydrostatic to effective stress ratio within the plastic zone. Peak values of Sh/Se are higher than the baseline plane-strain values when an out-of-plane stress is applied and occur at greater distances from the crack tip. This observation may have implications for fracture in the transition temperature range where ductile failure mechanisms become important. Constraint, as measured by the parameter Q in the dual parameter J-Q correlation, was found to decrease under pressure loading because of the action of the radial compressive stress. This decrease may produce an increase in cleavage fracture toughness relative to plane-strain values. It is important to recognize, however, that this relaxation of constraint does not apply to thermal stresses, which are the largest stresses in the pressure-vessel wall during a PTS transient.

Studies have been made of the effect of the reactor vessel dynamic response characteristics on crack arrest during a PTS event. The vessel first-mode frequency response time is much longer than the time required for crack propagation. It follows, therefore, that conditions may exist during the dynamic event where the crack arrests before the vessel reaches its equilibrium cracked configuration. The intent of these studies was to (1) determine the depth of crack penetration associated with the initial crack arrest under a range of dynamic response simulation conditions and (2) determine if the arrested crack would remain stable throughout the balance of the dynamic event.

The studies were conducted using a 180° thermoelastic dynamic analysis model of the reactor vessel wall. A PTS transient was selected; the OCA-P static equilibrium model had predicted it to produce crack arrest after a 50% penetration of the wall. The application-mode dynamic analysis showed an initial crack arrest at a crack depth corresponding to a 36% penetration of the wall. Subsequent dynamic loading, however, increased the crack-tip stress intensity until it exceeded the estimated dynamic fracture toughness of the material. Thereafter, the crack reinitiated and propagated to a final arrest at 46% of the vessel wall thickness. This arrest depth is not significantly less than the 50% depth given by the OCA-P static equilibrium model. It must be recognized, however, that the dynamic reinitiation toughness estimates were based on extrapolation of a relatively sparse data base of dynamic fracture-toughness data. Additional fracture-toughness data could modify the predictions of dynamic crack reinitiation. Note also that the influence of any dynamic crack arrest effect on the overall outcome of a PTS analysis may be negated when the PTS transient involves the recovery of high-pressure loading. Prior studies of such PTS transients show that crack-tip conditions will evolve long after the arrest of the initial crack to produce reinitiation and further propagation of the crack.

HSST program support of the Japanese EPI program continued. The goal of this program is to develop and

validate technology for the prediction of elastic-plastic crack growth in inhomogeneous materials such as weld metal. In the current reporting period, testing has been initiated on bimaterial specimens with a zone-to-zone yield stress ratio of 1.4. Data from these tests will be used in the crack propagation model development. Three-dimensional elastic-plastic, finite-element models are being used to analyze the test data and evaluate the performance of a number of elastic-plastic crack-growth estimating schemes. Effects of residual stress at the electron-beam weld between the materials of the bimaterial specimens are included in the analysis. Plans have been made for a comprehensive review of results and conclusions from the EPI program to be presented in a meeting tentatively scheduled to be held in conjunction with the ASME PV&P Division meeting in Denver, Colorado, in June 1993.

## 3 Material Characterization and Properties

The first phase of characterization testing of the A 533 B plate material used in the shallow-flaw fracture-toughness testing program was completed. Charpy V-notch (CVN) and tensile data were obtained for specimens cut from both the midthickness and surface regions of the plate. The value of $RT_{NDT}$ for material from the surface material was found to be 28°C lower than that for material from the midthickness of the plate. Note that specimens tested to date in the shallow-flaw fracture-toughness program have been cut from the midsection of the plate.

Investigation continued of the effects of thermal aging on the tearing toughness properties of type 308 stainless steel cladding material. The objective of this investigation is to provide data that will permit the previously reported reductions in tearing toughness of irradiated stainless steel cladding to be separated into irradiation and thermal-aging effects. In the current reporting period, tests on material aged for 1605 h at 288°C were completed. The tests showed a 16% decrease in the CVN upper-shelf energy; this is a significant portion of the CVN upper-shelf energy reduction (22%) previously reported for irradiated stainless steel cladding at the same test temperature. Thermal aging reduced the tearing initiation toughness at room temperature but not at prototypical reactor operating temperatures. Aging of specimens for testing in later phases of this program continues.

HSST Program support of the development of an ASTM combined $J_{Ic}$/J-R standard continued. Meetings were held to address issues associated with abnormal J-R test data patterns.

Investigation of local brittle zones and pop-ins on lower-bound fracture toughness of pressure vessel steels continued. This work will provide data that will contribute to resolution of licensing issues associated with the fracture-toughness curve to be used to define the low-temperature overpressure protection (LTOP) setpoint for operating reactors. In the current reporting period significant progress was made in the selection of a test material and test configuration to consistently produce pop-ins in fracture tests. This is a necessary prelude to the planned experimental phase of this program.

Investigation of the effect on fracture toughness of reinitiation of a crack from a previously arrested cleavage crack was completed at the University of Maryland. This investigation was initiated to resolve concerns that an arrested cleavage crack could produce fracture at stress-intensity factors lower than those required to fracture fatigue-sharpened cracks. Lower fracture toughness for cleavage precracked specimens was found only in tests conducted at relatively high temperatures (85°C).

## 4 Special Technical Assistance

The program continued to provide a service to NRC in the evaluation of irradiation embrittlement issues relating to the Yankee Rowe RPV. A sensitivity study was completed during this reporting period. Objectives for this study were to (1) assess the relative influence of key analysis input parameters on predicted PTS failure rates and (2) provide a means for rapidly revising the vessel failure rate predictions when more accurate vessel embrittlement estimates become available.

The OCA-P computer program was modified to perform the sensitivity analysis. Principal modifications were the additions of (1) a subclad and buried flaw analysis capability and (2) a spatial representation of the vessel irradiation fluence. The sensitivity analysis was completed. Results will be published in NUREG/CR-5872.

A review and interpretation of the Inglis equations for the nonsingular in-plane stresses at the tip of a crack were completed. Expressions were produced for the in-plane principal stresses on the plane of propagation of the crack. Results from this work were used in the investigation of the effect of out-of-plane stresses on fracture toughness reported in Task 1.

## 5 Fracture Analysis Computer Programs

There was no activity on this task during the current reporting period because of the diversion of resources to the higher priority Yankee Rowe PTS sensitivity studies reported in Task 4.

## 6 Cleavage Crack Initiation

Fracture toughness of shallow flaws has been found to be higher than that of deep flaws due to the relaxation of crack-tip constraint. Enhanced shallow-flaw fracture toughness can have a significant influence on the outcome of a PTS analysis because the majority of predicted crack initiations are observed to be from shallow flaws. This observation was the basis for implementation of the HSST Program of shallow-flaw testing on A 533 B material.

Determination of the center of rotation in the ligament remaining beneath a shallow crack is essential to interpretation of the test data. During the current reporting period two alternate experimental techniques for locating the center of rotation were evaluated. A technique using strain gages located on either side of the ligament neutral axis was found to give the most reliable and repeatable results and was selected for use in the production phase of the program.

Two techniques for calculating $J_c$ from the test results were evaluated. One used the energy derived from the total area under the load-displacement curve, while the other used only the plastic portion of that energy. The latter approach was found to give more consistent results and was used in the test data analysis. This analysis showed the ratio of lower-bound shallow-flaw toughness to deep-flaw toughness at –60°C to be 1.6. Constraint parameters were calculated for both the deep- and shallow-flaw specimens. Updated predictions of shallow-flaw fracture toughness made using deep-flaw toughness in conjunction with a modification of Irwin's $\beta_1$ correction factor showed the technique did not perform as well as had been reported previously.

Shallow-flaw fracture-toughness tests on full-thickness specimens cut from a PWR vessel from a cancelled plant are planned for the next phase of this program. These tests will provide data to resolve issues relating to (1) the effect of vessel fabrication processes on fracture toughness of the near-surface material and (2) transferability of the shallow-flaw fracture-toughness data. During the current reporting period the material to be used in these tests has been secured, and preliminary discussions have been held with the planned subcontractor. A specification for these tests will be completed early in FY 1992.

Research on the development of techniques for the generation of lower-bound fracture-toughness data using small-scale specimens was completed at the University of Maryland (UM). A report on this work is scheduled for publication in November 1991.

Effects of near-surface metallurgical gradients on fracture toughness are being investigated at UM. The objective for this research is to define the metallurgically induced fracture-toughness gradient in the near-surface region of plates and welds. Fracture-toughness gradients in this region can influence crack initiation from shallow surface flaws. Results from this work will be used to resolve issues relating to PTS analysis. In the current reporting period, ORNL has cut sections from the nozzle course of the cancelled Midland reactor vessel and provided the material to UM. UM has prepared the material for metallurgical examination. In a parallel action, heat treatment procedures have been developed at UM for generating toughness gradients in test material. Ultimately this research aims to relate metallurgical features identified in the reactor vessel material with similar features in the test specimens. Fracture-toughness data from the test specimens can then be related to specific areas of the reactor vessel near-surface region.

## 7 Cladding Evaluations

The University of Tennessee (UT) completed a study of the potential for tearing-induced crack propagation in cladding material to convert to cleavage fracture in the

reactor vessel base material. This study w[illegible] initiated in response to data from the Heavy-Section Steel Irradiation Program indicating low-tearing toughness for irradiated cladding. The study concluded that mode conversion and crack propagation from the cladding into the base material would not occur unless rapid loading and/or unstable crack propagation conditions were present in the cladding. Straining rates associated with stable crack propagation in the cladding were too low to influence fracture toughness in the substrate material to the extent that cleavage fracture could be initiated.

Other research activities planned for this task during this reporting period were deferred to accommodate an NRC request for a transfer of resources to address an unplanned evaluation of dynamic effects on crack arrest, as reported in Task 2. The Task leader did, however, visit Japan for discussions on the EPI program and PTS testing and analysis topics.

## 8 Pressurized-Thermal-Shock Technology

This task produces the PTS analysis developments required to support the PTS computer program development reported in Task 5. Research planned for the current reporting period was deferred at NRC request to make resources available for the Yankee Rowe PTS Sensitivity Study reported in Task 4.

## 9 Analysis Methods Validation

Validation of fracture-mechanics-based analysis methods is accomplished by comparing predictions from the technology with results obtained from large-scale fracture tests. Activities in this task are closely coupled with those of the CSNI Fracture Analysis Group (CSNI/FAG). The recently completed CSNI/FAG project for Fracture Analysis of Large Scale International Experiment (Project FALSIRE) has revealed a number of areas in which existing analysis methods did not perform well. Activities in this task during the current reporting period focused on completing an interpretive report on the Project FALSIRE findings. This is being done as a team effort with GRS of Colone, Germany. A meeting was held in Colone in May to coordinate arrangements for completion of the interpretive report. A paper on the projects findings was prepared and presented at the 11th SMIRT Conference in Tokyo, in August 1991.

One of the important results from the CSNI/FAG project FALSIRE was the recognition that the cause of deviations between analysis predictions and test results could not be effectively isolated in tests involving multiple variables. This finding has influenced the HSST Program planning for large-scale constraint effects tests. These tests are planned so each test introduces only one additional variable.

## 10 Fracture Evaluation Tests

This task performs fracture tests in support of all other tasks. In the current reporting period the segment of the production phase of the shallow-flaw fracture-toughness testing program assigned to ORNL was completed. Testing procedures and techniques developed during the development phase of the program worked well in the production tests. The remainder of the production tests will be performed by the David Taylor Research Center.

Planning was initiated for the full-scale shallow-flaw fracture-toughness tests and biaxial loading fracture-toughness tests. Both tests require large-capacity test machines. Preliminary discussions were held with potential testing subcontractors. These discussions resulted in the selection of the National Institute of Standards (NIST) in Rockville, Maryland, as the subcontractor for the full-scale shallow-flaw fracture-toughness tests. These tests will investigate the effect of prototypical surface effects on shallow-flaw fracture toughness. AEA Technology in the United Kingdom is a potential subcontractor for the biaxial fracture-toughness test. Their recently commissioned biaxial test facility appears to have the capacity required to meet the biaxial fracture-toughness test specification. However, additional analysis will be required before this preliminary evaluation can be confirmed. The large-scale biaxial tests will investigate the effect of out-of-plane stresses, which are generated during a PTS event, on crack-tip constraint and fracture toughness. Test material for both tests has been located and assigned.

# HEAVY-SECTION STEEL TECHNOLOGY PROGRAM SEMIANNUAL PROGRESS REPORT FOR APRIL–SEPTEMBER 1991*

## 1 Program Management

W. E. Pennell

The Heavy-Section Steel Technology (HSST) Program is conducted for the Nuclear Regulatory Commission (NRC) by Oak Ridge National Laboratory (ORNL). The program focuses on the development and validation of technology for the assessment of fracture-prevention margins in commercial nuclear reactor pressure vessels (RPVs).

RPV licensing issues of current concern can be grouped into three primary categories: (1) low-temperature overpressure protection (LTOP) setpoint criteria, (2) structural integrity of the pressure vessel when subjected to pressurized-thermal-shock (PTS) loading, and (3) criteria for the evaluation of fracture margins for reactor vessels containing low-upper-shelf (LUS) Charpy energy material. The current HSST Program is structured to provide the research results required for resolution of these issues. A summary of the program's principal research tasks is given in Fig. 1.1.

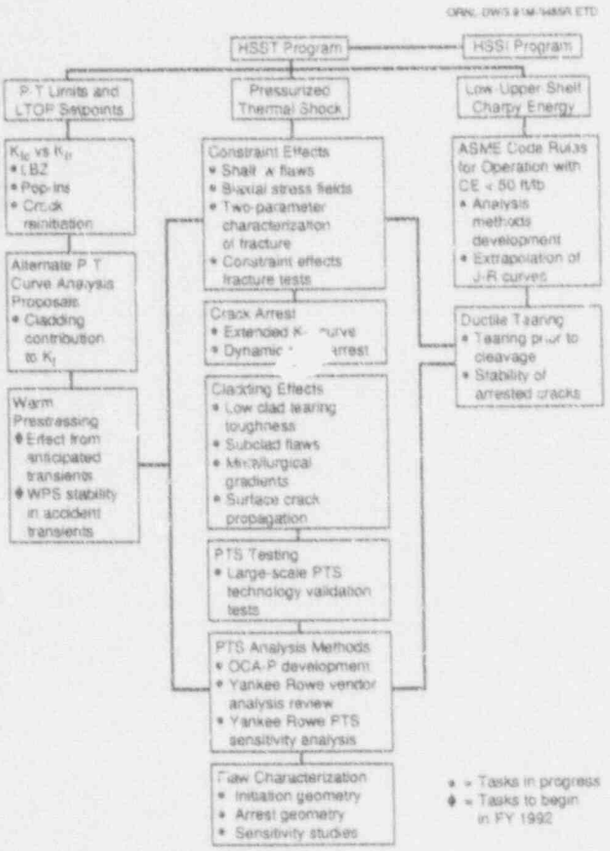


Figure 1.1 Summary of principal HSST Program research tasks

*This report is written in metric units. Conversions from SI to English units for all SI quantities are listed on a foldout page at the end of this report.

## Program

Management direction and control of the program are implemented using a ten-element Level 1 work breakdown structure (WBS) and a linked cost-schedule performance monitoring system. The current HSST Program Level 1 WBS is illustrated in Fig. 1.2. Each element of the Level 1 WBS represents a separate research or management task with a designated task leader.

At the close of the current reporting period the program cost and schedule variances were –0.6% and –12.0%, respectively. A midyear review resulted in the reallocation of program resources to accommodate the need to provide support to the licensing evaluation of the Yankee Rowe RPV. The –12% schedule variance was primarily because, at NRC request, the Yankee Rowe activities were extended to include scope beyond that covered in the midyear resource reallocation.

Staffing for the research tasks is drawn from the Engineering Technology, Metals and Ceramics, and Computing and Telecommunications Divisions at ORNL. Subcontracts with consultants, universities, and other research laboratories are used to gain access to special expertise and capabilities required for certain research tasks. A summary of resources applied to the HSST research tasks during this report period is given in Fig. 1.3.

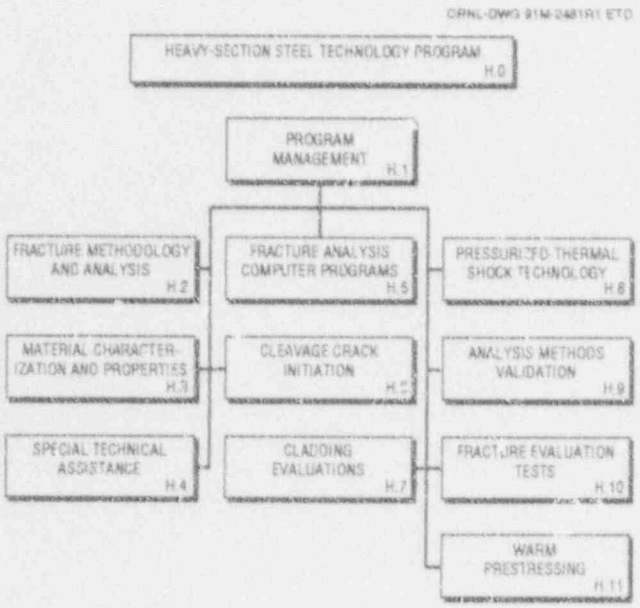


**Figure 1.2 Level 1 breakdown structure for HSST Program**

During this report period, discussions were held with four subcontractors and three consultants to define the program workscope for FY 1992. For FY 1992, consulting arrangements will give the program additional access to experts in the field of constraint effects on fracture toughness. Planned subcontracts will also provide the capability for performing large-scale fracture tests under out-of-plane biaxial loading conditions. These arrangements will permit the program to implement the experimental phase of the investigation of biaxial loading constraint effects on fracture toughness. This research will provide data to refine analysis of the response of reactor vessels to PTS transient loading.

Four sessions on various aspects of RPV integrity were organized and chaired by S. Bhandari of Framatome and W. E. Pennell of ORNL at the ASME PV&P Division Summer Annual Meeting in San Diego, California, in June 1991. Papers from these sessions, together with papers from two other sessions, were assembled at ORNL and published in ASME-Vol. 213 (MPC-Vol. 32), "Pressure Vessel Integrity—1991."

A number of program review presentations were given during the current reporting period; the most significant of these were (1) an overview of fracture issues relating to the analysis of PTS fracture margins given to USNRC Commissioner Rogers and (2) an ORNL Showcase Presentation on the role of fracture technology in nuclear plant life extension evaluations.

Proposals for the scope and objectives for a VTT (Finland)/ORNL fracture technology exchange agreement were prepared and forwarded to VTT after approval by NRC. The HSST program 189, which defines objectives and resource allocations for FY 1992, was also prepared and forwarded to NRC for review and approval.

During the current report period, HSST Program personnel published one semiannual progress report,[1] two topical NUREG/CR reports,[2,3] two presentations[4,5] (as NUREG/CP documents), two ORNL/NRC Letter Reports,[6,7] one paper in a peer-reviewed journal,[8] four papers[9–12] in technical society proceedings, and four papers in international proceedings.[13–16] Also, seven presentations were given at technical society meetings,[17–23] three presentations[24–26] were made at NRC-sponsored or associated meetings, and one

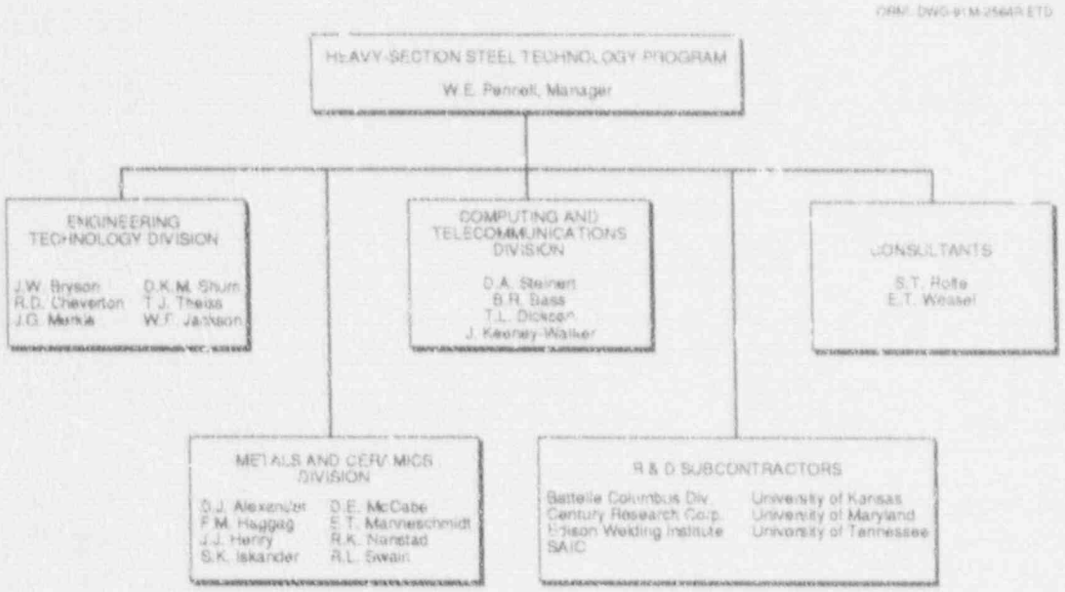


**Figure 1.3 Resources applied to HSST Program R&D tasks**

presentation[27] was made as an Oak Ridge National Laboratory Showcase.

A program management review of the potential effect of out-of-plane (OOP) stresses on crack-tip constraint and fracture toughness was completed. The review objective was to determine if the potential effects of OOP stresses on fracture toughness justified experimental investigation of this loading condition. Results from the previously reported ORNL investigation of circumferential flaws[2] were included in the review together with results derived from a model formulated to investigate the effect of OOP stresses on the $\sigma_b/\sigma_e$ stress ratio at the plastic-zone boundary. This latter model used the available plane-stress and plane-strain fracture-toughness data of Landes and McCabe[28] in conjunction with the stress-state-dependent, fracture-ductility formulation of Weiss[29] to estimate the effect of OOP stresses on fracture toughness. The primary conclusion from the review was that the predicted effect of OOP stresses on fracture toughness was dependent to an abnormal degree on the model used to make the prediction. It was further concluded that biaxial fracture tests would be required to resolve this issue.

## References

1. W. E. Pennell, Martin Marietta Energy Systems, Inc., Oak Ridge Natl. Lab., "Heavy-Section Steel Technology Program Semiann. Prog. Rep. October 1989–March 1990, USNRC Report NUREG/CR-4219, Vol. 7, No. 2 (ORNL/TM-9593/V7&N2), September 1991.*

2. D. K. M. Shum et al., Martin Marietta Energy Systems, Inc., Oak Ridge Natl. Lab., "Analytical Studies of Transverse Strain Effects on Fracture Toughness for Circumferentially Oriented Cracks," USNRC Report NUREG/CR-5592 (ORNL/TM-11581), May 1991.*

3. J. Keeney-Walker, B. R. Bass, and J. D. Landes, "An Investigation of Crack-Tip Stress Field Criteria for Predicting Cleavage-Crack Initiation," USNRC Report NUREG/CR-5651 (ORNL/TM-11692), September 1991.*

4. T. L. Dickson and T. J. Theiss, "Potential Impact of Enhanced Fracture Toughness Data on Pressurized-Thermal-Shock (PTS) Analysis," *Proceedings of the*

*U.S. Nuclear Regulatory Commission Eighteenth Water Reactor Safety Meeting, October 22–24, 1990*, Rockville, Md., USNRC Report NUREG/CP-0114, Vol 3, April 1991.*

5. W. E. Pennell, "Heavy-Section Steel Technology Program Overview," in *Proceedings of U.S. Nuclear Regulatory Commission Eighteenth Water Reactor Safety Information Meeting, October 22–24, 1991*, Rockville, Md., USNRC Report NUREG/CP-0114, Vol. 3, April 1991.*

6. T. L. Dickson and R. D. Cheverton, Martin Marietta Energy Systems, Inc., Oak Ridge Natl. Lab., "Probabilistic Fracture Mechanics Assessment of PWR Vessel Integrity Including Crack-Arrest Data Above MPa√m Unstable Ductile Tearing," ORNL/NRC/LTR-91/8, April 29, 1991.*

7. B. R. Bass, C. E. Pugh, and J. Keeney-Walker, Martin Marietta Energy Systems, Inc., Oak Ridge Natl. Lab., "Assessment of Ductile Fracture Methodology Based on Applications to Large-Scale Experiments," ORNL/NRC/LTR-91/17, September 16, 1991.*

8. J. G. Merkle, "An Application of the J Integral to an Incremental Analysis of Blunting Crack Behavior," pp. 392–432 in *Defect Assessment in Components—Fundamentals and Applications*, ESIS/EGF9, J. G. Blauel and K. H. Schwalbe, Eds., Mechanical Engineering Publications, London, 1991.†

9. T. L. Dickson, "Potential Impact of Enhanced Fracture Toughness on Fracture Mechanics Assessments of PWR Pressure Vessel Integrity for Pressurized-Thermal Shock," pp. 101–108 in *Proceedings of the ASME Pressure Vessel and Piping Conference*, PVP Vol. 208, San Diego, Calif., June 23–27, 1991.†

10. D. E. McCabe, "A Comparison on Weibull and $\beta_{Ic}$ Analysis in the Transition Range," pp. 141–148 in *Proceedings of the ASME Pressure Vessel and Piping Conference*, PVP Vol. 213, San Diego, Calif., June 23–27, 1991.†

11. J. G. Merkle, "A Summary of the Low-Upper-Shelf Toughness Safety Margin Issue," pp. 89–98 in *Proceedings of the ASME Pressure Vessel and Piping Conference*, PVP Vol. 213, San Diego, Calif., June 23–27, 1991.†

12. W. E. Pennell, "Heavy-Section Steel Technology Program: Fracture Issues," pp. 15–24 in *Proceedings of the ASME Pressure Vessel and Piping Conference*, PVP Vol. 213, San Diego, Calif., June 23–27, 1991.†

13. B. R. Bass et al., "Assessment of Ductile Fracture Methodology Based on Applications to Large Experiments," *Proceedings of 11th Conference on Structural Mechanics in Reactor Technology, Tokyo, Japan, August 18–22, 1991*, August

14. B. R. Bass, J. S. Parrott, and J. C. Thesken, "Applications of a 2-D Moving Finite Element Formulation to Elastic/Viscoplastic Dynamic Fracture Analysis," *Proceedings of 11th Conference on Structural Mechanics in Reactor Technology, Tokyo, Japan, August 18–22, 1991*, August 1991.†

15. T. L. Dickson and P. D. Cheverton, "Fracture Mechanics Assessment of PWR Vessel Integrity Incorporating Dynamic Crack Arrest Data Above 220 MPa," *Proceedings of 11th Conference on Structural Mechanics in Reactor Technology, Tokyo, Japan, August 18–22, 1991*, August 1991.†

16. J. Keeney-Walker, B. R. Bass, and W. E. Pennell, "Evaluation of the Effects of Irradiated Cladding on the Behavior of Shallow Flaws Subjected to Pressurized-Thermal-Shock Loading," in *Proceedings of 11th Conference on Structural Mechanics in Reactor Technology*, Tokyo, Japan, August 18–22, 1991, August 1991.†

17. D. J. Alexander, "Data Shifting and Curve Fitting for J-R Curves," presented to the Task Group on $J_{Ic}$ Test Method of E24.08, Indianapolis, Ind., May 6, 1991.

18. T. J. Theiss, "Influence of Crack Depth on the Fracture Toughness of Reactor Pressure Vessel Steel," presented at ASTM Symposium on Constraint Effects in Fracture, Indianapolis, Ind., May 8, 1991.

19. R. K. Nanstad, "Comparison of $K_{Ic}$ Curves and HSSI Program Data," presented to the Working Group on Flaw Evaluation of Section XI, Orlando, Fla., May 21, 1991.

20. J. G. Merkle, "Discussion of Methods for Calculating Tensile Instability in the Remaining Ligament," presented at ASME Section XI Working Group on Flaw Evaluation, Orlando, Fla., May 21, 1991.

21. D. E. McCabe et al., "Investigation of the Bases for Use of the $K_{Ic}$ Curve," presented at the 23rd ASTM National Symposium on Fracture Mechanics, College Station, Tex., June 18–20, 1991.†

22. J. G. Merkle, "Near Crack Tip Transverse Strain Effects Estimated with a Large Strain Hollow Cylinder Analogy," presented at the 23rd ASTM National Symposium on Fracture Mechanics, College Station, Tex., June 18–20, 1991.†

23. D. K. M. Shum and J. G. Merkle, "Crack Initiation Under Generalized Plane Strain Conditions," presented at the 23rd ASTM National Symposium on Fracture Mechanics, College Station, Tex., June 18–20, 1991.†

24. W. E. Pennell, "Review of the Heavy-Section Steel Technology (HSST) and Heavy-Section Steel Irradiation (HSSI) Programs," presented to the USNRC Office of Reactor Regulation, Oak Ridge, Tenn., May 16, 1991.

25. B. R. Bass and J. Keeney-Walker, "Comparison of Analysis Methodologies for Predicting Cleavage Arrest in a Deep Crack in a Reactor Pressure Vessel Subjected to Pressurized-Thermal-Shock Loading Conditions," presented at an NRC-sponsored Meeting on Dynamic Fracture Analysis, San Diego, Calif., June 27–28, 1991.

26. W. E. Pennell, "PTS — Current Issues and Research," presented at a meeting with USNRC Commissioner Kenneth C. Rogers, Oak Ridge National Laboratory, August 20, 1991.

27. W. E. Pennell, "Nuclear Plant Life Extension—The Role of ORNL Fracture Technology Research," presented at Oak Ridge National Laboratory, September 11, 1991.

28. J. D. Landes and D. E. McCabe, "Effect of Section Size on Transition Temperature Behavior of Structural Steels," *Fracture Mechanics: Fifteenth Symposium, ASTM STP 833*, 1984, pp 378–39.†

29. V. Weiss, Syracuse University, "Material Ductility and Fracture Toughness of Metals," *Proceedings of the International Conference on Mechanical Behavior of Materials, Kyoto, Japan, August 15–20, 1971*, The Society of Materials Science, 1972.†

---

*Available for purchase from National Technical Information Service, Springfield, VA 22161.

†Available in public technical libraries.

# 2 Fracture Methodology and Analysis

B. R. Bass*

## 2.1 Introduction

The following sections describe recent advances made in the coordinated effort being conducted under the HSST Program by ORNL and several subcontracting groups to [illegible] the experimental data base and the analytical tools [illegible] construct improved fracture models for RPV [illegible]

During this report period, work continued on an investigation of the relationship between positive straining parallel to the crack front and crack-initiation toughness, an analysis of the near-crack-tip region using modified-boundary-layer models, an analysis of a proposed large-scale biaxial test specimen, analytical studies of dynamic crack arrest in RPVs subjected to PTS loading, and the Joint Japanese/United States Elastic-Plastic Inhomogeneous (U.S. EPI) Program for the development of an engineering estimation scheme applicable to inhomogeneous materials and structures.

## 2.2 Applicability of Plane-Strain Fracture Toughness Toward the Evaluation of Circumferential Surface Cracks

The objective of this subtask is the development of analysis methods for estimating the decrease in crack-initiation toughness, from a reference plane-strain value, as a result of positive straining along the crack front of a circumferential flaw in an RPV. This objective is accomplished by examining the influence of a given magnitude of the transverse strain on the near crack-tip fields. The results from the stress and strain analyses (discussed in Sect. 2.1) are viewed in the context of various fracture prediction models, thereby providing a methodology for estimating the influence of positive transverse strain on fracture toughness.

### 2.2.1 Fracture Analysis of a Compact-Tension Specimen Subjected to Generalized Plane-Strain Loading (B. R. Bass* and J. Keeney-Walker*)

The effects of negative and positive out-of-plane strain on local crack-tip fields in a model of a IT-CT specimen are described in this section. Results presented here are an extension of studies previously performed on the same specimen and reported in Ref. 1 and Chap. 7 of Ref. 2. Analyses were carried out on a three-dimensional (3-D) finite-element model of a compact-tension (CT) specimen that assumed an incremental elastic-plastic constitutive formulation and generalized-plane strain (GPS) loading conditions. A parameter based on the area, $A_{CR}$, enclosed within a contour of critical maximum principal stress[3] ahead of the crack tip was used to correlate these local crack-tip fields with applied loading at initiation. Results of these correlations are presented for a range of imposed out-of-plane strain values and postulated critical maximum principal stresses.

The methodology employed here is based on a correlation procedure constructed by Anderson and Dodds[4] to remove the geometry dependence of cleavage fracture-toughness values for single-edge-notched bend (SENB) specimens of A36 steel for a range of crack depths. This procedure utilizes a local stress-based criterion for cleavage fracture and a detailed plane-strain, finite-element analysis. Dimensional analysis for small-scale yielding (taken from Ref. 4) implies that the principal stress ahead of the crack tip can be written as

$$\frac{\sigma_1}{\sigma_1} = f\left(\frac{J^2}{\sigma_0^2 A}\right), \qquad (2.1)$$

where $\sigma_0$ is the 0.2% offset yield strength, $\sigma_1$ is the maximum principal stress at a point, and A is the area enclosed by the contour on which $\sigma_1$ is a constant. The strategy employed in Ref. 4 utilizes a fracture criterion dependent upon achieving a critical volume $V_{CR}$ within which the principal stress is greater than $\sigma_1$. For a specimen subjected

*Computing and Telecommunications Division, Martin Marietta Energy Systems, Inc., Oak Ridge, Tenn.

*Computing a[illegible] Telecommunications Division, Martin Marietta Energy Systems, Inc., [illegible]ak Ridge, Tenn.

to plane-strain conditions, the volume is equal to the specimen thickness B times the area within the $\sigma_1$ contour on the midplane (V = BA). For a given J-value applied to the specimen, it would be expected that the area A within the $\sigma_1$ would increase with increasing out-of-plane strain values. Equation (2.1) is the appropriate normalization for small-scale yielding solutions when using the latter fracture criterion based on volume or area.

The 3-D model of the IT-CT specimen (described in Ref. 1) was analyzed using the ADINA finite-element program[5] and the material properties for A 533 B steel at –75°C taken from Ref. 6. An incremental elastic-plastic constitutive model was used for these analyses. For all cases, Young's modulus was taken as E = 205.9 GPa and Poisson's ratio as $\nu = 0.3$. The multilinear true-stress strain curves for the material are given in Ref. 5. A material-nonlinear-only (MNLO) formulation (small-strain theory) was used to model the strain response to deformation. A $2 \times 2 \times 2$ Gauss point rule was employed to compute the global stiffness matrix. Incremental loading was applied to the load pin hole of the model in the form of a cosine function with a resultant maximum load of 35 kN. In tests of IT-CT specimens at T = –75°C (described in Ref. 6) cleavage initiation was achieved at loads of 29 and 35 kN.

The 3-D model of the IT-CT specimen was analyzed for the load cases given in Table 2.1. In Table 2.1, the normalized out-of-plane strain for case 1 ($\varepsilon_z / \varepsilon_0 = -1.05$) was selected to yield a computed $J_I$ value equal to the experimentally determined $J_I$ value of 0.0263 MJ/m$^2$ reported in Ref. 5 for the initiation load of 35 kN. (The normalizing strain $\varepsilon_0$ is given by $\varepsilon_0 = \sigma_0/E$, where $\sigma_0 = 480$ MPa is the yield stress).

The relationship between the area $A_{CR}$ enclosed within the critical maximum principal stress contour defined by $\sigma_{pl} = \sigma_{CRIT}$ and the applied $J_I$ as a function of out-of-plane strain for the GPS model of the IT-CT specimen is shown in Figs. 2.1 to 2.3 for $\sigma_{CRIT}$ = 1375, 1400, and 1425 MPa, respectively. The J vs $A_{CR}$ correlations depicted in Figs. 2.1 to 2.3 exhibit a decreasing sensitivity to the magnitude of out-of-plane strain as the critical principal stress is increased from $\sigma_{pl}$ = 1375 to 1425 MPa. These results may provide an estimate of the elevation or reduction of critical load (or J) required for achieving a critical area for cleavage initiation $A_{CR}$ as a function of the out-of-plane strain. In particular, a critical value of $J_I$ measured at crack initiation under plane-strain conditions can be used to estimate the critical $J_I$ value required for initiation under generalized plane-strain (GPS) conditions ($\varepsilon_z/\varepsilon_0 \neq 0.0$), as shown in Figs. 2.1 and 2.2. If the estimate of Hahn et al.[7] for the cleavage microcrack propagation stress for individual grains of ferrite ($\sigma_{pl} \approx 1380$ MPa) is employed as the critical value, J vs $A_{CR}$ correlations imply a reduction of <9% (relative to plane-strain conditions) in applied $K_I$ values required to achieve a critical area $A_{CR}$ for cleavage initiation in the case of positive out-of-plane strain satisfying $\varepsilon_z/\varepsilon_0 = 0.5$ (Fig. 2.1). With increasing values of positive out-of-plane strain satisfying $\varepsilon_z/\varepsilon_0 > 0.5$, the J vs $A_{CR}$ relation no longer follows the monotonic trend of Fig. 2.1 as a function of the parameter $\varepsilon_z/\varepsilon_0$. This is illustrated in Fig. 2.2, where results for the case $\varepsilon_z/\varepsilon_0 = 0.7$ are given for critical maximum principal stress values of

**Table 2.1 Out-of-plane strain conditions imposed on GPS model of IT-CT specimen**

| Load case | Normalized out-of-plane strain[a] ($\varepsilon_z/\varepsilon_0$) | J at maximum load (kJ/m$^2$) | CTOD ($\delta_t$) at maximum load (mm) | $d = \delta_t/J/\sigma_0$ at maximum load (mm) |
|---|---|---|---|---|
| 1 | –1.05 | 26.412 | 0.02732 | 0.4964 |
| 2 | –0.5 | 22.703 | 0.02512 | 0.5311 |
| 3 | 0.0 (plane strain) | 22.594 | 0.02503 | 0.5317 |
| 4 | +0.5 | 22.679 | 0.02486 | 0.5262 |
| 5 | +0.7 | 24.170 | | |

[a]Maximum/minimum imposed uniform strains; maximum load of 35 kN applied at load pin hole; $\varepsilon_0 = \sigma_0/E$; $\sigma_0 = 480$ MPa.

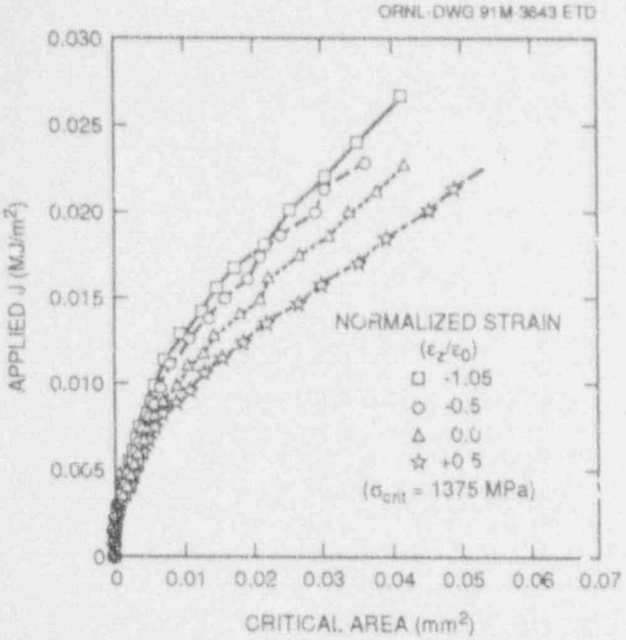


**Figure 2.1 Applied J vs area A within maximum principal stress contour of $\sigma_{pl}$ = 1375 MPa for IT-CT specimen subjected to four cases of out-of-plane strain**

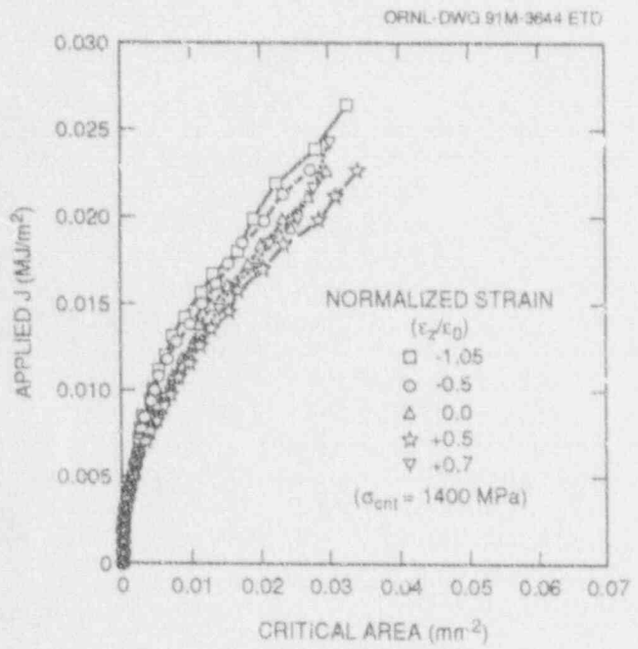


**Figure 2.2 Applied J vs area A within maximum principal stress contour of $\sigma_{pl}$ = 1400 MI a for IT-CT specimen subjected to five cases of out-of-plane strain**

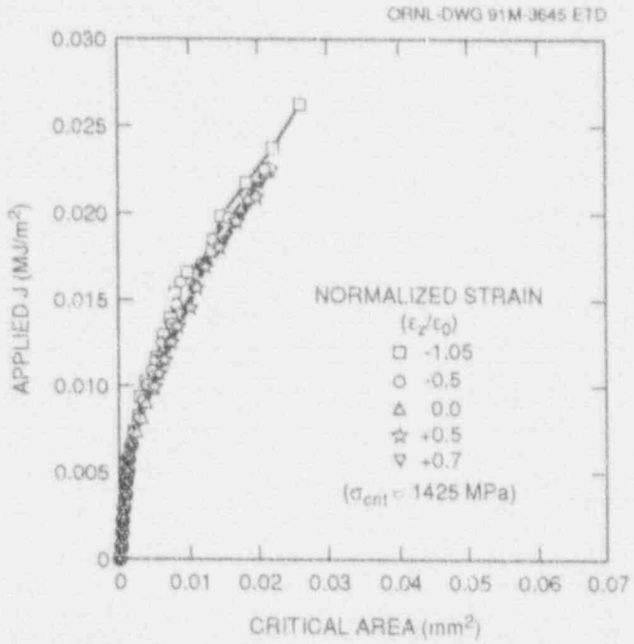


**Figure 2.3 Applied J vs area A within maximum principal stress contour of $\sigma_{pl}$ = 1425 MPa for IT-CT specimen subjected to four cases of out-of-plane strain**

$\sigma_{pl}$ = 1400 MPa. This onset of nonmonotonic behavior in the J vs $A_{CR}$ relations coincides with the development of a plastic zone at the back face of the CT specimen, as depicted in Fig. 2.4. These results imply that a correlation is not viable for the CT specimen model under conditions corresponding approximately to $\varepsilon_z/\varepsilon_0 > 0.5$.

The J vs $A_{CR}$ correlations shown in Figs. 2.1 to 2.3 illustrate that further development of the methodology depends on establishing the existence of critical $\sigma_1$ values that correlate fracture-toughness behavior over a range of transverse strain values. To accomplish this objective, studies were initiated to apply the methodology to existing fracture-toughness data to validate and calibrate the model in the plane stress-to-plane strain domain. Analyses of three-dimensional (3-D) finite-element models of compact specimens (from Ref. 8) having a common plan form of a 4T specimen and thickness varying from 0.4 to 4.0 in. are anticipated to provide critical $\sigma_1$ values for correlating toughness in the $\varepsilon_z/\varepsilon_0 < 0.0$ strain domain. These critical $\sigma_1$ values will then be used to estimate toughness correlations in the positive out-of-plane strain domain. Results from these calibration analyses will be reported in the

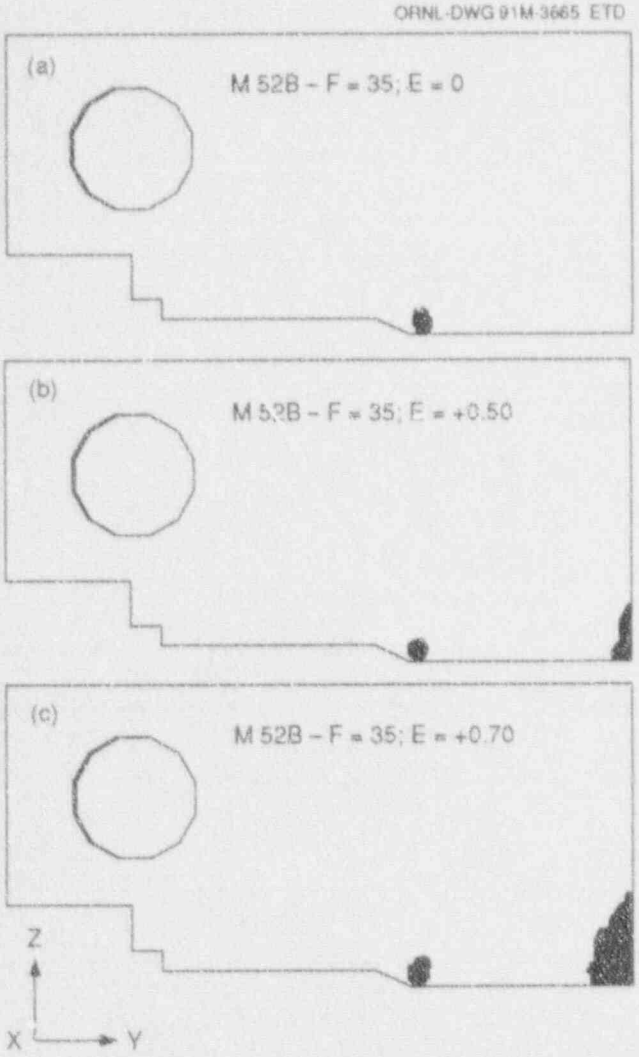


**Figure 2.4 Region of plasticity in GPS model of IT-CT specimen corresponding to maximum pin load of 35 kN and three values of out-of-plane strain. (*a*) $\varepsilon_z/\varepsilon_0 = 0.0$, (*b*) $\varepsilon_z/\varepsilon_0 = 0.5$, (*c*) $\varepsilon_z/\varepsilon_0 = 0.7$**

upcoming milestone report on circumferential flaw studies that will be completed in FY 1992. Ultimately, validation of the methodology in the positive strain domain must depend on application to measured data from the planned biaxial testing program.

### 2.2.2 Modified-Boundary Model of Near-Crack-Tip Region (D. K. M. Shum)

The primary focus of this subtask is on the development of a finite-element-based description of the near-crack-tip region that will provide a more detailed and realistic description of the near-crack-tip fields than was available in FY 1990. Results from these near-tip analyses will provide improved inputs to the various fracture-toughness prediction models developed in the first phase of this work, thereby providing the framework for evaluating and modifying the various fracture models.

A modified-boundary-layer formulation has been adopted in the finite-element description of the near-crack-tip region. In a modified-boundary-layer formulation, the in-plane geometry and loading conditions pertinent to a circumferential flaw are naturally incorporated into the analysis as remote boundary conditions, such as the imposition of remote K- or J-fields. Such an approach permits the evaluation of near-crack-tip stress and strain fields with a degree of accuracy not economically achievable with conventional application of the finite-element method to fracture problems. The modified-boundary-layer approach is used to evaluate the merits and implications of various fracture-toughness prediction models within the transverse strain context.

In addition to its relevance to the transverse straining issue, it is emphasized that the finite-element-based, near-tip model development from this subtask, in the form of a modified-boundary-layer model, is also expected to address various issues related to the transferability of small- and large-specimen toughness data to RPV applications. Specifically, these issues include the problem of estimating the elevation of toughness that occurs because of transverse contraction in a small surveillance specimen tested in the transition region, providing an explanation for the apparent toughness enhancement obtained in the ORNL wide-plate tests,* and the interpretation of shallow-flaw toughness values obtained within the HSST Program. The unifying feature in all these issues appears to be the role of the second parameter and the degree of transverse strain on the associated fracture problem. A brief description of the essential features of such an approach was given in a previous semiannual report.

*As an alternate explanation, G. R. Irwin, from the University of Maryland, has proposed that the elevation in crack-initiation toughness for the ORNL wide-plate tests[6] is due to crack-tip blunting that occurred during specimen fabrication. Maximum cleavage-initiation values of $K_J/K_{Ic} = 4$ were computed for the WP-1 series of tests.

Detailed small-strain and finite-strain solutions for the near-crack-tip stress and strain distributions for a number of material models, including a material similar to unirradiated A 533 grade B steel at 120°C, have been obtained using the finite-element program ABAQUS for various combinations of in-plane and transverse loading conditions. Specifically, the loading conditions examined are those for which the in-plane loading is characterized by the stress-intensity factor K (only), and the magnitude of the transverse strain ranges from $-1 < \varepsilon_z/\varepsilon_0 < 1$, where $\varepsilon_z$ is the magnitude of the transverse strain and $\varepsilon_0$ is the uniaxial yield strain in tension. Within the range of transverse strains considered is the case of plane strain where $\varepsilon_z/\varepsilon_0 = 0$. The plane-strain solutions serve as the reference solutions upon which the effects of transverse strain on toughness can be examined. Preliminary analysis of the finite-element results indicate the "crack-opening" stress distribution within the finite-strain region, within which the cleavage fracture response of a material is determined, agrees qualitatively with previous predictions based on a GPS slip-line description of the finite-strain region.

The effects of transverse strain on the near-crack-tip stress distribution, when the in-plane loading is characterized by K only, appear qualitatively similar to the effects of the in-plane T- and Q-stress on the near-crack-tip stress distribution of the associated plane-strain problem where K again serves as the in-plane loading parameter. It has been proposed that T- and/or Q-stress, in conjunction with K or J, could form the basis for a theoretically rigorous extension of conventional one-parameter fracture mechanics concept. To examine the relation between transverse strain and T- and Q-stress, detailed finite-element solutions for the near-crack-tip stress and strain distributions under various K-T and K-T-$\varepsilon_z/\varepsilon_0$ combinations have been generated. Interpretation of the detailed near-crack-tip solutions using various fracture-toughness models is continuing. Note that the effect of a given magnitude of the transverse strain or the T-stress on the near-tip fields is nonsymmetric. Specifically, a given positive magnitude of the transverse strain or the T-stress does not influence the near-tip fields from the reference plane-strain, small-scale-yielding solutions nearly as much as a given negative magnitude of these quantities. Interpretation of this asymmetry in terms of fracture prediction are included in the milestone report on circumferential flaw studies to be issued in FY 1992.

### 2.2.3 Analysis in Support of the Proposed ORNL Biaxial Test (D. K. M. Shum)

Finite-element analyses have been performed in support of the proposed ORNL biaxial test specimen using the commercial code ABAQUS. A material model that simulates the effects of irradiation on the tensile properties of RPV-grade materials was adopted. A detailed model of the central section of the proposed biaxial test specimen, corresponding to the location of maximum crack depth, has been constructed for the purpose of evaluating the near-crack-tip fields of this specimen under uniaxial and biaxial loading conditions. This detailed (full-field) model resolves the stresses and strains within the neighborhood of a few crack-tip-opening displacements (CTODs) ahead of the crack front while accurately incorporating the overall geometry of the proposed specimen. A 2-D, modified-boundary-layer, finite-element model of the crack-tip region of the biaxial specimen has also been developed to provide interpretation of the full-field and modified-boundary-layer models under plane-strain and GPS conditions. Analysis results are being incorporated in a report on circumferential flaw studies.

### 2.2.4 Constraint Effects for Circumferential Flaws (C. W. Schwartz*)

#### 2.2.4.1 Introduction

During this reporting period, work focused on further interpretation of our previously reported[9] analysis results for circumferential flaws and of the quantitative implications of these results for the elevation of fracture toughness for reactor-grade steels.

To review, the purpose of the previously reported analyses was to compare constraint in the circumferential flaw configuration with that in a corresponding reference plane-strain condition. The flaw geometry considered in these analyses is the limiting case of a continuous inner circumferential flaw in a cylindrical pressure vessel. Three different loading conditions were analyzed: (1) a reference plane-strain condition under axial loading only, (2) axisymmetric conditions under axial loading only; and (3) axisymmetric conditions under combined internal pressure, crack-face pressure, and axial loading. Details of the geometry, loading conditions, material properties, and other analysis

*University of Maryland, College Park, Maryland.

assumptions are given in Ref. 9. The principal finding from these analyses was that the crack-tip constraint, as quantified using the Q-stress approach proposed by O'Dowd and Shih,[10] was lowest for the axisymmetric/combined loading configuration, with progressively increasing constraint in the axisymmetric/axial loading and reference plane-strain configurations. The reduction in constraint in the axisymmetric/combined loading configuration was attributed to in-plane stress biaxiality caused by the radial compressive stresses in the combined loading case. For these pure mechanical loading conditions, the in-plane influence appears to dominate any out-of-plane influence caused by the tensile hoop strain parallel to the crack front. This dominance will diminish under PTS loading scenarios, however, when the crack plane stresses are generated primarily by thermal rather than mechanical loadings.

However, some problems and/or apparent inconsistencies were observed in these analysis results. Specifically, the trends in yield zone extent at the crack tip that should mirror the trends in crack-tip constraint were difficult to determine because of details of the finite-element mesh design. In addition and more important, the trends observed in the hydrostatic constraint factor $h = \sigma_m/\sigma_{eff}$ contradicted the trends indicated by the Q-stress approach; in terms of h, the axisymmetric/combined loading case exhibited the highest constraint, with progressively decreasing constraint in the plane-strain and axisymmetric/axial loading configurations. These results have been re-examined to address these points.

#### 2.2.4.2 Yield Zone Extent

The original analysis employed a conventional focused-element mesh design in the crack-tip region. The primary criterion in selecting a mesh design is that the element dimensions be sufficiently small to capture the stress/strain singularity at the crack tip. Although the discretization in the crack-tip region was very fine, with an element radial dimension at the crack tip of ~0.02 mm (r/a = 0.0000371), the elements increased in size with distance from the tip. For computing yield zone areas, the elements are thus the largest—and thus the resolution of the solution is the smallest—at the locations where the yield zones differ most among the three loading configurations, that is, the outer extremes of the yield zones.

To obtain a more precise calculation of yield zone extent, a new mesh was designed that replaced the focused element mesh at the crack tip with an assemblage of square elements. At the crack tip, the element side length equals 0.1 mm and increases somewhat through several transition zones with increasing distance from the crack tip.

Resolution of the crack-tip yield zone was excellent with the revised mesh, permitting precise calculations of the yield zone areas. The trends in yield zone area with applied load J are summarized in Fig. 2.5 for the axisymmetric/axial load and axisymmetric/combined load configurations. The range of J values in Fig. 2.5 corresponds to internal pressure values up to and slightly beyond the maximum allowable loading for a reactor vessel (~17.5 MPa or 2500 psi). Over this loading range, the two loading configurations exhibit virtually identical yield zones. Two explanations for this result are possible: (1) the differences in constraint between these two configurations are negligible, or (2) the effect of the constraint differences on the yield zone extent is insignificant. Although the implications for constraint as given by the Q-stress approach and by the hydrostatic constraint factor are somewhat contradictory, both measures predict constraint variations among the three loading configurations; thus it appears that the second explanation given previously is more plausible. Because yield zone area is an integrated or more "global" measure of constraint, it is conceivable that differences in the details of the crack-tip fields—particularly in the regions away from the tip but still within the yield zone—may produce similar aggregate levels of yielding while still producing different near-tip [i.e., with $r/(J/\sigma_0) \sim 10$] stress fields and associated constraint levels.

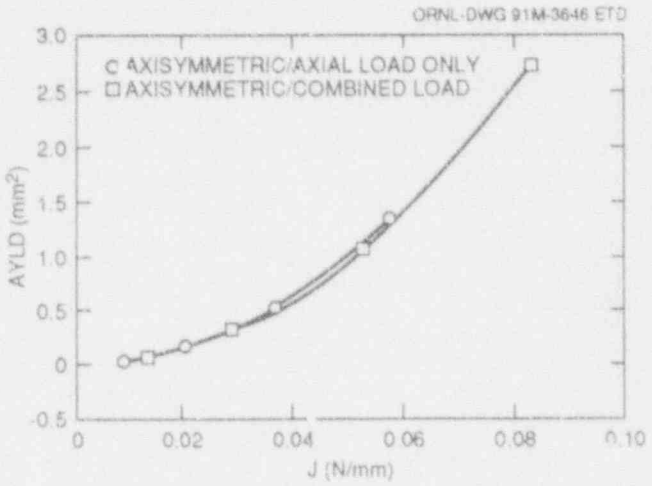


**Figure 2.5 Yield zone area as function of load level. Maximum load level corresponds to maximum allowable internal pressure loading for vessel**

### 2.2.4.3 Hydrostatic Coustraint Factor

Previous examinations[9] of the variation of the hydrostatic constraint factor h along the crack plane ($\theta = 0$) with distance from the crack tip found that h is slightly lower in the axisymmetric/axial load configuration than in the plane-strain configuration at similar distances and that h decreases with increasing load for both of these configurations. For the axisymmetric/combined load configuration, however, h was significantly greater than in both of the other two cases. This trend contradicts that observed in the Q-stress approach.

A more comprehensive view of the trends in h at the crack tip is given in Figs. 2.6 to 2.8, which show the contours of h within the near-tip region for the plane-strain, axisymmetrical/axial load, and axisymmetric/combined load configurations, respectively. The plane-strain (Fig. 2.6) and axisymmetric/axial load (Fig. 2.7) configurations exhibit nearly identical trends for h in the near-tip region. Close examination of the results for the axisymmetric/combined load configuration (Fig. 2.8) suggests a close similarity with the results for the other two loading cases for locations very near the crack tip, that is, for $r/(J/\sigma_0)$ within ~2. Unfortunately, it is within this zone that the small-strain formulation used in these finite-element calculations is invalid. At greater distances from the crack tip, the h contours for the axisymmetric/combined loading configuration are markedly different from the other two loading cases; that is, they indicate significantly higher constraint that extends for greater distances from the tip. This is a product of the high out-of-plane hoop stress in the combined loading case.

The inconsistent indications for constraint suggested by the hydrostatic constraint factor and the Q-stress approach has

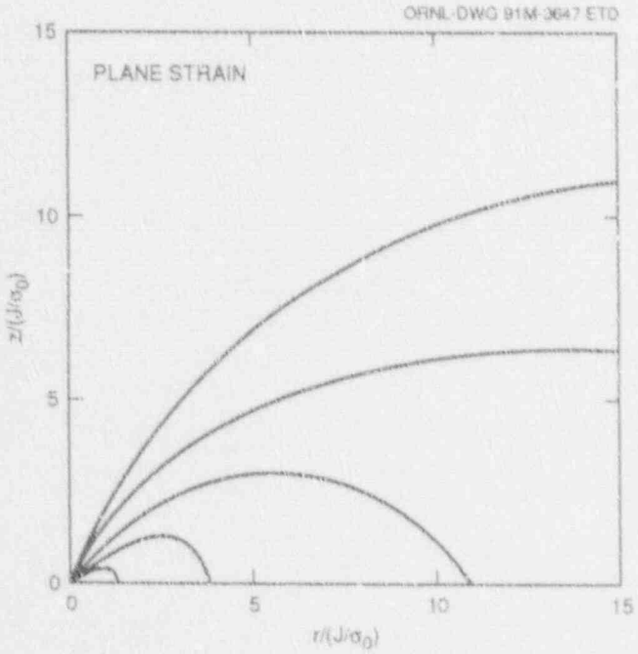


Figure 2.6 Contours of hydrostatic constraint factor, $\sigma_m/\sigma_{eff}$, in crack-tip region for plane-strain configuration under axial loading. Load level $p_a/\sigma_0 = 0.25$, $J/(a\sigma_0) = 1.13E\text{-}3$. Contours correspond to $\sigma_m/\sigma_{eff}$ equal to 1.5, 1.75, 2.0, 2.25, and 2.5 (outermost to innermost contours)

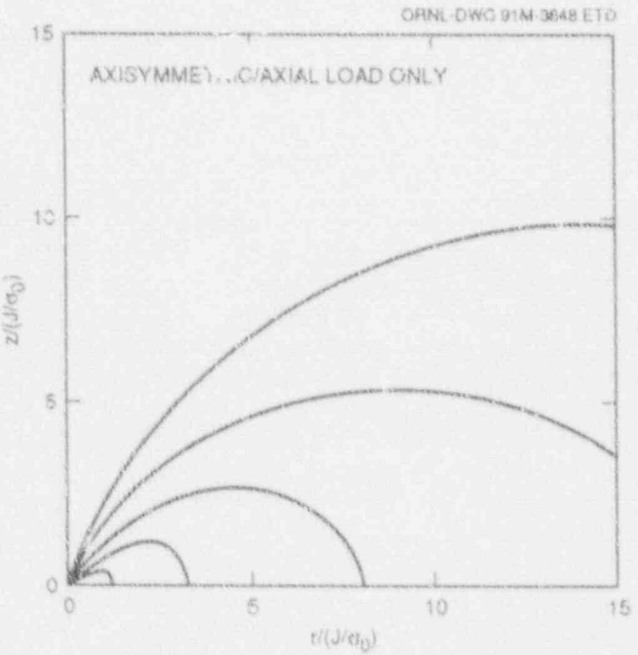


Figure 2.7 Contours of hydrostatic constraint factor, $\sigma_m/\sigma_{eff}$, in crack-tip region for axisymmetric configuration under axial loading. Load level $p_a/\sigma_0 = 0.25$, $J/(a\sigma_0) = 107E\text{-}3$. Contours correspond to $\sigma_m/\sigma_{eff}$ equal to 1.5, 1.75, 2.0, 2.25, and 2.5 (outermost to innermost contours)

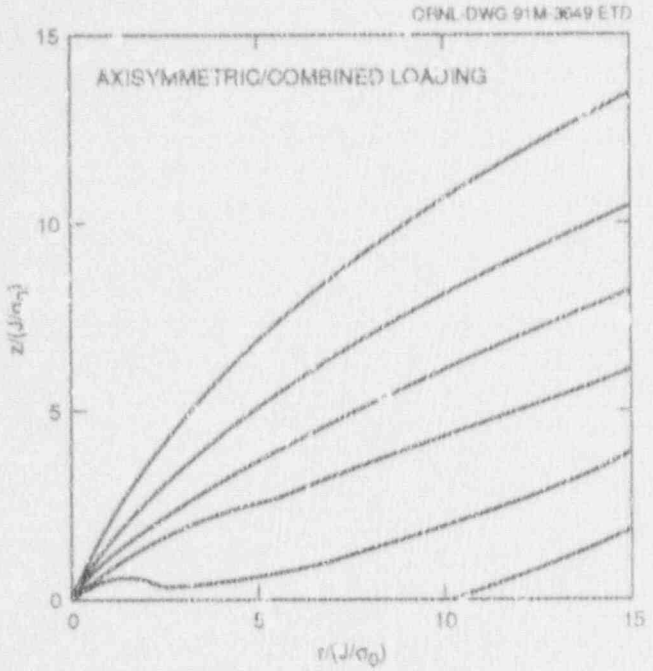


**Figure 2.8 Contours of hydrostatic constraint factor, $\sigma_m/\sigma_{eff}$, in crack-tip region for axisymmetric configuration under combined loading. Load level $p_s/\sigma_0 = 0.25$, $J/(a\sigma_0) = 1.54E\text{-}3$. Contours correspond to $\sigma_m/\sigma_{eff}$ equal to 1.5, 1.75, 2.0, 2.25, 2.5, and 2.73 (outermost to innermost contours)**

important implications for fracture in the transition region. The hydrostatic constraint factor is most relevant for ductile void-growth fracture mechanisms that are governed largely by stress triaxiality, while the Q-stress approach is most relevant for cleavage fracture mechanisms governed largely by maximum principal stress. In the transition region, both mechanisms are active. Additional analyses of the very near-tip fracture process zone [within $r/(J/\sigma_0) = 2$], using a large strain formulation, may provide some additional insight into the relationships between these two constraint measures. However, the question of which mechanism dominates, ductile void growth or cleavage, and thus which constraint measure (or combination of measures) is most relevant will require comparisons of analytical results with measured toughness values from experiments conducted over a range of constraint conditions.

### 2.2.4.4 Quantitative Effects of Constraint for A 533 B Steel

Application of the Q-stress approach to the analysis results for the circumferential flaw configurations under pure mechanical loading indicates that the Q value for the axisymmetric/combined loading condition may range down to –0.25 or –0.3 for J values corresponding to maximum allowable internal pressures in an actual reactor vessel. The next logical question is "What is the magnitude of the expected apparent toughness corresponding to this constraint loss?" A preliminary answer can be obtained by considering the experimental data obtained by Theiss and Bryson[11] on shallow-flaw SENB specimens of A 533 B steel.

Figure 2.9 shows the comparison between the $K_c$ values measured by Theiss and Bryson[11] and the computed Q. All data are for A 533 B steel at –60°C. The Q values were interpolated from the results of Al-Ani and Hancock[12] obtained from a 2-D analysis of the SENB configuration for a power-law constitutive model with a hardening exponent n equal to 13. The experimental data for a/W equal to 0.1 and 0.5 have each been averaged; in Fig. 2.9, these data are represented by boxes, with the center of the box representing the average and the extent of the box indicating the data range. For a/W = 0.15, only one data point is available and is indicated by an open circle on the figure. Upper and lower bounds for the $K_c$ vs Q trend are also delimited on the figure.

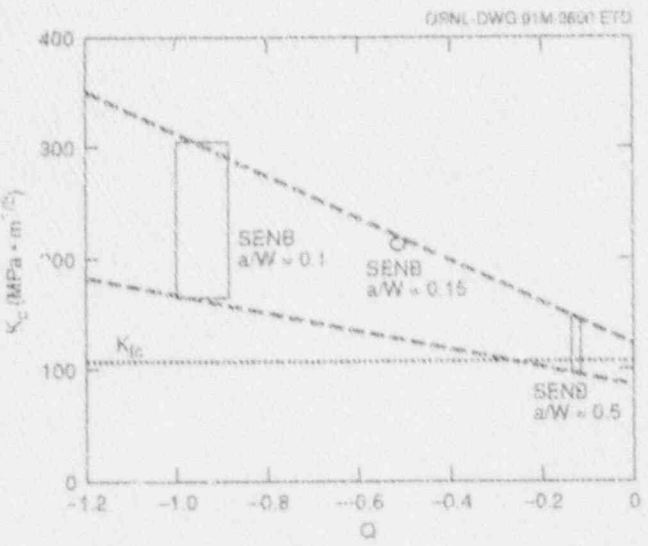


**Figure 2.9 $K_c$ as function of constraint measure Q as inferred from experimental data by Theiss and Bryson[11] for SENB specimens of A 533 B steel**

The cleavage fracture-toughness $K_{Ic}$ should correspond to the case of Q equal to zero, that is, the case of pure HRR-dominated fracture. This fracture toughness is illustrated by the dashed horizontal line in Fig. 2.9. For Q values from ~0.25 to ~0.3 corresponding to the circumferential flaw analysis results at the maximum allowable combined mechanical loading condition, Fig. 2.9 suggests that the apparent fracture toughness may be elevated by perhaps an average of 25 to 30%.

These admittedly limited analyses suggest that mechanically loaded circumferential flaws under cleavage-dominated conditions may exhibit usable increases in apparent fracture toughness. Certainly, more refined analyses of these and other experimental data are required to establish confidence in these types of quantitative predictions. Additional geometric, material property, and loading conditions must also be considered. Most importantly, the effect on constraint of the large thermal loading associated with PTS scenarios must still be investigated. The relative magnitudes of the thermal and mechanical loading components in the PTS loading will likely produce more severe constraint conditions at the crack tip.

## 2.3 Dynamic Fracture Analysis of Pressure Vessels

(J. Keeney-Walker,* B. R. Bass,* and W. E. Pennell)

### 2.3.1 Introduction

Analysis of PTS events in RPVs requires an understanding of conditions that govern initiation, rapid propagation, arrest, and ductile tearing of cracks. In PTS scenarios, inner-surface cracks in an RPV have the greatest propensity to propagate because they are located in the region of highest thermal stress, lowest temperature, and greatest irradiation damage. If such a crack begins to propagate radially through the vessel wall, it will extend into a region of higher fracture toughness due to the higher temperatures and less irradiation damage. Because crack initiation is a credible event in a PTS transient, assessment of vessel integrity requires the ability to predict all phases of a fracture event. This study examined several of the issues related to developing and evaluating fracture-mechanics methodologies that can be used for performing these assessments. Specifically, procedures for predicting cleavage arrest and reinitiation of a deep crack in the wall of an RPV were considered, including circumstances under which certain quasi-static methods can be used to approximate results from dynamic formulations. Levels of conservatism associated with applications of these methodologies to code-based analysis of RPVs were also considered.

Based on results from the Integrated Pressurized-Thermal-Shock (IPTS) Program[13–15] and other studies, NRC established the PTS rule (10 CFR 50.61) to insure the integrity of RPVs under PTS transients. Plant-specific analyses must be performed for any plant intended to operate beyond the screening criteria defined in the PTS rule. A typical quasi-static methodology for performing probabilistic deterministic and probabilistic fracture mechanics analyses is embodied in the OCA-P computer program,[16] which is referenced in the IPTS study. The OCA-P program was developed at ORNL specifically for simulating the cleavage fracture response of an RPV subjected to a PTS event.

Several recent studies[17,18] have been critical of the methodology incorporated into OCA-P for predicting crack arrest [i.e., linear elastic fracture-mechanics (LEFM) principles and static equilibrium assumptions] may be overly conservative when used in conjunction with the *American Society of Mechanical Engineers Boiler and Pressure Vessel Code* (*ASME B&PV Code*), Sect. XI, crack-arrest data.[19] Specifically, results from dynamic calculations are used in Refs. 17 and 18 to argue that currently accepted *ASME Code* procedures are overly conservative in crack-arrest predictions for the case where an initially shallow crack arrests deep in the wall of a vessel. The argument is based on the observation that the time interval for crack propagation is considerably less than the fundamental period of the structural response. In particular, the bending response of the structure that provides additional loading of a deep-arrested crack in a condition of static equilibrium is small during the crack propagation event; bending does not develop until well after crack arrest has occurred. Consequently, analyses, such as those performed with OCA-P, that incorporate influence coefficients based on full bending of the structure predict larger crack extensions and a higher apparent material toughness required for crack arrest than would be predicted by a dynamic analysis.

Several of these issues were examined quantitatively through static and dynamic analyses of a hypothetical RPV subjected to a PTS transient. Analyses were performed with

*Computing and Telecommunications Division, Martin Marietta Energy Systems, Inc., Oak Ridge, Tenn.

the OCA-P code to identify shallow cracks that initiate in cleavage and arrest deep in the wall of the RPV. The OCA-P predictions were compared with both application-mode and generation-mode dynamic analysis results based on postulated dynamic fracture-toughness models. The propensity for cleavage reinitiation of the arrested cracks was investigated using both static and dynamic initiation toughness relations. A radially constrained static model,[20] developed to approximate certain dynamic conditions at the time of crack arrest, was applied to the same PTS transient, and the results were comparable with those from the dynamic analyses.

## 2.3.2 Fracture Analyses

The PTS event selected for analysis from the USNRC/IPTS studies is the H. B. Robinson transient 922.B[13] (modified for a constant value of the heat-transfer coefficient). The vessel has an inner radius of 1981.2 mm, a wall thickness of 236.5 mm, and a cladding thickness of 5.6 mm. Based on an OCA-P analysis, a flaw having a depth of $a_0$ = 0.0239 m (a/W = 0.101) is predicted to initiate in cleavage at time t = 36 min and to arrest at a depth of $a_f$ = 0.1189 m (a/W = 0.503).

### 2.3.2.1 Finite-Element Model

In the static and dynamic thermoelastic analyses, a 2-D plane-strain, finite-element formulation was used to model the test vessel. The finite-element model employed in these analyses is depicted in Fig. 2.10 and consists of 1994 nodes and 613 eight-noded isoparametric elements. An MNLO formulation and a 2 × 2 numerical integration order was used in all the analyses. The values of the radial temperature distribution and internal pressure at the time of cleavage-crack propagation for this transient were used as the boundary conditions and assumed to be constant during the run-arrest event. The pressure at crack initiation was applied to the inner surface of the model using 2-D element pressure surfaces; crack-face pressure was not included. To provide the proper constraint for the thermal stresses, the material stress-free temperature was lowered so the average out-of-plane stress through the vessel approximated the average axial stress given by the relation (Pr/2t).

### 2.3.2.2 Finite-Element Analyses

Initially, quasi-static analyses were performed with ADINA/VPF[5,21] at the initial crack depth (a/W = 0.101) and at two other crack depths (a/W = 0.494 and a/W = 0.507) that were close to the arrest location determined by OCA-P. The computed $K_I$ values compare well with the OCA-P calculations (2% difference).

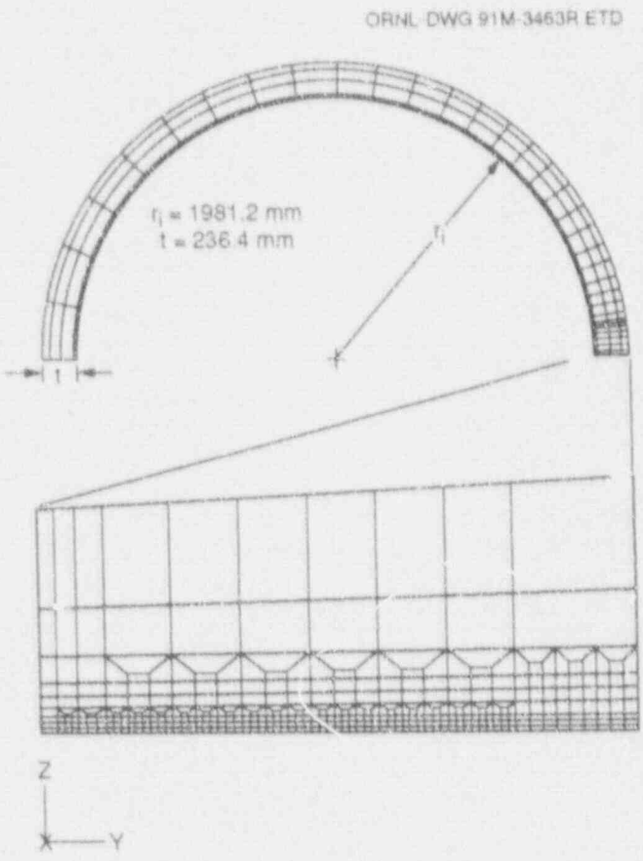


**Figure 2.10 Finite-element model of RPV**

Next, an application-mode dynamic analysis was performed using the ASME Sect. XI lower-bound toughness curves. In this case, the crack would arrest if $K_{ID}$ fell below $K_{Ia}$ or if the crack velocity drops below a threshold velocity of 2% of the shear wave velocity (~60 m/s). The crack would then reinitiate if the applied K increased above the $K_{Ic}$ value calculated for that particular temperature, $RT_{NDT}$, and crack depth. The crack arrested at an a/W = 0.358 and applied $K_I$ of 174 MPa•$\sqrt{m}$. After arrest, $K_I$ oscillates due to vessel bending and reaches a peak value of 262 MPa•$\sqrt{m}$ at 19.5 ms. This does not approach the value of $K_I$ needed for reinitiation from the $K_{Ic}$ curve.

In general, the fracture toughness of structural steels decreases with increasing loading rate. Thus, for any given

temperature, the fracture toughness measured in an impact test, $K_{Id}$, is generally lower than the fracture toughness measured in a static test, $K_{Ic}$. A procedure was developed for this study to determine the dynamic initiation toughness from measured data.[22] The application-mode dynamic analysis was repeated using the generated $K_{Id}$ curve to determine crack reinitiation. As shown in Fig. 2.11, the crack reinitiated at a $K_I$ value of 262 MPa•$\sqrt{m}$ and then arrested at a $K_I$ of 261 MPa•$\sqrt{m}$. After arrest, $K_I$ again oscillates with a peak value of 321 MPa•$\sqrt{m}$ at 37.6 ms, which is below the $K_{Id}$ curve.

To perform a generation-mode dynamic analysis, a crack position vs time relation must be constructed for the crack run-arrest event. In the application-mode analysis, the initial crack velocity and time of the first arrest are ~250 m/s and 0.466 ms, respectively. These were approximated in the analysis by an initial velocity of 350 m/s and an arrest time of 0.4 ms at an a/W of 0.507. To compare this with a faster-moving crack, an analysis was performed with a crack position vs time curve with an initial velocity of 800 m/s and an arrest time of 0.17 ms.

The results of these two analyses are depicted in Fig. 2.12, in which the calculated $K_I$ from OCA-P and the two generation-mode dynamic analyses are plotted vs a/W. The $K_I$ values at arrest, 142 and 189 MPa•$\sqrt{m}$ for the fast- and slow-moving cracks, respectively, are much lower than the static $K_I$ value of 311 MPa•$\sqrt{m}$. From Fig. 2.12 it is obvious that as the velocity of the crack increases and the time of arrest decreases, the value of $K_I$ at arrest decreases dynamic crack-arrest conditions using a methodology.

It was proposed in Ref. 18 that it might be possible to approximate the stress-intensity factor during crack extension by a static analysis that assumes the vessel is essentially stationary. A series of static thermoelastic analyses were performed at various crack lengths, with the vessel fixed radially on the outer edge at the radial displacement generated at the initial crack depth. The results of these analyses are depicted in Figs. 2.12 and 2.13. In Fig. 2.12, the calculated $K_I$ from OCA-P (static full-bending), generation-mode dynamic analyses (slow- and fast-moving cracks) and static analysis (radially constrained outer edge) is plotted as a function of a/W. The value of $K_I$ for the radially constrained static analysis at crack arrest (a/W = 0.507) is 124 MPa•$\sqrt{m}$, which is 13% lower than the dynamic analysis with the fast-moving crack.

It is apparent from these analyses that the calculated $K_I$ is greatly influenced by crack velocity. The difference between $K_I$ at arrest for the two different crack speeds is ~25%. Evidently, whether the constrained static analysis is a good approximation of a dynamic analysis depends on the crack position vs time relation chosen.

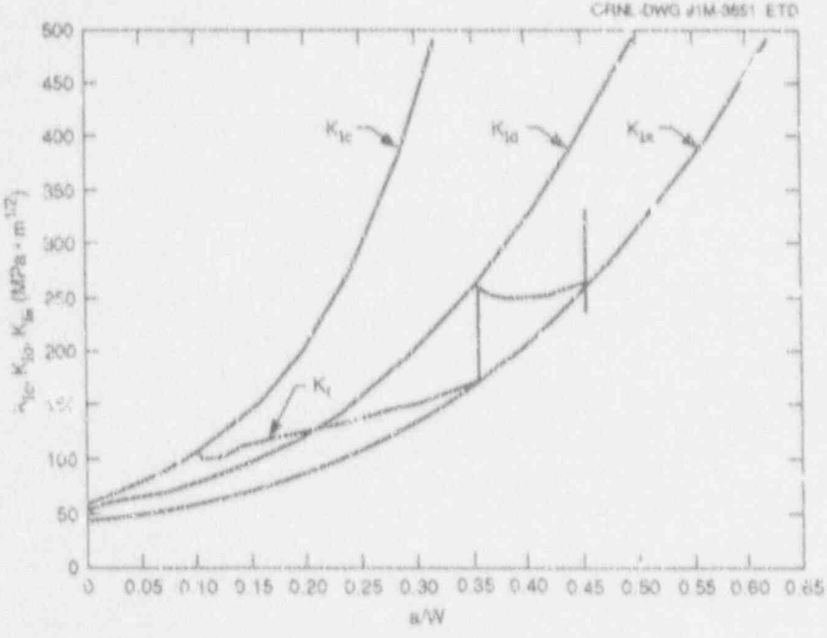


Figure 2.11 K vs a/W for application-mode dynamic analysis using initiation-toughness curve

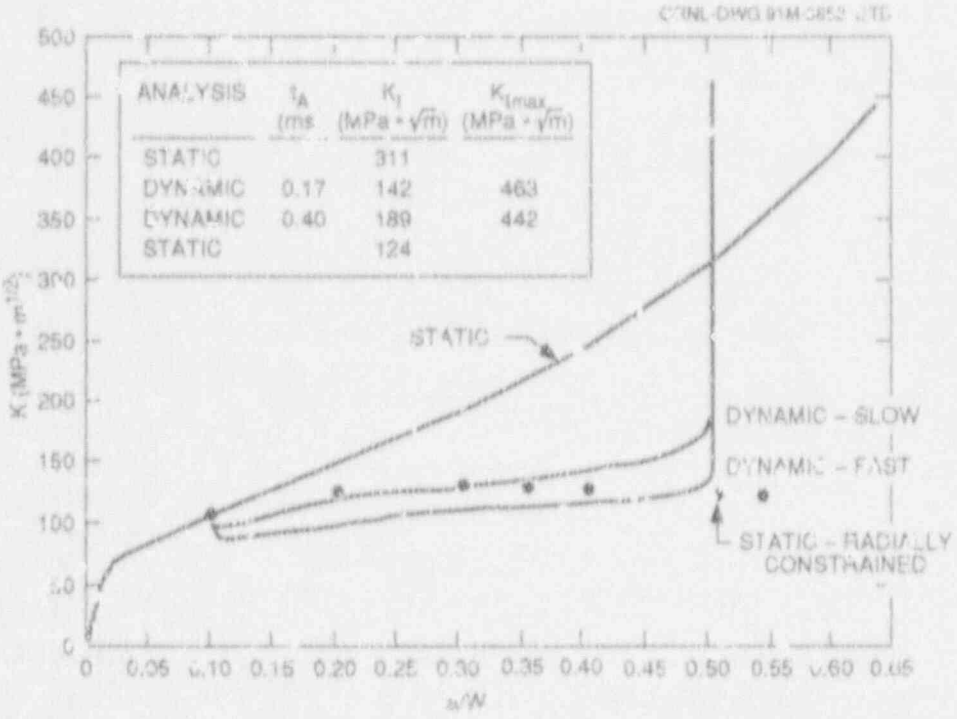


**Figure 2.13 Comparison of K vs a/W for static and generation-mode dynamic analyses**

A comparison of predicted crack-arrest depths for all the analyses is depicted in Fig. 2.13. The radially constrained static analysis underpredicted the first crack-arrest depth from the application-mode dynamic analysis by 17%, while the OCA-P static analysis overpredicted the second arrest value from the dynamic analysis by 9%.

The current analyses provide what is probably a lower-bound estimate of the influence of vessel dynamic response effects on crack arrest. The plane-strain analysis model of Fig. 2.10 incorporates the assumption of an infinite flaw length. Prior analyses [23,24] have shown that the stress-intensity factor at the deepest point on a semielliptical surface crack remains less than that for an infinite flaw even when the flaw surface dimension becomes very long. The stress-intensity factor time history for the period following the initial crack arrest will therefore be conservative for flaws of finite length. Incorporation of finite-length flaw stress-intensity factors into the analysis, together with a statistical rather than a lower-bound representation of $K_{Id}$, would preclude crack reinitiation in many cases. The initial crack arrest would then become the final arrest at that time in the PTS transient.

The analysis results of Fig. 2.13 show that without reinitiation, the crack depth-to-vessel wall thickness ratio (a/W) at arrest would be 0.36 rather than the value of 0.5 predicted by the OCA-P static equilibrium model. This difference could be very important in a probabilistic fracture-mechanics analysis because, beyond a critical depth, the arrested cleavage crack becomes unstable due to the onset of ductile tearing.

Another postarrest consideration is the effect of high-pressure transients, which have been determined to be the most probable from the IPTS studies. In these transients, $K_I$ can exceed $K_{Ic}$ for deeper crack depths, increasing the probability of crack reinitiation at a later time in the transient. Thus, even if an initial cleavage crack arrest takes place as a result of dynamic effect, a series of reinitiation/arrest events can lead to vessel failure.

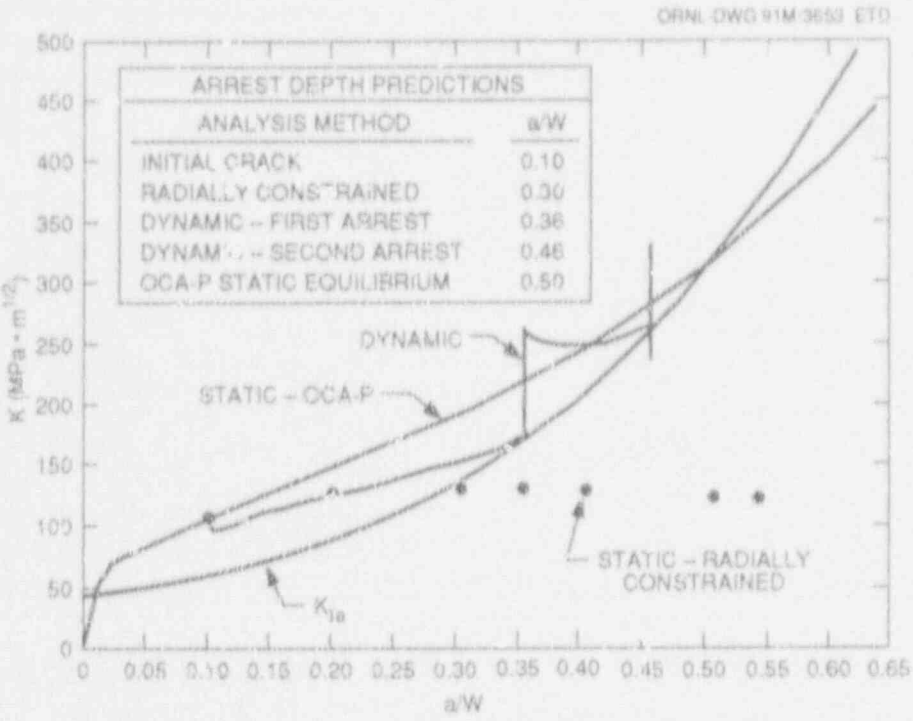


**Figure 2.13 Comparison of K vs a/W for static and application-mode dynamic analyses**

## 2.4 Elastic-Plastic Fracture Mechanics in Inhomogeneous Materials and Structures (B. R. Bass* and G. Yagawa†)

A meeting was held on August 20, 1991, in Tokyo, Japan, to review the planned workscope of the Joint Japanese/U.S. EPI Program for the current fiscal year (April 1, 1991 through March 31, 1992). The meeting was chaired by Professor G. Yagawa, University of Tokyo, who also serves as principal coordinator of the EPI Program.

The principal objective of the EPI Program is to investigate elastic-plastic crack-growth phenomena in inhomogeneous materials and structures, aiming at the development of estimation schemes of fracture resistance applicable to inhomogeneous structures. The Japanese consortium responsible for the EPI Program was organized in July 1988 as a subcommittee of the Nuclear Engineering Research Committee of the Japan Welding Engineering Society (JWES). The EPI subcommittee in Japan consists of 9 universities, 3 research institutes, and 21 companies.

The HSST Program, on behalf of NRC, is the sole United States participant in the EPI Program. The EPI Program is scheduled to be completed in August 1992.

Three working groups (WGs), Theoretical, Experimental, and Estimation Scheme, have been set up under the EPI subcommittee to carry out the objectives of the program. The Experimental WG generates experimental data on crack-growth behavior in inhomogeneous specimens to be used in evaluating the applicability of various fracture models to inhomogeneous materials and to provide the fracture models necessary for developing engineering estimation schemes. The Estimation Scheme WG is responsible for the development of engineering schemes to determine crack-growth resistance based on experimental and analytical results. Results from studies of the three WGs are reported in detail in interim EPI reports.[25-27]

### 2.4.1 Experimental WG Workscope

At the Tokyo meeting, Professor H. Homma (Tokyohashi University of Technology) presented a review of the work plan currently being performed within the Experimental WG. The highlight of this plan is a new testing program

*Computing and Telecommunications Division, Martin Marietta Energy Systems, Inc., Oak Ridge, Tenn.
†University of Tokyo, Tokyo, Japan.

being implemented to generate additional experimental data that will be used in developing an engineering estimation scheme. A bimaterial specimen is employed that consists of A 533 B steel (500- and 600-MPa yield and ultimate strength, respectively) and HT80 steel (700- and 800-MPa yield and ultimate strength, respectively) joined by an electron-beam weld. The motivation for this specimen design is to investigate the effect of two materials having a greater difference in yield stress than that provided by the previous EPI test specimens (for which the ratio of yield stresses was ~1.15). A high-toughness, heat-affected zone (HAZ) ~2 mm wide is associated with the weld. The plane of the crack is oriented normal to the weld line to provide for pure mode I loading. These specimens will be tested in an "as-welded" condition to avoid changing the material properties of the HT80 steel. Approximately 30 compact specimens having thicknesses of 6, 10, and 19 mm will be tested at room temperature with the crack tip either on the weld line or 3 mm from the weld line. Data generated from tests of these specimens will include $J_R$ curves, crack-growth data, and residual stress measurement. Three Japanese research organizations will participate in the testing program.

### 2.4.2 Theoretical WG Workscope

A review of the current work of the Theoretical WG was provided by Professor S. Aoki (Tokyo Institute of Technology). Five analytical studies are planned for this year. The first of these will involve 2-D, generation-phase, crack-growth analyses of the bimaterial A 533 B/HT80 specimens described previously. Experimental data (load and load-line displacement vs crack growth) from the testing program will be used with the finite-element models to evaluate the various path-area integral fracture parameters ($J$, $T^*$, $\hat{J}$, etc.) for different material combinations and crack-tip locations. A second study will investigate the effects of residual stress on crack growth in bimaterial A 533 B/weld-metal specimens. Initial thermal strains will be used to introduce residual stresses into 2-D finite-element models to compute effects on the integral parameters $J$, $T^*$, and $\hat{J}$. A third study will focus on the analysis of interfacial cracks in bimaterial specimens. Three-dimensional, elastic-plastic, finite-element models of stationary cracks will be employed. The fourth and fifth studies will examine surface cracks in both welded and clad specimens. Comparisons will be made between experimental data and analysis results obtained from 3-D elastic-plastic, finite-element models that use the line-spring methodology. At the meeting, A. Hiser (NRC) proposed that data produced by D. McCabe from the clad-beam test[28] should be used in these studies.

### 2.4.3 Estimation Scheme WG Workscope

Professor S. Yoshimura (University of Tokyo) provided a review of the current status of the Estimation Scheme WG. Applications of the General Electric/Electric Power Research Institute (GE/EPRI) method (based on fully plastic solutions) to a welded CT specimen with an initial crack tip located in the weld metal indicate that problems persist in the development of a simple estimation scheme. (The yield-stress ratio for the welded materials was ~1.15.) In this case, the best agreement with the experimentally measured $J_R$-curve was obtained from the use of base-metal properties in the GE/EPRI scheme, whereas the use of mixed properties (base-metal stress-strain relation and weld metal $h_1$, $h_3$ functions) provided the best agreement with the measured maximum applied load. Additional details of these problems are provided in Ref. 27.

### 2.4.4 Residual Stress Measurements

Professor Y. Arai (Saitama University) made a presentation on benchmark tests of residual-stress measurements in the EPI Program. The material used in these measurements was obtained from submerged-arc welded plates of A 533 B steel subjected to a postweld heat treatment of 600°C for 2 h. Comparisons were made between the results obtained from the acoustoelastic techniques of Professor Arai and those from a destructive strain-gage technique employed by Professor E. Rybicki in a study reported by the HSST Program at ORNL. The results of the acoustoelastic method overestimated the residual stresses when compared with results from the strain-gage method, presumably due to the existence of a relatively large stress gradient through the thickness of the specimens. Apparently, work will continue in the EPI Program to better understand the problems associated with these residual-stress measurements.

### 2.4.5 Proposed General Review Meeting

The meeting concluded with comments by ORNL staff concerning the need for a general review meeting on the achievements of the EPI Program following its scheduled completion in August 1992. A proposal was made that this meeting should take place in the United States in conjunction with a scheduled international conference to facilitate travel of the Japanese EPI team. It was tentatively agreed

that a suitable time for the meeting would be June 1993, either before or after the scheduled American Society of Mechanical Engineers Pressure Vessel and Piping (ASME/PVP) Conference, in Denver, Colorado. This time table would allow for completion of a final report on the EPI Program before the meeting. A discussion on the date, location, agenda, and invitees for the meeting will be finalized following additional negotiations involving the EPI Coordinator, the HSST Program Manager, and the NRC Technical Monitor.

## References


1. B. R. Bass, Martin Marietta Energy Systems, Inc., Oak Ridge Natl. Lab., "Heavy-Section Steel Technology Program Semiann. Prog. Rep. October 1989–March 1990," USNRC Report NUREG/CR-4219, Vol. 7, No. 2 (ORNL/TM-9593/V7&N2), September 1991.*

2. D. K. M. Shum et al., Martin Marietta Energy Systems, Inc., Oak Ridge Natl. Lab., "Analytical Studies of Transverse Strain Effects on Fracture Toughness for Circumferentially Oriented Cracks," USNRC Report NUREG/CR-5592 (ORNL/TM-11581), February 1991.*

3. J. Keeney-Walker, "A Numerical Study of Local Crack-Tip Fields for Modeling Cleavage Fracture Initiation," Master's Thesis, The University of Tennessee, Knoxville, Tennessee, May 1990.

4. T. L. Anderson and R. H. Dodds, Jr., Texas A&M University, College Station, Texas, Mechanics and Materials Center, "Specimen-Size Requirement for Fracture Toughness Testing in the Transition Region," Report MM-6586-90-5, May 1990.

5. K. J. Bathe, Massachusetts Institute of Technology, "ADINA—A Finite Element Program for Automatic Dynamic Incremental Nonlinear Analysis," Report 82448-1, 1975 (revised 1978).

6. D. J. Naus et al., Martin Marietta Energy Systems, Inc., Oak Ridge Natl. Lab., "Crack-Arrest Behavior in SEN Wide Plates of Quenched and Tempered A 533 Grade B Steel Tested Under Nonisothermal Conditions," USNRC Report NUREG/CR-4930 (ORNL-6338), August 1987.*

7. G. T. Hahn, A. Gilbert, and C. N. Reid, "Model for Crack Propagation in Steel," *J. Iron Steel Inst. (London)* 202, 677–684 (August 1964).†

8. D. E. McCabe and J. D. Landes, Westinghouse R&D Center, "The Effect of Specimen Plan View Size and Material Thickness on the Transition Temperature Behavior of A 533 B Steel," Research Report 80-1D3-REVEM-R2, November 1980.

9. C. W. Schwartz, "Influence of Out-of-Plane Loading on Crack-Tip Constraint," presented at the ASTM Symposium on Constraint Effects in Fracture, Indianapolis, May 1991.

10. N. P. O'Dowd and C. F. Shih, "Family of Crack-Tip Fields Characterized by a Triaxiality Parameter: Part I–Structure of Fields," *J. Mechanics and Physics of Solids* 39, 93–115 (1991).†

11. T. J. Theiss and J. W. Bryson, "Influence of Crack Depth on the Fracture Toughness of Reactor Pressure Vessel Steel," presented at the ASTM Symposium on Constraint Effects in Fracture, Indianapolis, May 1991.†

12. A. M. Al-Ani and J. W. Hancock, "J-Dominance of Short Cracks in Tension and Bending," *J. Mechanics and Physics of Solids* 39(1), 23–43 (1991).†

13. R. D. Cheverton and D. G. Ball, Martin Marietta Energy Systems, Inc., Oak Ridge Natl. Lab., "Pressurized-Thermal-Shock Evaluation of the H. B. Robinson Nuclear Power Plant," pp. 263–306, USNRC Report NUREG/CR-4183, Vol 1 (ORNL/TM-9567/V1), September 1985.*

14. R. D. Cheverton and D. G. Ball, Martin Marietta Energy Systems, Inc., Oak Ridge Natl. Lab., "Pressurized-Thermal-Shock Evaluation of the Calvert Cliffs Unit 1 Nuclear Power Plant," USNRC Report NUREG/CR-4022 (ORNL/TM-9408), September 1985.*

15. R. D. Cheverton and D. G. Ball, Martin Marietta Energy Systems, Inc., Oak Ridge Natl. Lab., "Preliminary Development of an Integrated Approach to the Evaluation of Pressurized-Thermal-Shock as Applied to the Oconee Unit 1 Nuclear Power Plant," USNRC Report NUREG/CR-3770 (ORNL/TM-9176), May 1986.*

16. R. D. Cheverton and D. G. Ball, Martin Marietta Energy Systems, Inc., Oak Ridge Natl. Lab., "OCA-P, A Deterministic and Probabilistic Fracture-Mechanics Code for Application to Pressure Vessels," USNRC Report NUREG-3618 (ORNL-5991), May 1984.*

17. E. Smith and T. J. Griesbach, "Simulating the Effect of Pressure Plus Thermal Loadings on Crack Arrest during a Hypothetical Pressurized Thermal Shock Event," PVP-Vol. 213/MPC-Vol. 32, pp. 41–46, Pressure Vessel Integrity, American Society of Mechanical Engineers, 1991.†

18. Combustion Engineering Inc., "Tests and Analyses of Crack Arrest in Reactor Vessel Materials," Final Report NP-5121 on EPRI Research Project 2180-3, 1987.†

19. *The American Society of Mechanical Engineers Boiler and Pressure Vessel Code*, Section XI, Rules for Inservice Inspection of Nuclear Power Plant Components, 1986.†

20. R. J. Fabi and D. J. Ayers, Combustion Engineering, Inc., "Calculating Dynamic Crack Arrest by Static Analogy," Electric Power Research Institute report NP-6223, March 1989.*

21. B. R. Bass et al., "Applications of ADINA to Viscoplastic-Dynamic Fracture Mechanics Analysis," *Computers and Structures* 32(3/4), 815–824, 1989.†

22. W. O. Shabbits, Westinghouse R&D Center, "Dynamic Fracture Toughness Properties of Heavy Section A533 Grade B Class 1 Steel Plate," WCAP-7623, HSST Technical Report No. 13, December 1970.*

23. J. G. Merkle et al., Union Carbide Corporation Nucl. Div., Oak Ridge Natl. Lab., "Heavy-Section Steel Technology Program Quar. Prog. Rep. July–September 1982," pp. 3–4, USNRC Report NUREG/CR-2571, Vol. 3 (ORNL/TM-8369/V3), January 1983.*

24. R. D. Cheverton and D. G. Ball, "A Reassessment of PWR Pressure Vessel Integrity During Overcooling Accidents, Considering 3-D Flaws," *J. Pressure Vessel Technology* 6, 375–382 (1984).†

25. G. Yagawa, Century Research Corporation, Tokyo, Japan, "Study on Elastic-Plastic Fracture Mechanics in Inhomogeneous Materials and Structures I," CRC-EPI-1, March 1989.

26. G. Yagawa, Century Research Corporation, Tokyo, Japan, "Study on Elastic-Plastic Fracture Mechanics in Inhomogeneous Materials and Structures II," CRC-EPI-2, March 1990.

27. G. Yagawa, Century Research Corporation, Tokyo, Japan, "Study on Elastic-Plastic Fracture Mechanics in Inhomogeneous Materials and Structures III," CRC-EPI-3, March 1991.

28. D. E. McCabe, Materials Engineering Associates, Inc., Lanham, Md., "Fracture Evaluation of Surface Cracks Embedded in Reactor Vessel Cladding," USNRC Report NUREG/CR-5326 (MEA-2329), March 1989.*

---

*Available for purchase from National Technical Information Service, Springfield, VA 22161.

†Available in public technical libraries.

# 3 Material Characterization and Properties

R. K. Nanstad

Primarily for internal management and budgetary control, the HSST Program created a separate task (Task H.3) for the work on material characterization and properties determinations. However, for the reader's convenience, some contributions to this report are placed within other chapters according to the larger tasks that correspond to the particular material studied.

## 3.1 Characterization of HSST Plate 013B in the L-S Orientation

(S. K. Iskander)

Much of the first phase of characterizing HSST Plate 013B for the Shallow-Flaws Task has been completed. Tests to determine the Charpy V-notch (CVN) curves in the L-S and T-L orientations, the drop-weight nil-ductility transition (NDT) temperature and the reference temperature, $RT_{NDT}$, for both surface and midthickness material have been completed. Tests are being performed to determine the tensile properties in the L-orientation as a function of temperature for both surface and midthickness material, thus completing all the tasks planned for the first phase. In the second phase, crack-initiation-toughness tests ($K_{Jc}$, $K_{Ic}$, or J-R) will be performed over the temperature range of interest using 25-mm compact specimens in the L-S orientation from the midthickness positions. A small number of 25-mm-thick, 50-mm-deep, single-edge, three-point bend SE(B) specimens will be tested at a single temperature and the results compared with those from the C(T) specimens to determine the effect of specimen geometry on the initiation toughness.

Results of the tests performed to date show a significant difference in the CVN impact energy test results between specimens from the midthickness and those from the surface of the characterization block. The results of the drop-weight tests have confirmed this difference in toughness properties. A detailed report of this study is being prepared.

HSST Plate 013 was manufactured by Lukens Steel, melt C4453, in accordance with ASTM Specification for Pressure Vessel Plates, Alloy Steels, Quenched and Tempered, Manganese-Molybdenum and Manganese-Molybdenum-Nickel Grade B, Class 1 (A 533 B Cl.1). A characterization block, designated as 13BA/5, was flame cut from the 187-mm-thick (7 3/8-in.) HSST Plate 013B. The characterization block, together with other flame-cut material designated to be machined into the shallow-flaw beam specimens, was given a postweld heat treatment (PWHT) of 621 ± 14°C (1150 ± 25°F) for 40 h to simulate the PWHT given to RPVs. The characterization has been performed in the L-S orientation, the same orientation as that in which the Shallow Flaws Task three-point bend beam tests are performed. HSST Plate 013A (the other half of HSST Plate 013) has been quite extensively characterized previously, but not in the L-S orientation.

Figures 3.1 and 3.2 show the results of the CVN testing in both the L-S and T-L orientations, respectively, and Table 3.1 gives a summary of the CVN impact energy test results as well as the results of drop-weight NDT temperature. The values of $RT_{NDT}$ are –43 and –15°C for material from the surface and midthickness material, respectively. The $RT_{NDT}$ determination was performed in accordance with Section III, Subarticle NB-2330, of the 1986 Edition of *ASME Boiler and Pressure Vessel Code*. For the PWHT HSST Plate 013B material, it was the CVN impact energy test results and not the NDT temperature that dictated the values of $RT_{NDT}$.

## 3.2 Thermal Aging of Stainless Steel Cladding (F. M. Haggag and R. K. Nanstad)

Thermal aging at relatively low temperatures (343°C) has been shown to significantly degrade the Charpy impact toughness of type 308 stainless steel welds. The stainless steel cladding applied to the inner surface of RPVs is very similar to that material. Hence, an experimental program was initiated to evaluate the effects of thermal aging on stainless steel cladding relative to its contribution to toughness degradation during irradiation experiments as well as long-term effects.

Since the irradiation of the three-wire series-arc cladding to the highest fluence of $5 \times 10^{19}$ neutrons/cm$^2$ (>1 MeV) was conducted at 288°C for 1605 h, tensile, CVN, pre-cracked CVN (PCVN), and compact fracture-toughness specimens were thermally aged at 288°C to times of 1605, 20,000, and 50,000 h. Test results from the 1605-h specimens are summarized below. Thermal aging at 288°C

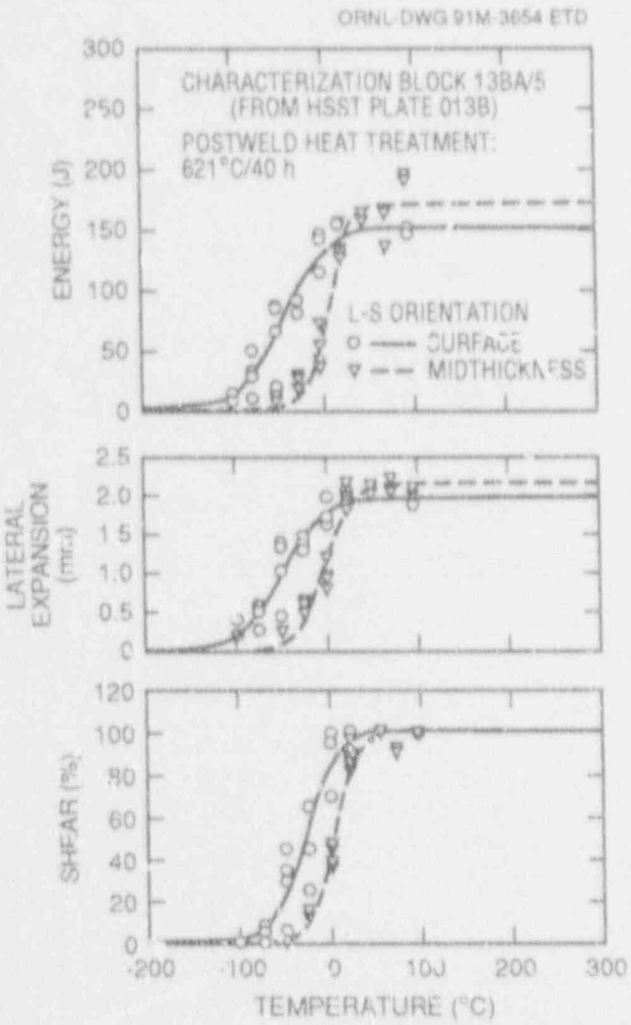


**Figure 3.1 Results of CVN testing in L-S orientation for characterization block 13BA/5 postweld heat treated at 621°C (1150°F) for 40 h**

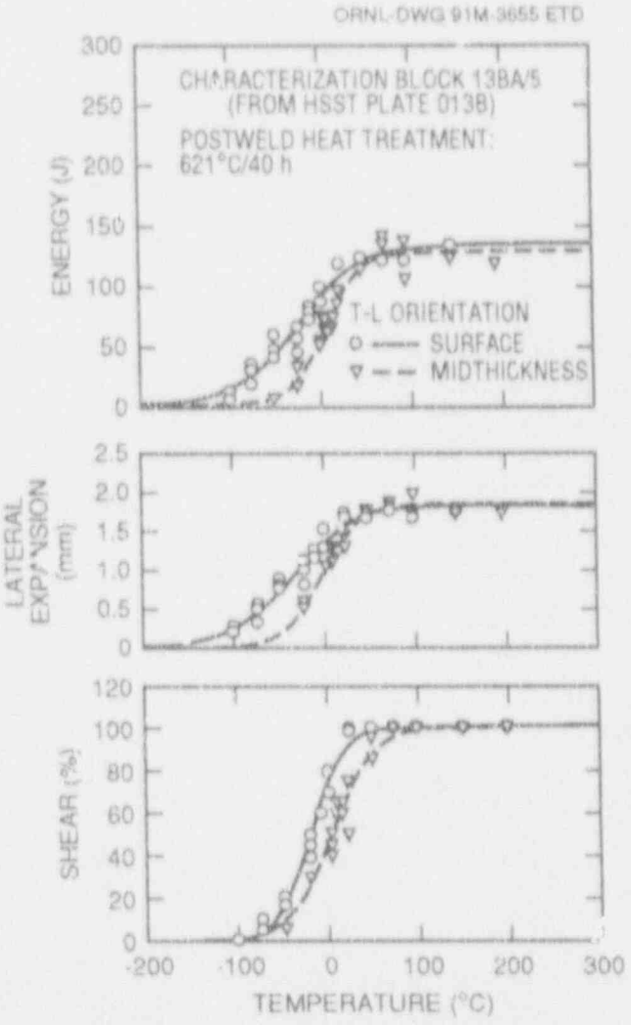


**Figure 3.2 Results of CVN testing in T-L orientation for characterization block 13BA/5 postweld heat treated at 621°C (1150°F) for 40 h**

of stainless steel cladding and the ferritic steel on which it is overlaid to accumulated times of 20,000 (expected to be completed by November 1992) and 50,000 h is in progress. Other cladding specimens are being aged at 343°C together with a type 308 stainless steel weld from another NRC program.

Thermal aging of the three-wire stainless steel weld overlay cladding at 288°C for 1605 h resulted in an appreciable decrease (16%) in the CVN upper-shelf energy (USE), but the effect on the 41-J transition temperature shift was very small (3°C). The combined effect following neutron irradiation at 288°C to a fluence of $5 \times 10^{19}$ neutrons/cm$^2$ (>1 MeV) was a 22% reduction in the CVN USE and a 29°C shift at the 41-J level. The effect of thermal aging on the tensile properties was very small or negligible. However, the combined effect after neutron irradiation was an increase (6 to 34% at test temperatures from 288°C to –125°C) in the yield strength and no apparent change in ultimate strength and total elongation.

The test results of the 12.7-mm-thick compact [0.5TC(T)] fracture-toughness specimens (all specimens were 10% side-grooved on each side and tested using a computerized

Table 3.1 Summary of CVN tests in the L-S and T-L orientations on material from characterization block 13BA/5 [flame-cut from HSST Plate 013B and postweld heat treated at 621°C (1150°F) for 40 h]

| Depth in plate | Results of fitting equation[a] A + B tanh [(T – $T_0$)/C] | | | | Upper-shelf energy (J) | Temperature (°C) at energy levels of | | NDT (°C) | Energy level at NDT (J) |
|---|---|---|---|---|---|---|---|---|---|
| | A[b] (J) | B[b] (J) | C $(°C)^{-1}$ | $T_0$ (°C) | | 41 J | 68 J | | |
| | | | | *L-S orientation* | | | | | |
| Surface | 77.3 | 74.6 | 47.4 | –39.1 | 152 | –64 | –45 | –55 | 53 |
| Midthickness | 86.3 | 83.6 | 23.7 | 8.8 | 170 | –6 | 4 | –30 | 9 |
| | | | | *T-L orientation* | | | | | |
| Surface | 68.4 | 65.7 | 70.3 | –23.9 | 134 | –55 | –24 | –55 | 41 |
| Midthickness | 65.5 | 62.8 | 38.7 | 7.3 | 128 | –9 | 9 | –30 | 19 |

[a]For purposes of fitting the tanh equation, the lower-shelf energy was prescribed to be 2.7 J (2 ft-lb) based on an average of five tests at –196°C of the WF-70 Midland weld.
[b]Upper-shelf energy (USE) = A + B; lower-shelf energy (LSE) = A – B.

Table 3.2 Unloading compliance J-R test results of 12.7-mm-thick three-wire stainless steel cladding fracture-toughness specimens (10% side-grooved on each side)

| Test temperature (°C) | Unirradiated | | | Irradiated | | | Aged[b] | | |
|---|---|---|---|---|---|---|---|---|---|
| | Specimen | $J_{Ic}$ (kJ/m²) | Tearing modulus | Specimen | $J_{Ic}$ (kJ/m²) | Tearing modulus | Specimen | $J_{Ic}$ (kJ/m²) | Tearing modulus |
| –75 | A13G | 116 | 62 | A15F | 79 | 29 | | | |
| –75 | H2 | 145 | 35 | A15G | 60 | 31 | | | |
| 20 | A13D | 132 | 203 | | | | H7 | 104 | 156 |
| 20 | A10G | 169 | 159 | | | | H8 | 144 | 182 |
| 30 | | | | A13A | 157 | 158 | | | |
| 50 | | | | A15C | 121 | 147 | | | |
| 120 | A10E | 136 | 233 | | | | H9 | 119 | 248 |
| 120 | H5 | 120 | 207 | A10F | 108 | 161 | AA03 | 94 | 282 |
| 120 | H3 | 114 | 214 | | | | | | |
| 200 | H6 | 95 | 220 | | | | | | |
| 200 | H4 | 100 | 221 | | | | | | |
| 288 | A15D | 76 | 278 | | | | H10 | 85 | 218 |
| 288 | A13C | 70 | 171 | A15A | 25 | 226 | AA04 | 93 | 209 |
| 288 | H1 | 83 | 185 | | | | AA02 | 59 | 230 |

[a]Irradiated 637 h at 288°C to a fluence of $2.4 \times 10^{19}$ neutrons/cm² (>1 MeV).
[b]Thermally aged at 288°C for 1605 h.

single-specimen unloading compliance technique) are summarized in Table 3.2 for the unirradiated, thermally aged (1605 h), and irradiated [637 h at 288°C to a fluence of $2.4 \times 10^{19}$ neutrons/cm$^2$ (>1 MeV)] material conditions. The deformation J-integral values of $J_{Ic}$ and tearing modulus at various test temperatures are also shown in Figs. 3.3 and 3.4, respectively. These results indicate that thermal aging reduced the initiation fracture toughness ($J_{Ic}$) at room temperature and at 120°C, however, there was no apparent effect at 288°C. The effect of thermal aging on the tearing modulus was insignificant (no reduction) for all test temperatures (room temperature, 120, and 288°C). The effect of thermal aging at 288°C on the $J_{Ic}$ at the test temperature of 288°C will be further clarified from $J_{Ic}$ tests following the 20,000-h aging. Furthermore, the effect of thermal aging on the dynamic fracture toughness ($K_{Id}$) will be reported shortly following the testing of PCVN specimens that were thermally aged with the other specimens.

## 3.3 ASTM Fracture-Toughness Testing Standards Development

(D. E. McCabe, D. J. Alexander, and R. K. Nanstad)

ORNL personnel participated in two meetings of the combined $J_{Ic}$/J-R curve standard. These meetings concentrated on ways to fit curves to data so that comparable $J_{Ic}$ values can be obtained from J-$\Delta a$ curve data with abnormal data patterns. Another issue is the incorporation of fracture-toughness determination from test specimens that fracture in a brittle manner (by cleavage). This effort was assisted by an HSST program prepared presentation on salient issues that differ from those that pertain to the testing of materials subject to ductile fracture. The objective was to assure compatibility with the work currently under way in the development of the ductile-brittle transition temperature standard.

A second draft of the proposed ASTM standard, "Test Practice (Method) for Fracture Toughness in the Transition Range," was developed for use at the ASTM task group meeting in San Diego in October. A presentation was given at this meeting.

## 3.4 Study of Low-Toughness Zones

### 3.4.1 ORNL Studies (D. E. McCabe)

Experiments on pop-in are currently under way. The test matrix was designed to isolate mechanical effects from the metallurgical effects of this phenomenon. Mechanical effects are evaluated best with bend bar tests and fixtures of variable compliance. The A710 steel, selected as one of the two test materials, proved to be the better material for such pop-in studies. Five bend bars were tested, and all gave pop-in behavior. However, the $K_{Jc}$ at the onset of pop-in varied as much as a factor of 2 between replicates, and the extent of crack jump was clearly a function of $K_{Jc}$ at pop-in. Hence, it seems that crack arrest is a function of stored elastic crack drive energy in the loading system. To clarify the point, a spring bar that will impart a strongly positive K-gradient into the loading system has been made. Five bend bars remain and will be used to confirm the observation.

Compact specimens of the same A 710 steel displayed only complete $K_{Jc}$ instabilities with no pop-ins. These were the first tests made, however, and the principal objective was to establish the optimum test temperature for pop-in behavior. The test setup was the usual one used on compacts with long pull rods. The compact specimens were side-grooved because it was believed that the increased constraint would promote pop-ins. After comparing these results with the bend bar results and discussions with J. D. G. Sumpter about this, it appears that side grooving was not the best choice. Compact specimens to be tested hereafter will not be side grooved, and the loading-system stiffness will be increased as much as possible.

Continuing work at Battelle-Columbus in support of the HSST Program will include effects of local brittle zones in tests on three selected weldments that had been made for previous crack-arrest programs. Specimens with cracks in the HAZ will be made and tested to demonstrate the effect of local brittle zones. Another part of the proposed Battelle work will be to try a proposed specimen design that can control biaxial stress ratio such that the effect of stress state on fracture toughness can be investigated using small specimens. Test specimen design is the principal objective of the first phase of the work.

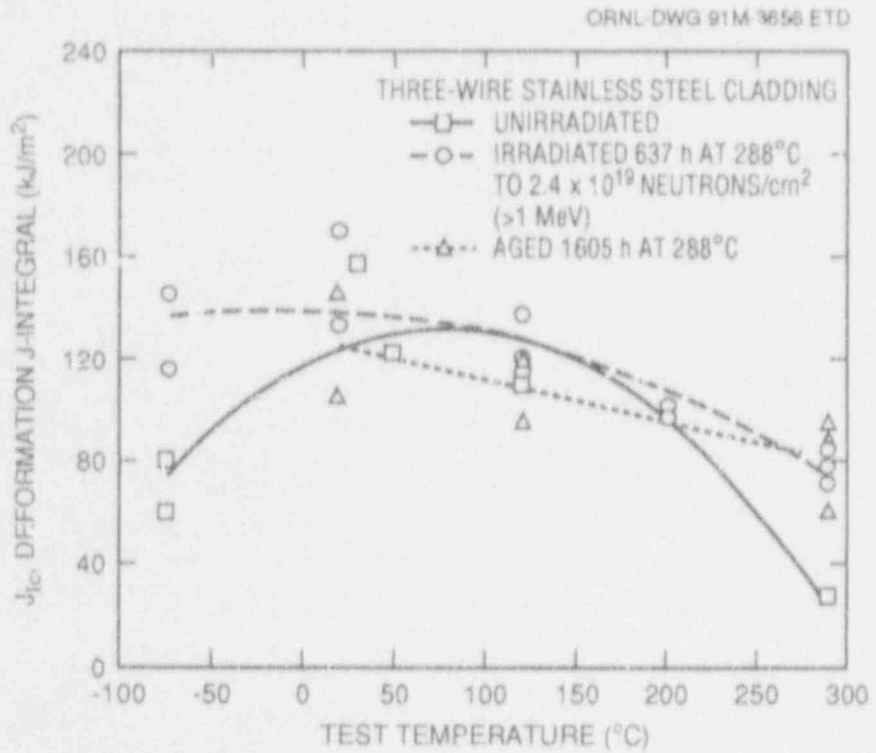


**Figure 3.3 Effects of neutron irradiation and thermal aging at 288°C on initiation fracture toughness, $J_{Ic}$, of three-wire type 308 stainless steel cladding at various test temperatures**

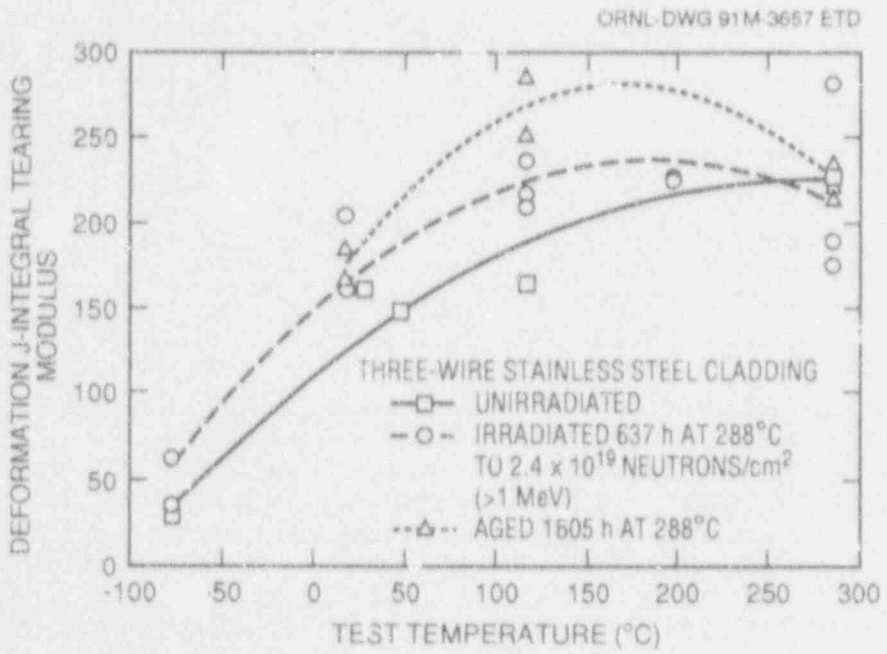


**Figure 3.4 Effects of neutron irradiation and thermal aging at 288°C on deformation J-integral tearing modulus of three-wire type 308 stainless steel cladding at various test temperatures**

### 3.4.2 University of Maryland Studies (G. R. Irwin)

#### 3.4.2.1 Initiation from Cleavage Cracks

Comparisons of cleavage initiation toughness were made using single-edge-notched bend (SENB) specimens of untempered A 508 steel, some with cleavage arrest precracks and some with fatigue precracks. Test temperatures of 23, 65, and 85°C were used. The $RT_{NDT}$ estimate was 65°C. Use of cleavage precracks caused more pop-in events. The K values at initiation of pop-in for cleavage precracked specimens were significantly lower than K for cleavage initiation in fatigue precracked specimens only at 85°C, where plastic yielding complicated interpretation of test results. A report on this work was completed in September 1991. This project required development of a practical method for insertion of cleavage arrest precracks. The method developed, employing wedge loading and deep chevron side grooves, is described in the report. Fractographic studies of features that assist initiation and reinitiation of cleavage are still in progress.

Completion of the report on these comparisons was delayed into September because of the need for further review of related complexities. The completed report, available in early October, will include results of this review.

### 3.4.3 Battelle Memorial Institute (A. R. Rosenfield, C. W. Marschall, and P. N. Mincer)

#### 3.4.3.1 Failure Analysis

A report describing and analyzing 20 failure analyses carried out between 1980 and 1990 was submitted to ORNL. The information was supplemented by data from a similar 1978 analysis.[1] It was concluded that the likelihood of failure is particularly large when there is a defect >25 mm and when the fracture-toughness/ yield-strength ratio is $<0.16 \cdot \sqrt{m} \approx 1.0 \sqrt{in.}$, provided the average value of toughness is used to determine this ratio. A survey of variability in fracture toughness suggested that the coefficient of variation is on the order of 20%, possibly less for upper-shelf behavior.

#### 3.4.3.2 Effect of Crack-Tip Morphology on Cleavage Crack Extension

Several years ago, Battelle investigators reported that arrested cleavage cracks led to significantly lower fracture-toughness values than did the fatigue precracks used in the standard ASTM fracture-toughness tests.[2,3] It was decided to extend these experiments. Research during this reporting period involved attempts to develop improved procedures for reinitiating an arrested cleavage crack in plate WP-1, an ASTM A 533 grade B steel that has been used in wide-plate tests. Initially, the fixture consisted of two flat support blocks, using line loading of a notched three-point bend specimen. The support blocks were separated by a distance that varied between one and two times the specimen height. This relatively small separation inhibits arm motion during crack propagation and, it was anticipated, reduces the size of the crack jump. The specimen also was bolted near both ends to the base plate to inhibit arm motion.

Earlier in FY 1991, chevron-notched specimens of WP-1 steel were precracked at –196°C to lower the load required to initiate a crack jump. To further decrease the crack jump, the specimens were wedge loaded at –70°C. Despite the lower initiation loads than previously achieved, the crack jump was still too long for a useful reinitiation experiment. Raising the precrack temperature to –50°C resulted in ligamentation, which would obscure the reinitiation data. It was concluded that WP-1 steel is too tough for accomplishing the goals of this task.

## References


1. T. P. Kich and A. R. Rosenfield, "Fracture Case Studies," in *Fracture Mechanics*, N. Perrone et al., Eds. (University of Virginia Press, Charlottesville, 1978), pp. 43–67.*

2. A. R. Rosenfield and P. N. Mincer, "Reinitiation of an Arrested Cleavage Crack," *Engineering Fracture Mechanics* 18, 1125–1129 (1983).*

3. A. R. Rosenfield, "Effect of Crack-Tip Morphology on Cleavage-Crack Extension," *Journal of Testing and Evaluation* 13, 202–205 (1985).*


*Available in public technical libraries.

# 4 Special Technical Assistance

J. G. Merkle

## 4.1 Yankee Rowe PTS Probabilistic Fracture-Mechanics Sensitivity Analysis

(T. L. Dickson,* R. D. Cheverton, J. W. Bryson, B. R. Bass, D. K. M. Shum, J. Keeney-Walker*)

### 4.1.1 Background Information

Following the ORNL review† of the Yankee Atomic Electric Company RPV evaluation report for the Yankee Rowe reactor,‡ NRC§ requested ORNL to perform a PTS probabilistic fracture-mechanics (PFM) sensitivity analysis for the vessel, using a specific small-break loss-of-coolant transient (SBLOCA-Case 7) as the loading condition. Subsequent discussions regarding the details of the methodologies to be used in performing the specified analyses were held between staff members of NRC and ORNL in meeting at Rockville, Maryland, on March 22 and May 14, 1991.

The two objectives of the study were to (1) provide NRC with results that could be used to assess the relative influence of key input parameters in the Yankee Rowe PTS analysis and (2) provide data that can be used for readily estimating the probability of vessel failure when a more accurate indication of vessel embrittlement becomes available.

### 4.1.2 Scope of the Sensitivity Analysis

The initial NRC request specified that the OCA-P computer code[1] be enhanced to calculate the conditional probability of failure for subclad and embedded flaws as well as for through-clad (surface) flaws. NRC also specified that the spatial variation of fluence be considered to the extent practical, and ORNL modified OCA-P to enhance this capability. All calculations were to be performed for fluences corresponding to the end of operating cycle 22.

Regions of the vessel with distinguishing features to be treated individually were the upper axial weld, lower axial weld, circumferential weld, upper-plate spot welds, upper-plate regions between the spot welds, lower-plate spot welds, and lower-plate regions between the spot welds. (Spot welds attach the cladding to the base material, except over the vessel welds, where the cladding is weld deposited.)

The fracture-analysis methods to be used in the analysis of the surface flaws were those represented by the established OCA-P methodology, which was developed during the IPTS Program.[2] Subclad and embedded flaws were not available in OCA-P, and thus the fracture-mechanics methodology for these flaws had to be developed. Because of the tight schedule, less precise methods than used for the surface flaws were acceptable.

The PFM sensitivity analyses for the weld regions were to be performed with copper concentration as the independent variable (0.15 to 0.35 wt % in increments of 0.05), while the analyses for the plates were to be performed with surface $RT_{NDT}$ as the independent variable. The upper-plate surface $RT_{NDT}$ values ranged from 121 to 163°C (250 to 325°F) in increments of –3.9°C (25°F), and the lower plate surface $RT_{NDT}$ values ranged from 121 to 204°C (250 to 400°F) in increments of –3.9°C (25°F).

### 4.1.3 Methods of Analysis

#### 4.1.3.1 Overview

The complete details of the models and methodologies implemented for performing the Yankee Rowe sensitivity analysis** are given below in a brief discussion of the fracture analysis methods applied for the three flaw types.

---

*Computing and Telecommunications Division, Martin Marietta Energy Systems, Inc., Oak Ridge, Tenn.

†R. D. Cheverton et al., ORNL/NRC Review of Reactor Pressure Vessel Evaluation Report for Yankee Nuclear Power Station, November 5, 1990.

‡Yankee Atomic Electric Company, "Reactor Pressure Vessel Evaluation Report for Yankee Nuclear Power Station," YAEC-1735, July 9, 1990.

§Facsimile from M. E. Mayfield (NRC) to W. E. Pennell (ORNL), February 15, 1991.

**T. L. Dickson et al., Martin Marietta Energy Systems, Inc., Oak Ridge National Lab., "Oak Ridge National Laboratory Pressurized-Thermal-Shock Probabilistic Fracture Mechanics Sensitivity Analysis for Yankee Rowe Reactor Pressure Vessel," USNRC Report NUREG/CR-5782 (ORNL/TM-11945), draft report sent to M. E. Mayfield, NRC, September 16, 1991.

#### 4.1.3.2 Fracture Analysis Methods—Basic Methodology

All fracture analyses were performed in accordance with LEFM theory. Based on this methodology, flaws are predicted to begin propagation (initiate) when the stress-intensity factor ($K_I$) is equal to the static crack-initiation fracture toughness ($K_{Ic}$) or the dynamic-loading fracture toughness ($K_{Id}$). Arrest of a fast-running crack is predicted when $K_I = K_{Ia}$, the crack-arrest toughness. Dynamic loading is introduced when one portion of a crack front initiates under static loading conditions, thereby subjecting the remaining stationary part of the crack front to dynamic loading.

In the fracture analysis of flaws residing in welds, the $K_I$'s corresponding to crack tips that reside in the first inch of base metal include the effect of a 6-ksi tensile residual stress. The $K_I$'s for crack tips in the cladding and the remainder of the base material do not include the effect of residual stresses.

In the fracture analyses of subclad and embedded flaws, dynamic effects have been included to the extent of including the dynamic-loading fracture toughness ($K_{Id}$) for specific crack-initiation events. The $K_{Id}$ curve was approximated by shifting the $K_{Ic}$ curve ~0.5°C (33°F), and it was used in the prediction of crack initiation in the base material at the time step for which the cladding was predicted to fail.

#### 4.1.3.3 Types of Flaws

The basic types of flaws considered are surface flaws and embedded flaws, of which a subclad flaw is a special category. All flaws analyzed were considered to be normal to the surface and oriented in either an axial (longitudinal) or azimuthal (circumferential) direction. All other flaws that might exist were ignored.

The length of an initial flaw in the axial or circumferential direction is more likely to be short than long, but upon propagation, short flaws have a tendency to become long flaws.[3] Previous studies have indicated that under thermal-shock loading, a semicircular surface flaw has a greater potential for surface extension than other short flaws and about the same potential for surface propagation as that for radial propagation of a long surface flaw of the same initial depth. Thus, the assumption was made that all initial surface flaws were semicircular, in which case the spatial distribution (z,j) of the fluence could be considered for the first initiation event, but the $K_I$ values used were those for a very long flaw.

Initial embedded flaws were also assumed to be short so that the spatial distribution of the fluence could be considered. Even though the shorter embedded flaws have less potential for propagating, the embedded-flaw $K_I$ values used were for long flaws. In any subsequent studies, the more realistic shorter flaw should be considered.

#### 4.1.3.4 Fracture Analysis Method for Surface Flaws

Surface flaws are flaws that penetrate from the inner surface of the vessel into the cladding and base metal. The stress-intensity factors ($K_I$) used in the PFM analyses of surface flaws were calculated in the usual OCA-P manner, that is, a superposition technique that applies a large number of $K_I$ influence coefficients (calculated by a 2-D finite-element method) and the stresses induced in the uncracked vessel as a function of time and radial position in the pressure-vessel wall (calculated by a 1-D finite-element thermal and stress analysis). Note that all surface-flaw $K_I$'s used in these analyses are for flaws of infinite surface length.

It is of interest to note that the ASME Sect. XI procedure[4] for calculating $K_I$'s for surface flaws was also included in the specialized code for performing the Yankee Analysis. The values calculated by the ASME methodology are very close to those calculated by the OCA-P methodology (discussed above) for very shallow flaws; however, they diverge for greater depths, with the ASME values being higher. Probabilities of failure for surface flaws, calculated using the ASME $K_I$ methodology, are higher than those using the OCA-P $K_I$ methodology by approximately a factor of 2.

The flow chart logic for performing the deterministic fracture mechanics analysis of each of the probabilistically simulated embrittled vessels containing a surface flaw is included in Fig. 4.1.

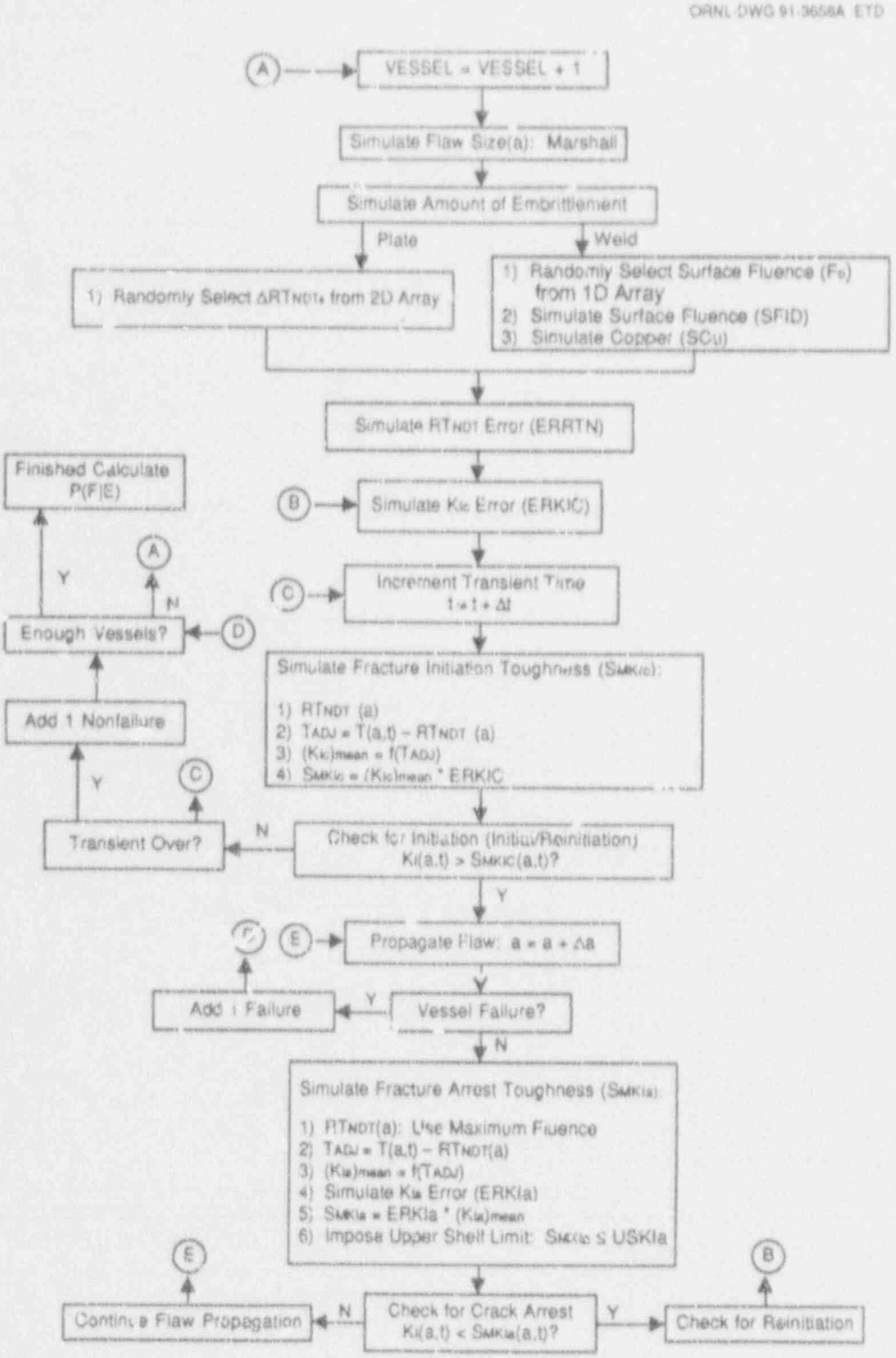


**Figure 4.1 Probabilistic fracture-mechanics methodology for surface flaws**

#### 4.1.3.5 Fracture Analysis Method for Subclad Flaws

A subclad flaw is a flaw that has its inner crack tip at the clad/base interface, and thus its outer crack tip is in the base metal. The outer flaw tip is checked for initiation according to LEFM principles. If the subclad flaw size reaches the critical size for which cladding is predicted to fail, the subclad flaw is converted to a surface flaw, and the $K_I$'s for surface flaws are then used to predict initial initiation, crack arrest, and subsequent reinitiation of the outer crack tip. At the time step corresponding to cladding failure, dynamic effects were simulated by using a value of $K_{Id}$, instead of $K_{Ic}$, to predict crack initiation in the base material.

If the cladding does not fail, the probability of initiation of the subclad flaw is less than that of a surface flaw. Analyses of thermal-shock experiments performed at ORNL indicate that at times of maximum loading, the $K_I$ for a subclad flaw is ~34% less than that for a surface flaw.[5] Based on these experimental results, the stress-intensity factors for predicting the initial initiation of subcritical (cladding has not failed) subclad flaws were calculated by reducing $K_I$ for a surface flaw (with the crack tip at the same radial wall location) by 35%.

Subclad flaws that exist in the plate regions between the spot welds are treated differently than the subclad flaws at the circumferential welds and plate regions in the spot welds. These subclad flaws are treated like surface flaws, that is, the $K_I$'s are not reduced by 35%, because the clad/base interface is separated by a 3-mil gap. ADINA-T, a general purpose multidimensional finite-element thermal analysis program,[6] was used to calculate the thermal response of the plate region between the spot welds, assuming the 3-mil gap to be filled with water. The insulating effect of the gap slightly reduces the severity of the thermal load. Also, the insulating effect of the gap results in higher fracture toughness.

The flow chart logic for performing the deterministic fracture mechanics analysis of each of the probabilistically simulated embrittled vessels containing a subclad flaw is included in Fig. 4.2(*a*) and (*b*).

#### 4.1.3.6 Fracture Analysis Method for Embedded Flaws

An embedded flaw is considered to be a flaw that resides entirely in the base metal. In the probabilistic analysis, the location of the inner tip of the embedded flaw is probabilistically simulated, that is, located randomly along a discrete mesh between the clad/base interface and the vessel outer wall. The flaw has equal probability of being located at any one of the discrete mesh points in the base metal. Note that the calculated probability of failure is sensitive to the discrete mesh size used as possible locations for the embedded inner crack tip. Mesh convergence analyses were performed, and it was determined that a discrete mesh spacing of 0.005 in. is converged with respect to the probability of failure.

The mathematical representation[7] of the ASME Sect. XI procedure was used to calculate $K_I$'s that were used to predict the initial initiation for the embedded flaws.

The inner tip of the embedded flaw is checked for initiation according to LEFM principles. If the inner tip initiates, it is assumed that the flaw propagates all the way through the cladding, because the flaw is propagating into a region of higher embrittlement and higher thermal stress. Therefore, an initiated embedded flaw is converted to a surface flaw. Surface flaw $K_I$'s are then used to predict subsequent initiation and arrest. Dynamic effects (as described previously for subclad flaws) are included for the time step at which the flaw breaks through the cladding.

The flow chart logic for performing the deterministic fracture mechanics analysis of each of the probabilistically simulated embrittled vessels containing an embedded flaw is included in Fig. 4.3(*a*) and (*b*).

### 4.1.4 Results

The detailed results of the Yankee Rowe pressurized-thermal-shock probabilistic fracture-mechanics sensitivity analysis will be published in USNRC Report NUREG/CR-5782.

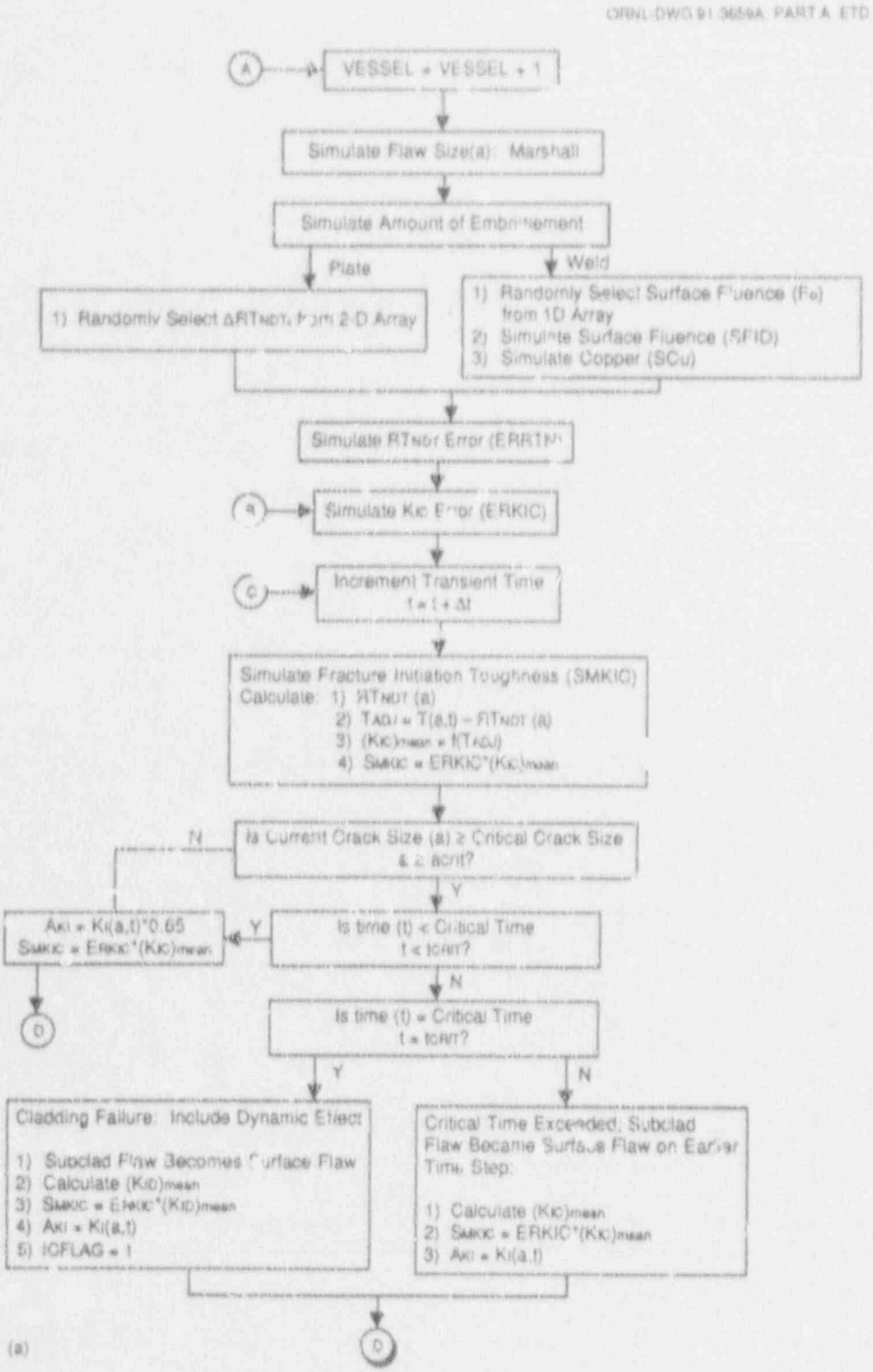


Figure 4.2 Probabilistic fracture-mechanics methodology for subclad flaws

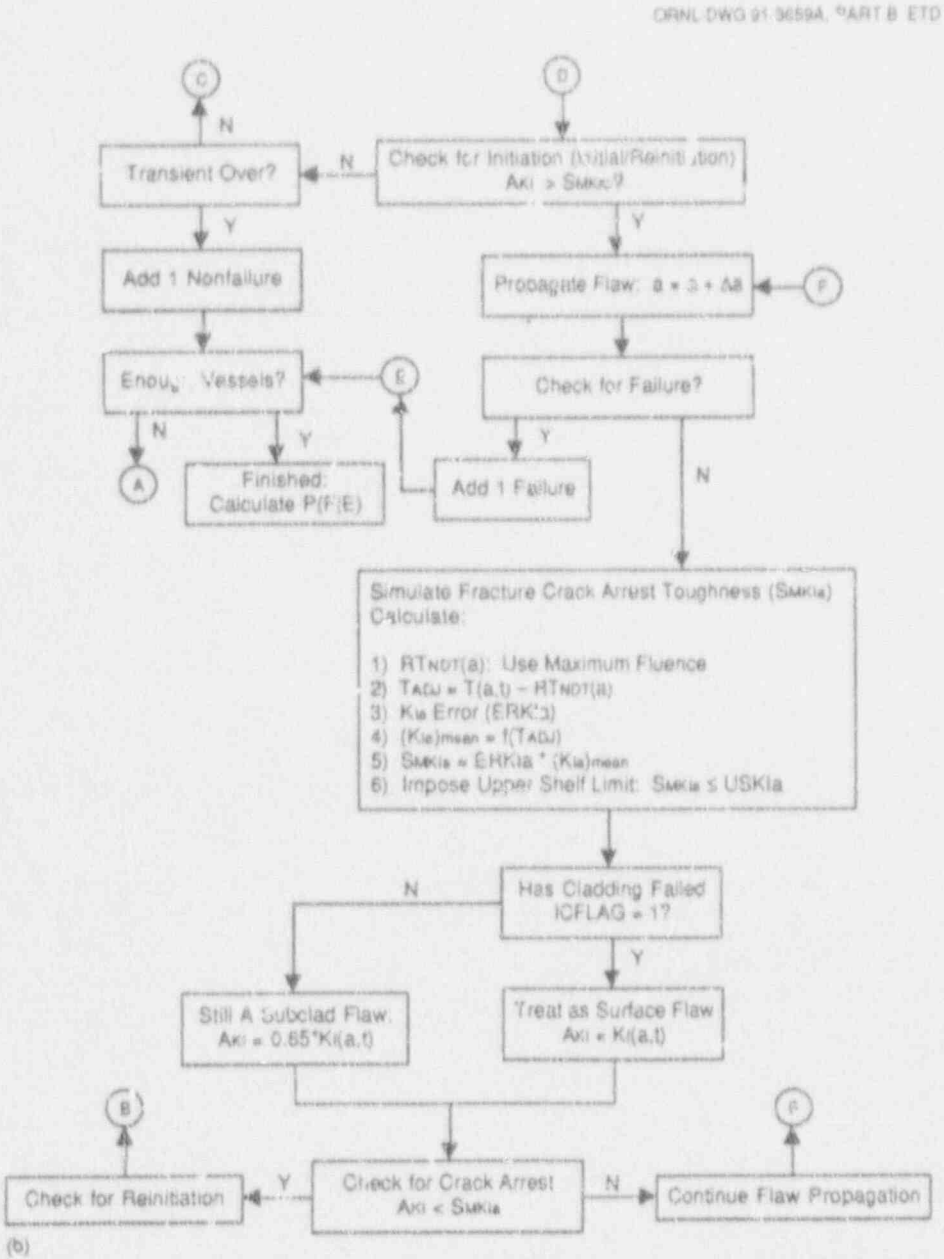


Figure 4.2 (continued)

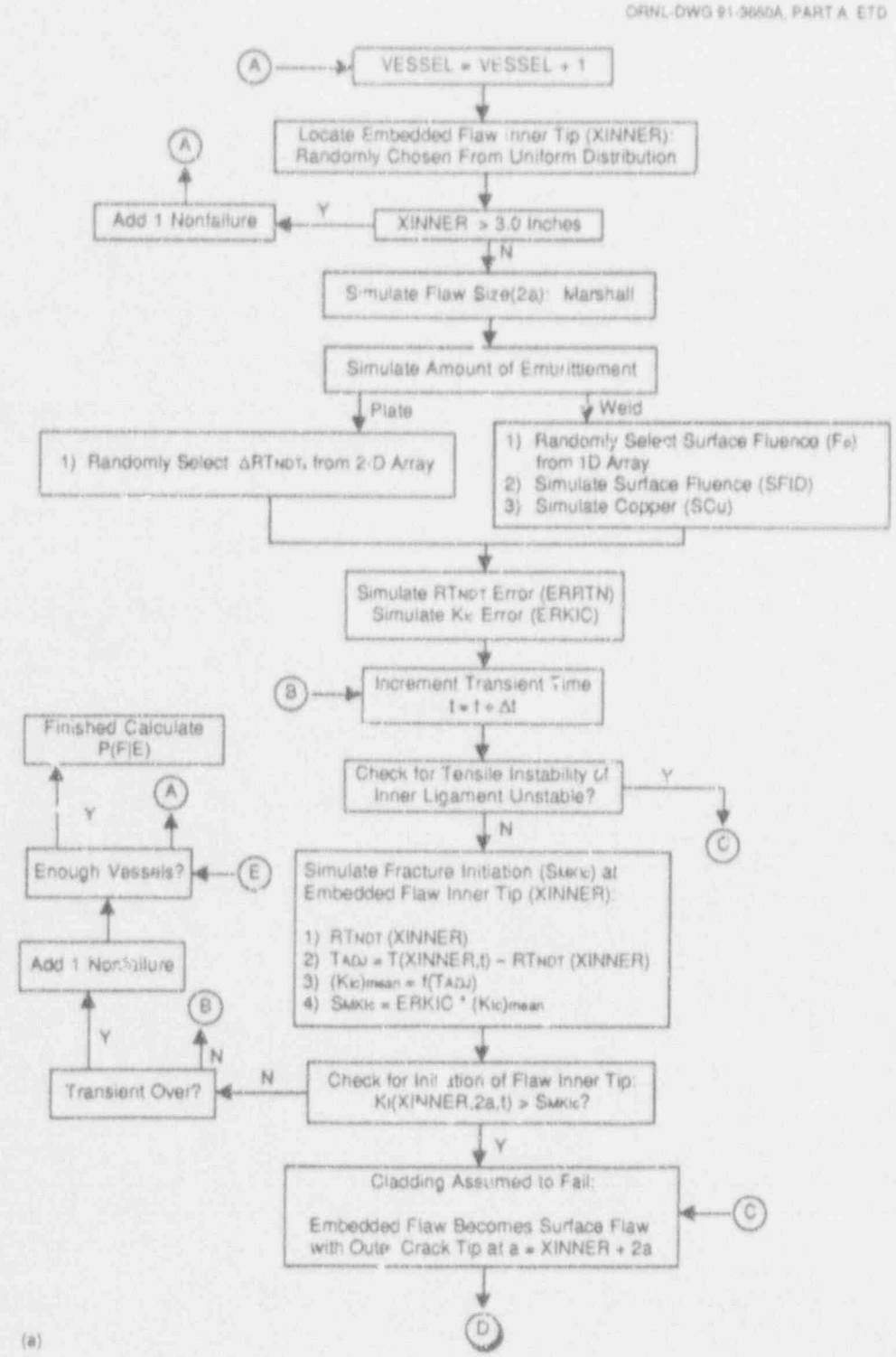


Figure 4.3 Probabilistic fracture-mechanics methodology for embedded flaws

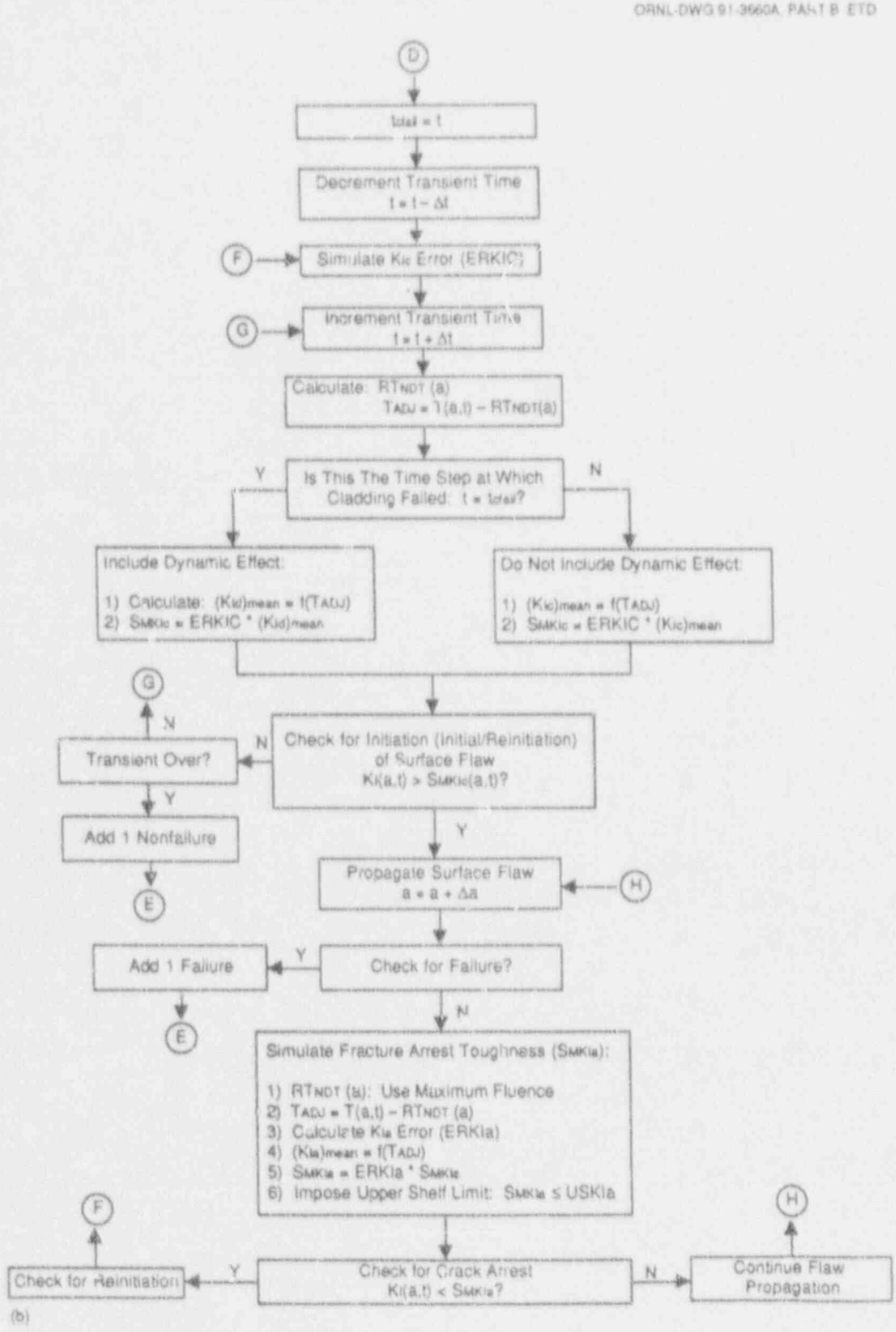


Figure 4.3 (continued)

## 4.2 Review of Inglis' Analysis for the Cases of Equibiaxial and Uniaxial Loading of a Through Crack in a Wide Plate (J. G. Merkle)

### 4.2.1 Introduction

Circumferentially oriented cracks in pressure vessels are subject to positive transverse strains. To gain an improved understanding of the effects of positive transverse strains on fracture toughness, it is necessary to determine the effect of biaxial nominal stresses on the near-crack-tip stress and strain field. Most fracture mechanics analyses are performed on the basis of near-crack-tip stress distributions, which are only the universal singular portions of the unique complete solutions for individual geometries. In most cases, this approach suffices. However, for estimating constraint effects, it may be necessary to employ complete solutions to take into account nonsingular differences between the near-crack-tip principal stresses. Such solutions for elastic conditions have been found by Inglis[8] for a through crack in a wide plate, by Sneddon[9] and Bell[10] for a buried circular crack, and by Green and Sneddon[11] for a buried elliptical crack. The results obtained by Inglis provide an opportunity to study the effects of the in-plane horizontal applied stress on triaxial constraint. However, Inglis presented a final algebraic solution only for the case of equibiaxial tensile loading. In a discussion in ASTM STP 381, Liu[12] presented results for the uniaxial case graphically, as shown in Fig. 4.4, but not analytically. Therefore, the object of this study is to derive both the biaxial and the uniaxial load case stress distributions, on $\beta = 0°$, from the equations given by Inglis.

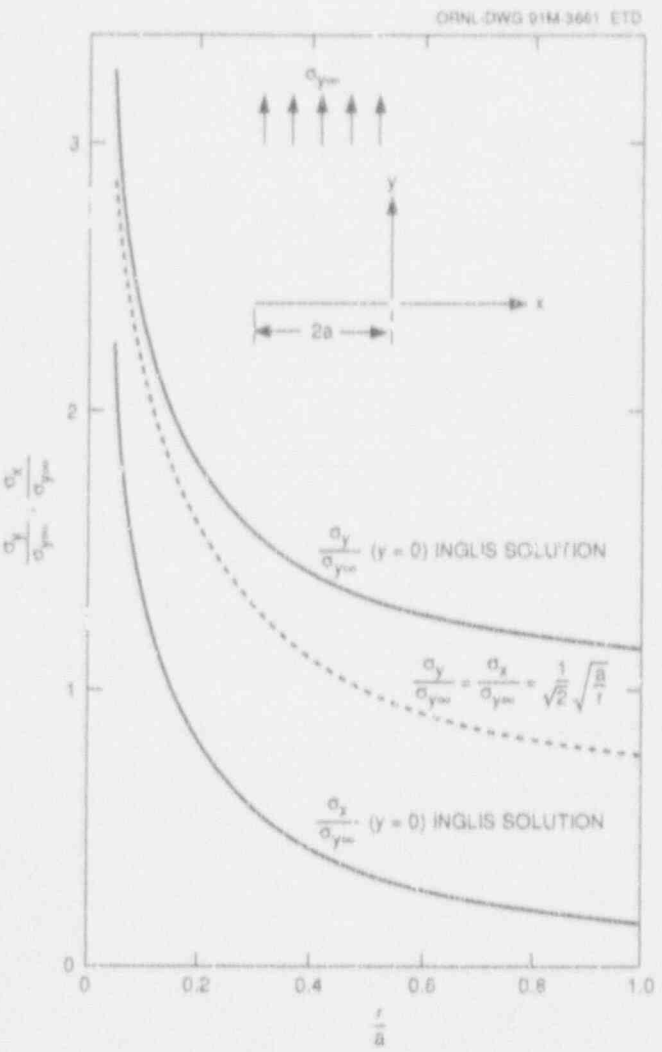


**Figure 4.4 Comparison of Inglis' complete solution for crack-tip stresses in uniaxially loaded center-cracked plate with one-term LEFM approximation**

Inglis[8] analyzed the stresses around an elliptical hole in an elastic flat plate under arbitrary biaxial loading. The primary coordinate system used was a curvilinear coordinate system consisting of concentric ellipses and orthogonal hyperbolae, all having the same focal distance, denoted by c. On each ellipse, the parameter $\alpha$ is constant, and on each hyperbola the parameter $\beta$ is constant. The parameter $\beta$ is also the parametric angle of the ellipses.

In a rectangular coordinate system, the coordinate axes x and y are the lines along which only x and y vary, respectively. In a curvilinear coordinate system it is not possible to establish coordinate values for arbitrary points with only two curves because the lines of constant coordinate values are neither parallel nor of identical shape. Therefore, a network of isoparameter lines (coordinate lines) must be drawn and used as the primary graphical expression of coordinates. This fact has a bearing on the definition of subscripts for stresses. In rectangular coordinates, $\sigma_{ij}$ means the stress on the plane normal to the i axis, acting in the j direction. In curvilinear coordinates, $\sigma_{ij}$ means the stress acting on the plane normal to which only the coordinate i changes, acting in the direction in which only the coordinate j changes. The meaning is the

same in both cases, but in the latter case the wording must be modified to remain accurate. Inglis[8] used the symbol R for the remotely applied stress normal to the crack plane. In this discussion, that stress will be represented by the symbol $\sigma_{y\infty}$. Referring to Fig. 4.5, and using the subscript definitions just explained, on $\beta = 0°$,

$$R_{\beta\beta} = \sigma_y \tag{4.1}$$

and

$$R_{\alpha\alpha} = \sigma_x \ . \tag{4.2}$$

### 4.2.2 Equibiaxial Loading

Inglis[8] included the stress equations for this case in his paper. On $\beta = 0°$, the principal stresses are

$$\sigma_y = \frac{\sigma_{y\infty}\sinh 2\alpha(\cosh 2\alpha + \cosh 2\alpha_o - 2)}{(\cosh 2\alpha - 1)^2} \tag{4.3}$$

and

$$\sigma_x = \frac{\sigma_{y\infty}\sinh 2\alpha(\cosh 2\alpha - \cosh 2\alpha_o)}{(\cosh 2\alpha - 1)^2} \ . \tag{4.4}$$

For an ellipse, the focal distance, c, and the semimajor and semiminor axes, a and b, respectively, are related by

$$c^2 = a^2 - b^2 \ . \tag{4.5}$$

For a crack, $b = 0$ and therefore $c = a$.

Therefore, on the plane $\beta = 0$,

$$x = a \cosh \alpha \ , \tag{4.6}$$

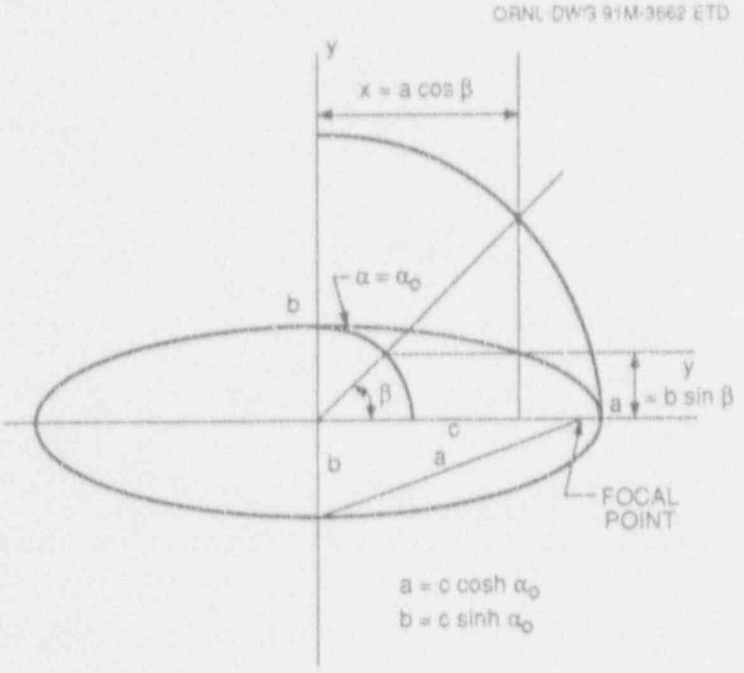


**Figure 4.5** Coordinate definition for Inglis' analysis

from which it follows that

$$\cosh\alpha = \frac{x}{a} \qquad (4.7)$$

and

$$\cosh\alpha_o = 1 \ . \qquad (4.8)$$

Because

$$\cosh 2\alpha = 2\cosh^2\alpha - 1 \ , \qquad (4.9)$$

$$\cosh 2\alpha_o = 1 \ , \qquad (4.10)$$

and substituting Eq. (4.10) into Eqs. (4.3) and (4.4), it can be seen that $\sigma_x = \sigma_y$ on $\beta = 0$.

Because

$$\sinh 2\alpha = 2\cosh\alpha\sqrt{\cosh^2\alpha - 1} \ , \qquad (4.11)$$

it follows, by using Eq. (4.7), that

$$\sinh 2\alpha = 2\left(\frac{x}{a}\right)\sqrt{\left(\frac{x}{a}\right)^2 - 1} \ , \qquad (4.12)$$

and, from Eqs. (4.7) and (4.9),

$$\cosh 2\alpha = 2\left(\frac{x}{a}\right)^2 - 1 \ . \qquad (4.13)$$

Substituting Eqs. (4.10), (4.12), and (4.13) into Eqs. (4.3) and (4.9) gives

$$\frac{\sigma_y}{\sigma_{y\infty}} = \frac{\sigma_x}{\sigma_{x\infty}} = \frac{\left(\frac{x}{a}\right)}{\sqrt{\left(\frac{x}{a}\right)^2 - 1}} \ . \qquad (4.14)$$

An alternate expression can be obtained by using

$$x = a + r \ , \qquad (4.15)$$

where r is distance from the crack tip. Substituting Eq. (4.15) into Eq. (4.14) gives

$$\frac{\sigma_y}{\sigma_{y\infty}} = \frac{\sigma_x}{\sigma_{x\infty}} = \frac{\left(1 + \frac{r}{a}\right)}{\sqrt{2\frac{r}{a} + \left(\frac{r}{a}\right)^2}} \ , \qquad (4.16)$$

which agrees with a result given by Paris and Sih[13] in ASTM STP 381.

### 4.2.3 Uniaxial Loading

Inglis' paper[8] contains a general set of equations, from which the stress components in a plate containing an elliptical hole can be obtained, once a set of multiplying coefficients representing particular stress boundary conditions are determined. Since Inglis gave the coefficients for uniaxial loading, it is straightforward to obtain the principal stress equations for $\beta = 0$. The results are

$$\frac{\sigma_y}{\sigma_{y\infty}} = \frac{\left(1 + \frac{r}{a}\right)}{\sqrt{2\frac{r}{a} + \left(\frac{r}{a}\right)^2}} \ , \qquad (4.17)$$

the same as for the equibiaxial case, and

$$\frac{\sigma_x}{\sigma_{y\infty}} = \frac{\sigma_y}{\sigma_{y\infty}} - 1 \ . \qquad (4.18)$$

Liu's curves[12] in Fig. 4.4 agree with Eqs. (4.17) and (4.18). These results are evidence of the geometry and load-type dependent nonsingular horizontal T-stress, familiar to photoelasticians,[14] now under widespread analytical investigation.

## References


1. R. D. Cheverton and D. G. Ball, Union Carbide Corp. Nuclear Division, Oak Ridge Natl. Lab., "OCA-P, A Deterministic and Probabilistic Fracture Mechanics Code for Application to Pressure Vessels," USNRC Report NUREG/CR-3618 (ORNL-5991), May 1984.*

2. D. L. Selby et al., Martin Marietta Energy Systems Inc., Oak Ridge Natl. Lab., "Pressurized Thermal Shock Evaluation of the H. B. Robinson Nuclear Power Plant," USNRC Report NUREG/CR-4183 (ORNL/TM-9567), September 1985.*

3. R. D. Cheverton et al., Martin Marietta Energy Systems, Inc., Oak Ridge Natl. Lab., "Pressure Vessel Fracture Studies Pertaining to the PWR Thermal Shock Issue: Experiment TSE-7," USNRC Report NUREG/CR-4304 (ORNL-6177), July 1985.*

4. *The American Society of Mechanical Engineers Boiler and Pressure Vessel Code*, Section XI, Rules for Inservice Inspection of Nuclear Power Plant Components, Appendix A, Analysis of Flaws, Article A-3000, Method for $K_I$ Determination, 1989.†

5. W. J. McAfee et al., "A Specimen and Method for Evaluating the Effect of Cladding on the Behavior of Subclad Flaws," ASME Pressure Vessel and Piping, PVP Vol. 213/MPC Vol. 32—Pressure Vessel Integrity, American Society of Mechanical Engineers, June 1991.†

6. K. J. Bathe, Massachusetts Institute of Technology, "ADINAT—A Finite Element Program for Automatic Dynamic Incremental Nonlinear Analysis of Temperatures," December 1978.†

7. R. C. Cipolla et al., Electric Power Research Institute, "Computational Method to Perform the Flaw Evaluation Procedure as Specified in the ASME Code, Section XI, Appendix A," EPRI Report NP-1181, September 1979.†

8. C. E. Inglis, "Stresses in a Plate Due to the Presence of Cracks and Sharp Corners," *Transactions of the Institute of Naval Architects* (British), Vol. 55, pp. 219–230, 1913; also *Engineering* (London) 95, 413 (1913); reprinted in Fracture Mechanics Retrospective, Early Classic Papers (1913–1965), ASTM RS-1, J. M. Barsom, Ed., American Society for Testing and Materials, 1987.†

9. I. N. Sneddon, "The Distribution of Stress in the Neighborhood of a Crack in an Elastic Solid," pp. 229–260 in *Proc. of the Royal Society, London*, Series A, Vol. 187, London, England, 1946.†

10. J. Clarence Bell, "Stresses from Variously Loaded Circular Cracks," Paper No. 12752, *Journal of the Structural Division*, ASCE, ST2, February 1977, pp 355-376.†

11. A. E. Green and I. N. Sneddon, "The Distribution of Stress in the Neighborhood of a Flat Elliptical Crack in an Elastic Solid," pp. 159–163 in *Proc. of the Cambridge Philosophical Society*, Vol. 46, 1950.†

12. H. W. Liu, Discussion of paper by V.Weiss and S. Yukawa entitled, "Critical Appraisal of Fracture Mechanics," pp. 23-29 in *Fracture Toughness Testing and Its Applications*, ASTM STP 381, American Society for Testing and Materials, Philadelphia, 1965.†

13. P. C. Paris and G. C. Sih, "Stress Analysis of Cracks," pp. 30-83 in *Fracture Toughness Testing and Its Applications*, ASTM STP 381, American Society for Testing and Materials, Philadelphia, 1965.†

14. M. A. Schroedl and C. W. Smith, "Local Stresses Near Deep Surface Flaws Under Cylindrical Bending Fields," pp. 45-63 in *Progress in Flaw Growth and Fracture Toughness Testing*, ASTM STP 536, American Society for Testing and Materials, Philadelphia, 1973.†

---

*Available for purchase from National Technical Information Service, Springfield, VA 22161.

†Available in public technical libraries.

# 5 Fracture Analysis Computer Programs

T. L. Dickson*

## 5.1 Background Information

No specific tasks were performed under this task during this reporting period; however, the OCA-P code was considerably enhanced to meet the specified objectives of NRC in performing the Pressurized-Thermal-Shock Probabilistic Fracture Mechanics (PTS PFM) Sensitivity Analysis for the Yankee Rowe reactor pressure vessel.† Refer to Task 4.0 for more details of the methods used in the Yankee Rowe PTS PFM Sensitivity Analysis.

It is anticipated that the enhancements performed to OCA-P for this specific study will be further refined and generalized and will become part of the FAVOR (Fracture Analysis of Vessels: Oak Ridge) PTS PFM code to be developed under this task beginning in FY 1992.

## 5.2 Enhancements

Specific enhancements to the OCA-P code for the Yankee Rowe study anticipated to become part of the FAVOR code development include the ability to model variational fluence fields, subclad flaws, and embedded flaws. Another enhancement is the revision of the user input and output data formats for probabilistic fracture mechanics analyses, aiming to make the program more "user friendly" and to provide better documentation (an audit trail) of the results of the PTS PFM analysis; this enhancement is anticipated to be considerably refined during the next year.

Additional PFM postprocessing capability has also been added to the PFM code. This capability enables the user to examine what combinations of parameters tend to dominate initial initiations, reinitiations, crack arrests, and stable (terminating event) crack arrests.

---

*Computing and Telecommunications Division, Martin Marietta Energy Systems, Inc., Oak Ridge, Tenn.

†T.L. Dickson et al., Martin Marietta Energy Systems, Inc., Oak Ridge Natl. Lab., "Oak Ridge National Laboratory Pressurized-Thermal-Shock Probabilistic Fracture Mechanics Sensitivity Analysis for Yankee Rowe Reactor Pressure Vessel," USNRC Report NUREG/CR-5782 (ORNL/TM-11945) (to be published February 1992).

# 6 Cleavage-Crack Initiation

T. J. Theiss

This task emphasizes cleavage initiation toughness and the specimens used to evaluate cleavage fracture toughness. Begun in FY 1990, the task is currently divided into four subtasks: (6.1) Shallow-Crack Fracture-Toughness Testing, (6.2) Lower-Bound Initiation Toughness, (6.3) Gradient Effects on Fracture Toughness, and (6.4) Thickness Effects on Fracture. The fourth subtask was added at the midyear review to study the influence of thickness on toughness by testing six additional deep-crack beams with varying thicknesses. The testing portion of subtasks 6.1 and 6.4 is reported as part of Task 10, Fracture Evaluation Tests. In conjunction with the shallow-crack fracture-toughness testing program, HSST continued support for the joint Edison Welding Institute (EWI) and The Welding Institute (TWI) project to develop shallow-crack fracture-mechanics tests.

## 6.1 Shallow-Crack Fracture-Toughness Testing (T. J. Theiss and S. T. Rolfe)

The current testing portion of the shallow-crack program is divided into two phases: development and production.[1] During the development phase, the experimental techniques necessary for shallow-crack testing are to be verified. A limited data base of shallow-crack fracture-toughness values appropriate for application to RPV analyses will be generated as part of the production phase. During the previous reporting period, the development phase of the experimental shallow-crack program was completed and discussed.[2] Additional interpretation of the development phase data is reported herein. Previous shallow-crack work has been detailed in prior semiannual reports and in open literature.[2–4] Chapter 10, Fracture Evaluation Tests, reports details of the testing. The FY 1991 portion of the production beams was begun and completed during this reporting period.

### 6.1.1 Rotation Factor Development

The plastic component of CTOD is determined experimentally from the plastic component of CMOD and the rotation factor. The plastic displacement of the crack flanks is assumed to vary linearly with distance from the plastic center of rotation. In this way, the plastic CMOD can be related to the plastic CTOD. The plastic center of rotation is located ahead of the crack tip at a distance equal to the rotation factor (RF) multiplied by the remaining ligament (W-a).[5] Numerous experimental and analytical techniques have been used to determine the rotation factor,[5–12] although no single technique seems to be universally accepted and the various experimental and analytical determinations sometimes appear contradictory,[7] especially for shallow-crack specimens. The rotation factor in ASTM E1290 is given to be 0.4 but is a function of specimen geometry and material.

In the HSST shallow-crack study, two experimental methods were used to determine the rotation factor. The first method used dual clip gages located at different distances from the crack mouth. Clip gages were mounted directly on the crack mouth and elevated 8.89 mm (0.35 in.) above the crack mouth. The second technique located the neutral axis of the beam ahead of the crack tip using strain gages, assuming that the plastic center of rotation was located at the neutral axis of the beam. Because the rotation factor relates the plastic component of CMOD to the plastic component of CTOD, only plastic strains were used to determine the rotation factor. The dual clip gage technique produced values of the rotation factor that varied significantly from 0.4 and were not constant as a function of load. However, the rotation factors determined using the strain-gage technique were close to 0.4 and were relatively insensitive to load once plastic strains became nontrivial. The rotation factors from strain gages were averaged for the deep- and shallow-crack geometries and were used in the CTOD calculations. The average rotation factor varied from 0.46 for the deep-crack specimens to 0.50 for the shallow-crack specimens. Individual values of the rotation factor using both techniques are shown in Table 6.1. The rotation factor used for the CTOD toughness calculations is the average of the values from the strain-gage technique for each crack depth as shown in Table 6.1.

A parametric evaluation was performed to assess the sensitivity of CTOD toughness on the rotation factor. This evaluation indicated that the plastic component of CTOD is not overly sensitive to the value of the rotation factor. Shallow-crack beams are less sensitive to the rotation factor than deep-crack beams. A 25% increase in rotation factor increases the plastic CTOD by about 5 and 17% for the shallow- and deep-crack geometries, respectively. The rotation factor is insensitive to beam thickness and absolute beam dimensions, varying only with a/W ratios for a given material.

Table 6.1 Rotation factor data

| HSST beam | a/W | Strain gages | Dual clip gages |
|---|---|---|---|
| 3 | 0.10 | 0.48 | 0.64 |
| 4 | 0.52 | N/A[a] | N/A |
| 5 | 0.52 | N/A | N/A |
| 6 | 0.52 | N/A | N/A |
| 7 | 0.11 | N/A | N/A |
| 8 | 0.10 | 0.53 | 0.64 |
| 9 | 0.10 | 0.47 | N/A |
| 10 | 0.15 | N/A | 4.07 |
| 11 | 0.089 | 0.50 | 9.64 |
| 12 | 0.53 | 0.40 | 0.00 |
| 13 | 0.094 | N/A | 0.73 |
| 14 | 0.094 | 0.48 | N/A |
| 15 | 0.092 | 0.52 | N/A |
| 16 | 0.53 | 0.52 | 2.35 |
| | Average deep | 0.46 | |
| | Average shallow | 0.50 | |

[a] N/A = not applicable.

### 6.1.2 Development Phase

The CTOD fracture toughness for the development beams has been updated to reflect the latest rotation factor determinations and checks of the test data. Table 6.2 includes a summary of the critical CTOD toughness, $\delta_c$, and supporting data. These data have been checked and verified and are included in the test reports now issued for each development beam test. Chapter 10 includes additional information on the test reports and includes a representative report (Appendix 10.1).

Fracture toughness was determined for each beam in terms of the J integral using two slightly different techniques. Little or no crack growth took place in these tests, so ASTM E813 is not strictly applicable. In the first technique, J was computed using a total energy approach utilizing the total area under the load vs load-line-displacement (LLD) curve and a single $\eta$ factor estimated from finite-element analyses of the HSST deep- and shallow-crack beams. The second technique calculates J by dividing the elastic and plastic components of energy, using only the plastic component of area under the load vs LLD curve and a plastic $\eta$ factor.[7] The equations[7] used to determine the J-integral toughness follow:

$$J_c = J_{el} + J_{pl} \quad , \tag{6.1}$$

where

$$J_{el} = K_c^2(1 - \nu^2)/E \quad , \tag{6.2}$$

$$J_{pl} = \eta_{pl} U_{pl}/[B(W - a)] \quad , \tag{6.3}$$

The two J-integral techniques gave reasonably close values of J-integral toughness, averaging about ±10% different. However, the second technique yielded more consistent values of J as a function of thickness. Thus, the J-integral toughness values using the divided energy technique are considered more reliable; these are given in Table 6.3 and included in the test reports.

Examination of the data in Tables 6.2 and 6.3 shows that $J_c$ toughness values are consistent with the $\delta_c$ calculations. The $J_c$ ratio of the mean shallow-crack toughness to deep-crack toughness is 2.8 for the beams tested at –60°C (–76°F). The ratio of the shallow-to-deep lower-bound toughness is 2.0, which is consistent with the shallow-crack elevated toughness expressed in terms of CTOD.

Because $J_c$ and $\delta_c$ are related according to $J_c = m \times \sigma_f \times \delta_c$,[13] comparing $J_c$ and $\delta_c$ allows m, the constraint parameter, to be determined as a function of crack depth. Plots of J vs CTOD show a linear relationship between the two toughness expressions. The constraint parameter, m, for each test was determined using the critical toughness ($J_c$ and $\delta_c$) and the estimated flow stress $\sigma_f$. Use of the critical toughness is in keeping with Sumpter's contention that $\eta_{pl}$ is valid only for a perfectly plastic material after limit load.[7] Table 6.3 shows the constraint values calculated for each test. The average constraint parameter was 1.6 for deep-crack specimens and 1.1 for shallow-crack specimens.

Although the J-integral and CTOD toughness expressions are generally consistent with each other, the CTOD toughness was considered more reliable than the J integral because the experimental load vs CMOD records were more consistent and repeatable than the load vs LLD records. The previous semiannual (October 1990–March 1991) included $K_c$ estimates that computed the shallow-

Table 6.2 HSST development beam data with CTOD toughness[a]

| HSST beam | Temperature (°C) | S (mm) | B (mm) | W (mm) | a (mm) | a/W | Measured elastic compliance (mm/kN) | Failure load (kN) | Measured failure CMOD (mm) | Toughness CTOD (mm) |
|---|---|---|---|---|---|---|---|---|---|---|
| 3 | –35.6 | 406 | 50.6 | 99.7 | 10.0 | 0.101 | $3.09 \times 10^{-4}$ | 600 | 0.808 | 0.59 |
| 4 | –60.6 | 406 | 50.7 | 99.5 | 51.8 | 0.520 | $3.38 \times 10^{-3}$ | 128 | 0.461 | 0.048 |
| 5 | –55.3 | 406 | 50.6 | 99.1 | 51.2 | 0.517 | $3.14 \times 10^{-3}$ | 140 | 0.442 | 0.049 |
| 6 | –59.2 | 406 | 50.6 | 99.5 | 51.9 | 0.522 | $3.52 \times 10^{-3}$ | 185 | 0.758 | 0.12 |
| 7 | –59.4 | 406 | 50.7 | 94.2 | 10.2 | 0.108 | $3.27 \times 10^{-4}$ | 483 | 0.250 | 0.14 |
| 8 | –59.5 | 406 | 50.8 | 94.2 | 9.63 | 0.102 | $3.12 \times 10^{-4}$ | 657 | 0.652 | 0.48 |
| 9 | –62.3 | 406 | 50.9 | 94.0 | 9.52 | 0.101 | $3.09 \times 10^{-4}$ | 552 | 0.508 | 0.35 |
| 10 | –60.2 | 406 | 50.9 | 94.3 | 14.0 | 0.149 | $4.77 \times 10^{-4}$ | 489 | 0.434 | 0.24 |
| 11 | –56.7 | 864 | 102 | 93.9 | 8.36 | 0.0890 | $3.08 \times 10^{-4}$ | 472 | 0.312 | 0.20 |
| 12 | –56.7 | 864 | 102 | 94.7 | 49.8 | 0.526 | $4.44 \times 10^{-3}$ | 117 | 0.574 | 0.061 |
| 13 | –59.6 | 864 | 102 | 94.0 | 8.81 | 0.0938 | $3.29 \times 10^{-4}$ | 502 | 0.514 | 0.36 |
| 14 | –57.4 | 864 | 152 | 92.5 | 8.69 | 0.0939 | $2.25 \times 10^{-4}$ | 723 | 0.504 | 0.35 |
| 15 | –58.5 | 864 | 153 | 94.5 | 8.66 | 0.0917 | $2.14 \times 10^{-4}$ | 684 | 0.257 | 0.15 |
| 16 | –57.8 | 864 | 153 | 94.0 | 50.0 | 0.532 | $2.81 \times 10^{-3}$ | 170 | 0.530 | 0.060 |

[a]Notes: Rotation factors given in Table 6.1. Yield stress = 476 MPa at T = –60°C and 440 MPa at T = –35°C. The yield stress was estimated from room-temperature values and adjusted for the lower temperatures. E = 206,850 MPa, ν = 0.3.

and deep-crack toughness in the same manner.[2] This technique tends to overestimate the shallow-crack toughness. For these reasons, $K_c$ was calculated[13] from CTOD using the following relation:

$$K_c = (m \times \sigma_f \times E' \times \delta_c)^{1/2} , \qquad (6.4)$$

where m = 1.6 and $E' = E/(1 - \nu^2)$ for deep-crack specimens, and m = 1.1 and E′ = E for shallow-crack specimens.

The plane-strain value of E′ was used for the deep-crack specimens in spite of not meeting the validity requirements of ASTM E399 because the experimental data in this program indicate little or no influence of beam thickness on the data. Table 6.4 gives the toughness of each beam in terms of $K_c$. The ratio of shallow-to-deep toughness in terms of $K_c$ is approximately equal to the square root of the ratio in terms of CTOD. The lower-bound, shallow-crack toughness is ≈60% greater than the lower-bound, deep-crack toughness at –60°C. The spread of the data is also reduced, expressing the toughness in terms of $K_c$.

For comparison, $K_c$ was calculated directly from the J-integral values in Table 6.4 in addition to using CTOD and Eq. (6.4). The two methods of determining $K_c$ are very consistent. The maximum difference between $K_c$ using the two techniques was 12%; the average difference was <5%.

The previous semiannual report[2] includes estimates of the plane-strain toughness from the deep- and shallow-crack data using the Irwin $\beta_c$ correction. In addition, the $\beta_c$ correction was modified to "predict" the shallow-crack toughness from deep-crack data with good success. These calculations have been repeated using the updated $K_c$ calculations, and the results are not as promising as previously believed. The agreement between "predicted" and actual shallow-crack toughness is reasonably good, although the modified $\beta_c$ correction tends to overestimate the actual shallow-crack toughness. The actual $K_c$, adjusted $K_c$, and "predicted" shallow-crack $K_c$ values are given in Table 6.4.

Table 6.3 J-integral toughness and constant parameter, m, determination

| | ...lastic ... | $\eta_{pl}$ | $J_c$ (MPa-mm) | $\sigma_f$ (MPa) | m |
|---|---|---|---|---|---|
| ... | | 1.13 | 260 | 525 | 0.87 |
| 4 | | 2.00 | 42 | 558 | 1.6 |
| | 4.1 | 2.00 | 48 | 550 | 1.8 |
| | ... | 2.00 | 100 | 556 | 1.6 |
| 7 | | 1.16 | 92 | 556 | 1.2 |
| 8 | | 1.14 | 280 | 556 | 1.1 |
| 9 | 372 | 1.13 | 170 | 561 | 0.89 |
| ... | 187 | 1.34 | 140 | 557 | 1.1 |
| 11 | 376 | 1.07 | ... | 552 | 0.97 |
| 12 | 16.9 | 2.00 | 50 | 552 | 1.5 |
| 13 | 1134 | 1.09 | 210 | 556 | 1.1 |
| 14 | 1876 | 1.09 | 230 | 552 | 1.2 |
| 15 | 400 | 1.08 | ... | 552 | 1.1 |
| 16 | 10.7 | 2.00 | 46 | 556 | 1.4 |
| | | | | m (deep) = | 1.6 |
| | | | | m (shallow) = | 1.1 |

Table 6.4 Actual and "predicted" toughness values using modified Irwin $\beta_c$ correction[a]

| HSST beam | $K_c$ actual (MPa·$\sqrt{m}$) | $K_{Ic}$ (MPa·$\sqrt{m}$) | $K_c$ predicted (MPa·$\sqrt{m}$) |
|---|---|---|---|
| 4 | 99 | 81 | 127 |
| 5 | 99 | 81 | 129 |
| 6 | 153 | 102 | 127 |
| 12 | 111 | 98 | 103 |
| 16 | 110 | 105 | 98 |
| Average deep flaw | 114 | 93 | 117 |
| 7 | 131 | 74 | 235 |
| 8 | 244 | 93 | 246 |
| 9 | 211 | 88 | 245 |
| 10 | 172 | 91 | 181 |
| 11 | 156 | 75 | 282 |
| 13 | 212 | 86 | 265 |
| 14 | 208 | 85 | 271 |
| 15 | 135 | 103 | 271 |
| Average shallow flaw | 184 | 87 | 250 |

[a]Notes: Average of deep-crack adjusted values was used to "predict" toughness for shallow-flaw specimens. Only tests conducted at T ≤ -60°C are included.

### 6.1.3 Production Phase

The production phase of the shallow-crack program was initiated during this reporting period. A total of 18 production beams have been tested. Additional testing information, including the test matrix in Table 10.2, is supplied in Chap. 10. The goal of the production phase of tests is to produce a limited data base of toughness values appropriate for reactor vessel analyses with shallow flaws. This objective is being fulfilled by testing deep- and shallow-crack beams primarily in the lower transition region. The temperature limits between which a shallow-crack beam would exhibit the increase in toughness need to be determined.

All beams tested to date have been cut from the center portion of the source plate (HSST Plate 13B) where the material properties are homogeneous. It is planned that some shallow-crack beams will be taken from the surface portion of Plate 13B where metallurgical gradients exist that further increase the fracture toughness (i.e., "skin effects"). Surface material is being sampled in these tests because shallow surface flaws in a reactor vessel would be located in material possessing a similar skin effect.

Data analysis to determine the CTOD and J-integral toughness consistent with that performed for the development beam tests has not yet been performed. However, preliminary estimates of the production beam tests indicate results consistent with the development phase tests. The production phase tests are being conducted at multiple temperatures; these indicate that the shallow-crack toughness curve is similar in shape to the deep-crack toughness curve but is shifted about 13°C (55°F). Shallow crack beams have been tested on the lower shelf and, as expected, showed linear, elastic behavior with no toughness increase. Figure 6.1 shows the results of all of the shallow-crack testing and the six additional deep-crack beam (see Sect. 6.4) tests in terms of $K_c$ vs temperature. The CTOD toughness is converted to $K_c$ using the technique described in the previous semiannual. The development beam tests use the same conversion to $K_c$ to show the consistency

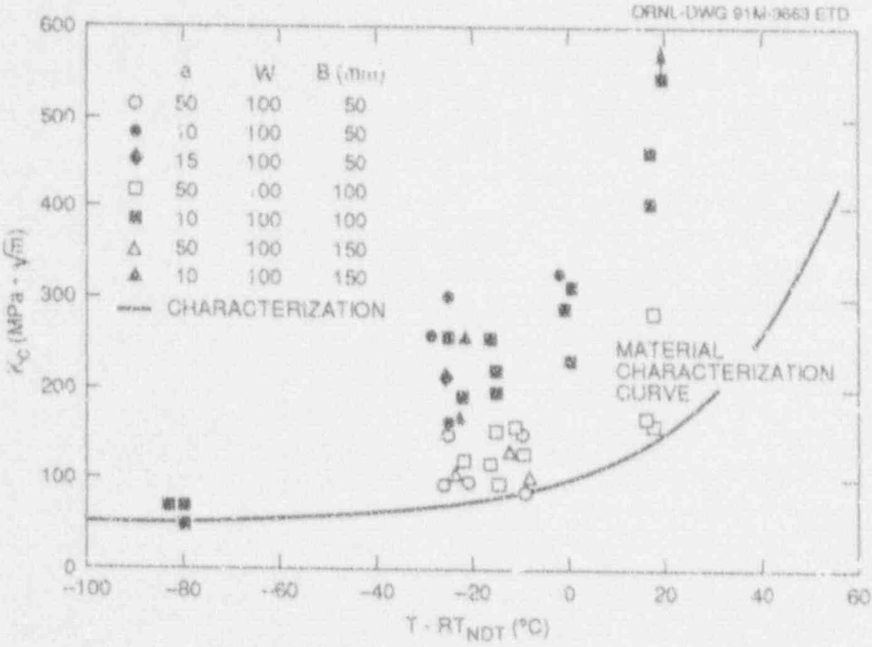


**Figure 6.1 Preliminary $K_c$ vs temperature toughness data**

between the development and production beam results. Additional analyses will be conducted to calculate J-integral toughness and the constraint parameter, m, for the production beams to refine the $K_c$ toughness values.

### 6.1.4 Future Work

The application of the shallow-crack, fracture-toughness data to reactor vessel analyses remains the final goal of the program. To reach that goal, more specimens should be tested with multiple crack depths and at several temperatures within the transition region. Comparisons between shallow-crack beams taken from center and surface portions of the source plate should be made. The results generated to date are encouraging but not conclusive as to how to apply the data to an RPV. Prior experimental work within the HSST Program has included tests on thick-walled vessels containing relatively shallow flaws.[14] These tests offer a means to validate the technology for applying shallow-flaw toughness data to an RPV.

In addition, numerical analyses of the test specimen and the application (i.e., an axially oriented flaw in an RPV) need to be performed and interpreted. These analyses will provide a means for checking transferability of the test results to an RPV.

The fracture toughness of RPV weld and plate material needs to be determined in full-thickness clad specimens with shallow flaws under prototypic PTS conditions. Comparison of results from these tests with previous test results would provide a qualitative definition of the effect of near-surface conditions on fracture toughness.

## 6.2 Lower-Bound Initiation Toughness

(W. L. Fourney, G. R. Irwin, J. W. Dally, X. J. Zhang, and R. Bonenberger)

A new experimental method has been developed by the research group at the University of Maryland (UM) to measure the lower-bound initiation toughness in reactor-grade steel. The method uses two relatively small specimens (notched round bar and modified Charpy) subjected to dynamic loading as the fracture specimens.[2,15] Lower-bound initiation toughness is achieved through enhanced constraint in the specimens and dynamic loading. The notched round bar specimen provides enhanced constraint compared with similarly sized plate specimens. The modified Charpy specimen is side-grooved, which enhances the constraint.

A report on lower-bound initiation toughness values obtained from modified instrumental Charpy testing was delivered to the NRC during the reporting period.[16] A second report, which will cover the determination of lower-bound initiation toughness from notched round bars and the effects of precompression of these bars on the initiation toughness, will be delivered to ORNL in October 1991.

## 6.3 Gradient Effects on Fracture Toughness (G. R. Irwin, W. L. Fourney, X. J. Zhang, and T. J. Theiss)

The purpose of this subtask is to investigate the influence of metallurgical and thermal gradients on fracture toughness. Metallurgical gradients are known to exist and influence fracture toughness in large plates. The toughness as expressed in terms of the Drop-Weight Nil-Ductility Transition Temperature ($DW_{NDT}$) of the center portion of a large plate can be 65°C (120°F) less than the $DW_{NDT}$ of the surface portion of the same plate. Metallurgical gradients are important in considering shallow flaws in a reactor vessel because shallow flaws are located near the plate surface in the region of greatest metallurgical toughness. Thermal gradients have also been suggested as a possible influencing factor of fracture toughness.

Two separate studies are being conducted to investigate the influence of metallurgical gradients on fracture toughness. The material for the first metallurgical gradient study is from the Midland vessel and is taken from the nozzle course. The test piece is full thickness and includes cladding and a weld (WK-70 and WF-67 chemistry) section. The second study is being performed on AISI 1045 steel.

In the first study, metallographic examinations of the heavy-section slab, provided by ORNL, are in progress. After substantial wet-grinding, the slab surface was polished and etched. This permitted the selection of regions of special interest. Preliminary studies of inhomogeneity features, using microhardness indents and views at higher magnification, have been done. The ongoing work will center attention on metallurgical features related to fracture toughness.

A series of experiments is under way to examine the effect of metallurgical gradients on crack propagation and crack arrest behavior. The program plan is divided into three phases. Phase I consists of developing and analyzing suitable procedures for creating metallurgical gradients in steel specimens. In phase II, fracture tests (crack propagation, crack arrest and possibly dynamic reinitiation) will be performed to determine the respective fracture-toughness properties. Phase III will attempt to relate the microstructure, propagation toughness, and cleavage characteristics of the fracture surface by examining the fractured specimens with scanning electron microscopy.

The gradients in the specimen are developed by employing an unorthodox heat-treating procedure. This procedure, illustrated in Fig. 6.2, involves a nonuniform quench of a steel specimen. The illustration shows a bar of length L immersed in the quenching fluid to a depth d and held at this level until the temperature of the bar reaches equilibrium with the quenching fluid. This action will produce a wide variation in the quench rates at various locations on the specimen. At the quench end, the cooling rate will be very high, and significant amounts of martensite will be produced to give a very hard but brittle structure. At the other end of the bar, the cooling rate will

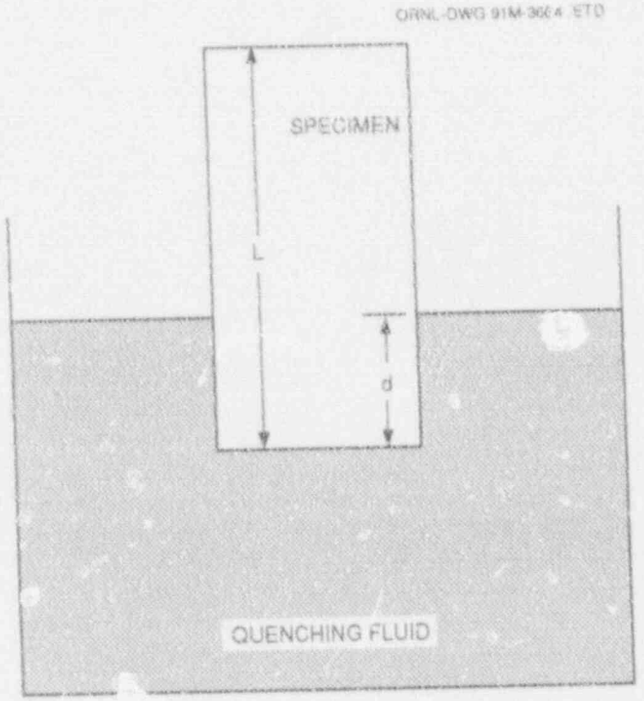


**Figure 6.2 Unorthodox quenching procedure being used in gradient study**

be very slow, and the structure will be similar to that generated by air cooling (normalized). The metallurgical structure at this end of the bar will be mostly pearlite. Between the two ends of the bar, the metallurgical structure should undergo a transition from a martensite-rich structure to one that is coarse pearlite.

Steel bars approximately 50 × 150 × 305 mm (2 × 6 × 12 in.) in size are being used to determine the effectiveness of the unorthodox heat-treating process in developing a gradient bar. Quenching is done in a water bath at room temperature [21°C (70°F)]. Following the quench, the hardness of the bar is determined at various cross sections along the length of the bar. Metallurgical specimens from different locations will be prepared, and the grain size and metallurgical structure will be identified with optical photomicrographs.

Initially, a medium carbon, hot-rolled steel (AISI 1045) is being employed in the heat-treating studies. This steel is available in hot-rolled bars of the correct size and can be used to establish heat-treating procedures that will be applicable to reactor-grade steels such as A 533 B. After the heat-treating procedures for the 1045 carbon steel are established, they will be adapted to A 533 B reactor-grade steel. This material will be provided to UM by ORNL. It is anticipated that this sample of material will be "characterized" so that its physical properties and fracture properties are known.

To date, one of the AISI 1045 steel specimens has been heat treated and studied. The maximum temperature attained during the heating operation was 784°C (1444°F), and the bar was submerged to a depth of 150 mm (6 in.) during the water quench. After quenching, the bar was sectioned transverse to its length, and hardness profiles were determined for many of these sections. A substantial hardness gradient was produced along the length of the specimen, ranging from 81 HRA (83 HRB) near the normalized end to 79 HRA (56 HRC) at the quenched end. Pronounced gradients also exist from the bar's surface to the interior at certain cross sections, especially the sections that were submerged in the quenching bath. This result is expected because the cooling rate at the surface, in contact with the water, is greater than the cooling rate at the interior of the bar. A complete hardness profile has not yet been determined due to difficulties encountered during sectioning of the specimen, particularly in the quenched region. Efforts are progressing on purchasing equipment for sectioning the very hard regions of the steel and for increasing the maximum temperature limit of the furnace.

## 6.4 Thickness Influence on Toughness

(T. J. Theiss)

At the midyear review, six deep-crack beams were added to the program to investigate the influence of thickness on fracture toughness. Information on the testing of these beams is included in Chap. 10. These beams complement the deep-crack beams in the development phase of the shallow-crack program by testing beams 50, 100, and 150 mm (2, 4, and 6 in.) thick at a separate temperature. It is generally accepted that the "validity" criteria in ASTM E399 place very stringent requirements on the beam thickness required for plane-strain fracture toughness. The deep-crack tests can provide experimental evidence of a more appropriate validity criteria if the results from tests of differing thicknesses give the same toughness in spite of not meeting the current criteria. Full analyses of these data are not available at this time; however, preliminary analysis indicates similar results comparing the deep-crack tests conducted at –60°C (–75°F) and those at –46°C (–50°F). The influence of beam thickness appears minimal at both temperatures, although the data exhibit scatter. Results from the six additional beam tests along with the preliminary development and production beam data are shown in Fig. 6.1.

## References

1. T. J. Theiss, Martin Marietta Energy Systems, Inc., Oak Ridge Natl. Lab., "Recommendations for the Shallow-Crack Fracture Toughness Testing Task Within the HSST Program," USNRC Report NUREG/CR-5554 (ORNL/TM-11509), August 1990.*

2. T. J. Theiss, Martin Marietta Energy Systems, Inc., Oak Ridge Natl. Lab., HSST Program Semiann. Prog. Rep. October 1990–March 1991, pp. 35–43, USNRC Report NUREG/CR-4219, Vol. 8, No. 1 (ORNL/TM-9593/V8&N1), February 1992.*

3. T. L. Dickson and T. J. Theiss, "Potential Impact of Enhanced Fracture-Toughness Data on Pressurized-Thermal-Shock Analysis," pp.35–53 in *Proc. of the U.S. Nuclear Regulatory Commission Eighteenth Water Reactor Safety Information Meeting, Rockville,*

*Md., October 22–24, 1990*, USNRC Report NUREG/CP-0114, Vol. 3, April 1991.*

4. T. J. Theiss, G. C. Robinson, and S. T. Rolfe, "Preliminary Test Results from the Heavy-Section Steel Technology Shallow-Crack Toughness Program," pp. 125–129 in *Proceedings of the ASME Pressure Vessel & Piping Conference*, PVP Vol. 213/MPC-Vol. 32, pp. 125-129, Pressure Vessel Integrity, ASME, 1991.†

5. W. A. Sorem, R. H. Dodds, Jr., and S. T. Rolfe, "An Analytical Comparison of Short Crack and Deep Crack CTOD Fracture Specimens of an A36 Steel," *WRC Bulletin 351*, Welding Research Council, New York, February 1990.†

6. J. A. Smith and S. T. Rolfe, "The Effect of Crack Depth to Width Ratio on the Elastic-Plastic Fracture Toughness of a High-Strength Low-Strain Hardening Steel," *WRC Bulletin 358*, Welding Research Council, New York, November 1990.†

7. J. D. G. Sumpter, "$J_c$ Determination for Shallow Notch Welded Bend Specimens," *Fatigue Frac. Eng. Mater. Struct.* 10(6), 479–493 (1987).†

8. B. Cottrell et al., "On the Effect of Plastic Constraint on the Ductile Tearing in a Structural Steel," *Eng. Fract. Mech.* 21(2), 239–244 (1985).†

9. Q.-F. Li, "A Study About $J_i$ and $\delta_i$ in Three-Point Bend Specimens with Deep and Shallow Notches," *Eng. Frac. Mech.* 22(1), 9–15 (1985).†

10. D.-Z. Zhang and H. Wang, "On the Effect of the Ratio a/W on the Value of $\delta_i$ and $J_i$ in a Structural Steel," *Eng. Frac. Mech.* 26(2), 247–250 (1987).†

11. G. Matsoukas, B. Cottrell, and Y.-W. Mai, "On the Plastic Rotation Constant Used in Standard COD Tests," *Int. J. Frac.* 26(2), R49–R53 (1984).†

12. T. L. Anderson, H. I. McHenry, and M. G. Dawes, "Elastic-Plastic Fractures Toughness Tests with Single-Edge Notched Bend Specimens," in *Elastic-Plastic Fracture Test Methods: The User's Experience, ASTM STP 856*, E. T. Wessel and F. J. Loss, Eds. (American Society for Testing and Materials, Philadelphia, 1985), pp. 210–229.†

13. J. M. Barsom and S. T. Rolfe, *Fracture and Fatigue Control in Structures*, Prentice-Hall, Englewood Cliffs, N.J., 1987.†

14. R. D. Cheverton, S. K. Iskander, and D. G. Ball, "Review of Pressurized-Water-Reactor-Related Thermal Shock Studies," Fracture Mechanics: Nineteenth Symposium, ASTM STP 969, T. A. Cruse, Ed. (American Society for Testing and Materials, Philadelphia, 1988), pp. 752–766.†

15. J. W. Dally, "Lower Bound Initiation Toughness with a Modified Charpy Specimen," Master's Thesis, University of Maryland, College Park, Md., 1990.

16. J. W. Dally et al., University of Maryland, "Lower-Bound Initiation Toughness with a Modified Charpy Specimen," USNRC Report NUREG/CR-5703, (ORNL/Sub/79-7778/7), prepared at University of Maryland for Martin Marietta Energy Systems, Inc. Oak Ridge Natl. Lab., November 1991.

---

*Available for purchase from the National Technical Information Service, Springfield, VA 22161.

†Available in public technical libraries.

# 7 Cladding Evaluations

J. Keeney-Walker*

## 7.1 Objective

The objective of this task is to achieve a more comprehensive representation of the effects of cladding in the probabilistic analysis of vessel fracture. Specific parameters of interest are (1) the effects of dynamic loading and irradiation on the toughness of cladding, (2) the possibility of fracture-mode conversion due to high strain rates associated with a propagating crack, and (3) the propensity for ductile tearing of shallow through-clad surface cracks in low-toughness cladding.

During this report period, a draft report was received in support of the work on parameters (1) and (2). Also, a technical paper was presented at the 11th International Conference on Structural Mechanics in Reactor Technology (SMiRT) held in August in Tokyo, Japan. Discussions were held in Japan with researchers concerning the EPI Program and ongoing large-scale PTS experiments being conducted in Japan.

## 7.2 Study of the Effect of Cladding on Reactor Vessel Integrity

(J. D. Landes, The University of Tennessee)

The influence of the stainless steel cladding on the toughness of the composite clad metal-base structure has not been entirely resolved. While many studies have found beneficial effects of the cladding,[1–4,†,‡] these benefits are often smaller than anticipated.[2,†] In some cases, the accompanying tough heat-affected zone (HAZ) may play an important role by providing a crack-arrest region, thus contributing to any beneficial effect of the cladding.[1,5] On the other hand, the low-tearing resistance of the cladding may cause a problem when the crack front propagates into the base metal, resulting in an overall detrimental effect.

Fracture-toughness tests have shown the stainless steel cladding material to have relatively low resistance to ductile tearing in the unirradiated condition.[5,6] Irradiation at the fluence level experienced near end-of-license periods for a commercial pressurized-water reactor (PWR) can further reduce the tearing resistance in the cladding material. This allows a tearing flaw to initiate more easily in the clad material than in the reactor base metal. During a PTS, such a flaw may provide a site for a brittle initiation of fast fracture in the reactor vessel material. For this fracture mechanism to be of concern, the fracture toughness of the reactor base metal material must be reduced below that attained in statically loaded fracture tests for irradiated base material. This reduction in fracture toughness could come from a combination of irradiation and high strain rates associated with the ductility propagating crack. Strain rates associated with a crack propagating in the low-toughness cladding might provide the loading condition needed to reduce the base metal fracture-toughness level. Certainly, the effect of a cladded crack in the PTS scenario is important and should be considered further.

The objective of this work is to look at the various effects of irradiation and dynamic loading reported in the literature and to apply them in an estimation procedure to assess the danger of a crack in the cladding to pressure vessel integrity. To do this, a four-step work plan was performed.

1. The available fracture-toughness data bases for both irradiated and unirradiated reactor vessel stainless steel and low-alloy steel base material were studied to identify any data that will provide information on strain-rate effects.
2. The available fracture-toughness data bases for both nuclear-grade steels and non-nuclear structural materials were used to determine strain-rate effects.
3. A procedure was developed for estimating the effect of strain rate on both the brittle-fracture and ductile-tearing toughness of nuclear pressure vessel cladding and base material, based on the information determined in the first two steps.
4. The procedure of step three was applied to existing fracture-toughness data for RPV cladding and base metal; estimated fracture toughness curves covering the range of strain rates anticipated were produced.

---

*Computing and Telecommunications Division, Martin Marietta Energy Systems, Inc., Oak Ridge, Tenn.

†"White Paper on Reactor Vessel Integrity Requirements for Level A and B Conditions," prepared by ASME Section XI Task Group on Reactor Vessel Integrity Requirements, January 1991, available through EPRI.

‡S. K. Iskander et al., "Experimental Results of Tests to Investigate Fly Behavior of Mechanically Loaded Stainless Steel Clad Plates," to be published as a USNRC NUREG report.

These four steps were followed in this work. In addition, a model was developed to look at the effects of the lowered fracture toughness in terms of an actual structural component. The results were used to examine the effect of the degraded toughness on lowering the load-bearing capacity of the structural model. Finally, strain rates associated with a crack propagating in the ductile cladding material were estimated to assess the possibility of a fracture-mode conversion due to high strain rates at the crack tip.

An analysis of the dynamic strain rates associated with a propagating crack shows that normal crack-growth rates that occur as a result of stable R curve behavior do not elevate the crack-tip strain rates to the level needed to shift the $K_{Ic}$ transition temperature. The analysis infers that the high crack-tip strain rates occur only as a consequence of a rapid loading rate or the unstable crack propagation that may occur from a ductile fracture instability.

## 7.3 Effect of Irradiated Cladding on the Behavior of Shallow Flaws

(J. Keeney-Walker* and B. R. Bass*)

Further studies of the cladding problem scheduled for the report period were delayed due to diversion of staff resources to the analytical studies described in Sect. 2.3 of this report. This change in priorities was made at the request of the NRC technical monitor for the HSST Program.

The potential for stainless-steel cladding to influence the fracture behavior of shallow cracks on the inner surface of an RPV was studied. Shallow through-clad surface cracks were analyzed using finite-element techniques, elastic-plastic constitutive models, and $J_R$-methodology to determine the propensity for ductile tearing in low-toughness cladding. The clad-yield stress at the temperature of interest in this study (138 MPa) was at the low end of the range of accessible data (130 to 290 MPa). Results indicated that ductile tearing of the cladding is unlikely to occur for the crack geometries, material properties, and pressurized-thermal-shock loading assumed in the model.

This study is discussed in detail in Ref. 7. A technical paper[8] describing this study was presented at the 11th International Conference on Structural Mechanics in Reactor Technology (SMiRT) in August in Tokyo, Japan.

## 7.4 Discussions of EPI Program and PTS Experiments in Japan

(J. Keeney-Walker*)

### 7.4.1 Introduction

Detailed discussions were held in Japan in May 1991 with Japanese researchers concerning the EPI Program and ongoing, large-scale PTS experiments in Japan. The principal objective and the organizational structure of the EPI Program are discussed in Sect. 2.4 of this report.

The Japanese PTS integrity studies were initiated in FY 1983 as a national project by Japan Power Engineering and Inspection Corporation (JAPEIC) under contract with the Ministry of International Trade and Industry (MITI). During the period of these studies, a number of interactions have occurred between the JAPEIC participants and the HSST Program staff concerning PTS experiments in the respective countries. In a recent interchange, JAPEIC provided the HSST Program with a problem statement on the Japanese Step-B PTS experiment for inclusion in the recently completed CSNI Project FALSIRE (see Chap. 9). Discussions described here focused on the recent Step-C PTS experiment and on the large-scale, warm-prestressing experiments being carried out by JAPEIC. A summary of the discussions held at several university and research institutions is presented in the following section concerning the EPI Program and PTS studies.

### 7.4.2 Department of Nuclear Engineering, University of Tokyo

Professor G. Yagawa, chairman of the EPI subcommittee and Professor S. Yoshimura, task leader of the Estimation Scheme WG, provided an overview of current and future efforts in the EPI Program with an emphasis on the near-term experimental and numerical tasks. The major computational/analytical task of the past fiscal year (which ran to the end of March 1991) was the round-robin analysis of stationary as well as growing cracks in welded CT specimens of A 533 grade B class 1 steel. The round-robin task, completed at the end of 1990, involved participants

*Computing and Telecommunications Division, Martin Marietta Energy Systems, Inc., Oak Ridge, Tenn.

from five universities and four industrial organizations in Japan. According to the round-robin problem statement, participants were requested to perform static and/or generation-phase, crack-growth analyses based on crack growth (Δa) vs load-line displacement (δ) relations measured in the experiments. The side-grooved CT specimens (19 mm thick) used in these experiments consisted of four different configurations: (1) homogeneous base metal, (2) base metal/weld metal with the crack tip in the HAZ, (3) base metal/weld metal with the crack tip on the fusion line, and (4) base metal/weld metal with the crack tip in the weld metal. The problem statement included the necessary information for each specimen concerning geometry, material properties, measured load (P) vs δ curves, and measured relations among P, δ, and Δa. Participants were requested to provide calculated results for applied load per unit thickness—$J_{PATH}$ calculated on integral paths; $J_{MC}$, $J_D$, and [illegible] ained with conventional estimation formulas (i.e., Me[illegible]-Corten, ASTM E-813, and modified Ernst, respectively); and crack-tip opening angle (CTOA) and displacement (CTOD). The analysis matrix was designed such that at least two analyses were carried out for each test by different participating organizations. The results of these analyses have been compiled and reported in detail in the third EPI report.[9]

Several different tasks are scheduled to be performed by the members of the Experimental WG in 1991. Residual stress measurements have been performed on a portion of a welded plate of A 533 grade B class 1 steel fabricated and tested in 1989 under the EPI Program. These measurements were conducted on an "as-welded" segment (i.e., not stress relieved by heat treatment) by Professor H. Kobayashi of the Tokyo Institute of Technology using an acousto-elastic technique. Similar measurements on stress-relieved welded segments from the same plate were previously performed by Professor Kobayashi for the EPI Program and by Professor E. Rybicki of the University of Tulsa for the HSST Program; Professor Rybicki utilized a destructive strain-gage technique for his measurements.

Comparisons between the stress-relieved and not stress-relieved plates indicated that the maximum residual stress after the heat treatment and machining decreased by half. The mean values of residual stresses in the thickness direction measured by the strain-gage method were much smaller than those of the acousto-elastic method, which may be due to the large stress gradient. Plans are under way to conduct fracture analyses with residual stresses to determine their effects precisely. Additional experiments on crack growth in CT specimens and 3PB specimens have been carried out using specimens 6, 10, and 19 mm thick. These data were compared with data generated previously using specimens 19 mm thick to study size effects. The effects of (1) specimen thickness and crack orientation on initiation toughness, (2) crack-tip location on crack-growth resistance, and (3) specimen configuration are reported in Ref. 9.

Also, measurement techniques of crack-tip behavior (grid method and Moiré interferometry) were examined by the University of Tokyo with the assistance of computer image-processing techniques. Another type of specimen being utilized this year focuses on the growth of surface cracks in welded plates. Professor Kikuchi of the Science University of Tokyo is testing surface-cracked specimens with ratios of crack depth to surface length (a/c), satisfying $0.2 \leq (a/c) \leq 0.8$, using a 3PB-type of applied load. In each case, the crack plane is perpendicular to the weld direction, with the fusion line coinciding with the minor axis of the semielliptical crack. These specimens are depicted in Figs. 2.11 and 2.12 in Ref. 10.The results indicate that the crack-growth distributions were symmetrical with respect to the center line of the surface crack irrespective of weldment and that the CTOA values of welded specimens were much smaller than those of homogeneous specimens.

At the University of Tokyo, Professors Yagawa and Yoshimura are analyzing large-scale growth in welded CT specimens using computer image processing. Measurements of nonlinear fracture-mechanics parameters (with emphasis on the T*-integral) using caustic and Moiré interferometry techniques are being conducted by Professor T. Nishioka at Kobe University. Professor H. Homma at Toyohashi Institute of Technology is using fracture tests under nonisothermal conditions to study the effects of thermal gradients on the fracture-initiation process.

Professor Yoshimura indicated that the new welded plate similar to that tested in 1989 by the EPI Program has been fabricated by Kawasaki Steel from a different heat of A 533 grade B class 1 steel and will be utilized in a testing program to augment the data compiled from the first plate. The plate was cut into one base plate and seven welded plates and sent to several institutions for varied experimental work including material property determination, small-specimen testing, and residual stress effects on the fracture behavior. (See Sect. 2.4.1 for additional details concerning the testing program.)

### 7.4.3 Komae Research Laboratory, Central Research Institute of Electric Power Industry

Technical discussions concerning fracture-mechanics studies at the Central Research Institute of Electric Power Industry (CRIEPI) covered topics related to light-water reactor (LWR) and fast-breeder reactor (FBR) programs. Recently, a simplified fracture-mechanics model has been developed that does not use finite-element analysis to predict creep-fatigue crack-growth behavior in FBRs. The model contains contributions of stress redistribution (elastic-plastic) and primary creep (non-Norton). Based on applications to tests of 304 stainless steel at 550°C, predictions of crack-growth behavior from this model have been good for 2-D crack problems. The accuracy of the model has also been examined through finite-element analysis. Future plans include taking into account 3-D and thermal stress effects.

A tour of the material test facilities in the Materials Section focused on testing capabilities for FBR developments. The experimental equipment included a 1000-ton fatigue machine being used for leak-before-break (LBB) tests of large 304 stainless steel wide plates at 550°C. Fourteen tests have been performed at various conditions, that is, room temperature/high temperature, through notch/surface notch, and base metal/weld joints. At high temperatures (550°C), the surface notch propagates first in the depth direction and then in the surface direction. Thus, a condition of LBB would be expected. Further tests are planned that combine various temperatures and materials. Also on display was a 100-ton fatigue machine being used for vessel model tests under transient-thermal conditions, performed to demonstrate the validity of inelastic analysis. Additional testing facilities included approximately 30 conventional fatigue machines with capacity up to 10 tons and temperature of 1000°C, approximately 30 creep machines for temperature up to 1000°C, two tensile-test machines, and a thermal ratcheting machine for testing FBR vessels.

### 7.4.4 Department of Mechanical Engineering Sciences, Tokyo Institute of Technology

Discussions concerning the EPI Program focused primarily on computational studies of interfacial crack models and on acoustic techniques for nondestructive measurements of residual stresses in welds. Professor S. Aoki, Task Leader of the Theoretical WG in the EPI Program, is leading a study to develop a fracture model for cracks at the interface between two dissimilar materials in structures having welded or adhesive joints. The large-strain, finite-element model utilizes Gurson's constitutive relation for porous, plastic solids to incorporate the effects of microvoid nucleation and growth on near crack-tip fields. Currently, this model is being developed to predict combinations of material properties that lead to so-called "strong" or "weak" bonds at the interface between "hard" and "soft" materials. In particular, it is desirable to predict whether the interface crack will extend along the interface (weak bond) or extend into the softer material (strong bond). In results obtained thus far, it has been shown that the microvoids have a larger effect on the crack-tip blunting and stress fields for a bimaterial than for a homogeneous material. It was also found that the plastic strain and the microvoid volume fraction are localized in a few narrow bands that grow into the softer material from the intersection of the interface and the blunted crack tip at inclinations of ~15–45°.

Professors H. Kobayashi and Y. Arai have developed and employed acousto-elastic techniques for nondestructive measurement of residual stresses. Recently, these techniques were applied to the determination of residual stresses in segments of the welded plate of A 533 grade B class 1 steel tested in the EPI Program. The technique is based on the principle that, in a state of plane stress, differences in principal stress and principal directions of stress can be measured from the relative differences in the velocities and the principal directions of ultrasonic shear waves. In recent studies, they evaluated the influence of material anisotropy on the measured acousto-elastic effect and applied these techniques to welded plates. Results of their studies have been compared with the measurements of residual stresses in welded segments from the same plate performed by Professor Rybicki for the HSST Program using destructive strain-gage techniques. The acousto-elastic method overestimated the residual stress as compared to the strain-gage method, which is assumed to be due to the large stress gradient.

### 7.4.5 Takasago R&D Center, Mitsubishi Heavy Industries

Discussions with Dr. K. Hojo and staff concentrated on recent developments in the Japanese PTS integrity studies, including the current status of the testing program being carried out at the Takasago R&D Center. The stated

objectives of the PTS integrity studies in Japan are to gain public acceptance for RPV integrity against PTS events and to develop a data base for life extension. To meet these objectives, a research program involving both experimental and analytical studies has been developed. The experimental program for investigating crack behavior under PTS conditions features a large-scale, flat-plate specimen with a thickness approximating that of an RPV. A special PTS test facility has been constructed at Takasago to apply thermomechanical loading to the flat plate to approximate PTS loading conditions. The facility contains a horizontal testing machine with a capacity of 2000 tons in tension and 500 tons in bending. A large-scale, thermal-hydraulic loop with a flow-rate capacity of 10 $m^3/s$ and bulk-coolant temperature of –32°C is used to thermally shock the flawed surface of the plate. Surface flaws are generated in the plate by electrodischarge machining followed by fatigue-sharpening with a cyclic-bending load. Some of the current analytical studies include the development of a probabilistic fracture-mechanics code for creep-fatigue crack growth (PCCF), which shows the effects of loading conditions on failure probability. Also, a crack-shape estimation technique using the Reversing Direct Current Potential Method (RDCPM) has been developed and compares well with analytical computations.

Large-scale PTS tests completed at the Takasago facility include (1) a preliminary verification test involving brittle-crack initiation, (2) Step-A test verifying no-crack initiation under PTS conditions at end of design life, (3) Step-B test investigating crack behavior for upper-shelf conditions, and (4) Step-C test investigating crack behavior in material with a toughness gradient. Dr. Hojo indicated that the data and analysis results from the Step-C test remain proprietary to MITI and cannot be released. This position is consistent with our previous experiences with JAPEIC and is related to the well-known political sensitivity associated with the interpretations of these PTS tests in Japan. The next series of PTS tests (large-scale models) is now under way at Takasago and is designed to study and validate the effects of WPS. The test material is A 533 grade B class 1 steel with a 6:1 surface flaw and depth of 10 to 20 mm. Two out of five tests have been carried out. In both tests, the stress-intensity factor at crack initiation exceeded the material initiation toughness curve. Dr. Hojo offered no comment on this result, but the measured crack depth is in a range that could be susceptible to shallow-flaw loss-of-constraint effects. The third specimen is in the machine ready to be tested. This series is expected to be completed in 1 year.

Two points should be made concerning potential use of the Step-C PTS data by the HSST Program. First, the Step-C experiment is being considered as a candidate for inclusion in Phase II of the CSNI/PAG Project FALSIRE (see Chap. 9), which will be initiated in FY 1992. Second, it would be beneficial if dual-parameter approaches to fracture characterization currently being studied under Task 2 could be applied to the large- and small-scale specimen data. One objective here would be to reconcile the differences in toughness measured by the Japanese for the two specimens using single-parameter approaches. The dual-parameter approaches have been applied previously to wide-plate fracture initiation test data[11] by the HSST Program with some success.

### 7.4.6 Department of Ocean Mechanical Engineering, Kobe University of Mercantile Marine

A hybrid numerical–experimental method has been developed by Professor T. Nishioka to measure mode I and mixed-mode fracture parameters using a laser-caustic (shadow pattern) method. The method of caustics is an optical technique that has been used to measure stress-intensity factors in both static and dynamic fracture mechanics problems. In applications of this method, high-speed photographs of the reflected caustic patterns around the crack tip are taken using a laser-generated light source. Professor Nishioka has developed a finite-element technique aided by computerized symbolic manipulation for simulating the formation process of caustic patterns in elastoplastic materials. The simulated and actual caustic patterns can then be compared, and the relation between computed-fracture parameters, such as the T*-integral, and the size of the caustic pattern can be obtained for various optical arrangements. In effect, the caustic pattern is used to calibrate the finite-element model of the specimen from which the T*-integral can be evaluated. This technique is being applied at Kobe in support of the testing program of the Experimental WG in the EPI Program. Applications have been applied to PMMA using the transmitted caustic method and A 508 steel using the reflective caustic method for double cantilever beam (DCB) specimens. Professor Nishioka has also begun experiments using the Moiré interferometry method to determine the deformation behaviors of the crack tip in inhomogeneous CT specimens of A 533 B. Initial experiments have shown that fine-specimen grating could not be used to measure displacement fields for high loading but that the plastic zones were clearly visible.

Professor Nishioka provided a tour of his laboratory facilities in the Department of Mechanical Engineering and described the experimental setup for high-speed, laser-caustic photography used in conjunction with a tensile testing machine. He has recently received a new camera, Cordin Model 330, which has a maximum speed of $2 \times 10^6$ frames/s with a storage capacity of 80 frames. This has significantly improved the high-speed photographic capabilities. The tour also included visits to the wave and superconducting propulsion laboratories and training ship.

Near-term contributions to the EPI Program by Professor Nishioka will be concerned primarily with additional measurements of nonlinear-fracture parameters (i.e., T*-integral) in CT specimens of RPV steels using the laser-caustic technique. He also participated in the 1990 round-robin analysis of the EPI Program, performing analyses of two base metal/weld metal CT specimens with the crack tip located in the HAZ and on the fusion line.

### 7.4.7 Department of Energy Engineering, Toyohashi Institute of Technology

The testing program organized by the Experimental WG of the EPI Program was the primary subject of discussion with Professor Homma, who serves as task leader of that group. Professor Homma discussed the experimental work currently under way at Toyohashi. The objective of one of his studies is to determine whether there is a thermal gradient effect on cleavage initiation in pressure vessel steels. In other words, he seeks to determine if cleavage initiation is a function of temperature "pointwise" or whether it extends over a finite region in front of the crack tip. In the first phase of these studies, he performed tests on PMMA to validate techniques. Recently, a fracture experiment under an anisothermal condition was performed using the single-edge notched specimens taken from the heat-treated base plate of A 533 B class 1 steel. The purpose of the present experiment is to examine the effects of gradual change of material toughness on fracture behaviors. Pressure vessel materials may be subjected to such situations on the occasion of the TS and PTS events. The ligament length of the specimen was 113 mm, and the crack tip was cooled down to −10°C using liquid nitrogen, while the temperature at the face of the specimen behind the crack was set to be 10°C. As a result, the temperature gradient at the crack tip was about 0.250°/mm. For comparison, fracture-toughness tests were performed using CT specimens by varying temperature from −50 to 10°C. For simplicity, the stress-intensity factor was evaluated by neglecting thermal stress effects. Only one data point was obtained this year. They did not observe any significant effects of anisothermal conditions on the fracture behavior. This might be because the temperature gradient used was not large enough. Next year a steeper temperature gradient will be applied to the specimen, and experiments are being planned for PMMA in which the cooled and heated edges will be switched.

A tour of the laboratory facilities at Toyohashi included a briefing on the operation of the computer-assisted Charpy-impact-testing system developed under the direction of Professor Niinomi. The system incorporates four Charpy machines, the largest of which has a 50-kg-m capacity. The laboratory also includes one 50-ton tensile machine, a 1-ton tensile machine, and several fatigue-testing machines. Various programs utilize the machines for testing of ferritic steels, aluminum alloys, plastics, ceramics, and composites.

## References


1. S. K. Iskander and R. K. Nanstad, "Observations on the Behavior of Surface Flaws in the Presence of Cladding, Advances in Fracture Research," pp. 3525–3534 in *Proceedings of the 7th International Conference on Fracture (ICF7)*, Vol. 5, March 1989.*

2. A. Pellissier-Tanon et al., "French Verification of PWR Vessel Integrity," EPRI NP-7713, Final Report of Project 2975-2, February 1990.*

3. R. D. Cheverton et al., "Thermal Shock Experiments with Flawed Clad Cylinders," *Nuclear Engineering and Design* 124 (1990), 109–119, Norris-Holland.*

4. S. K. Iskander et al., Martin Marietta Energy Systems, Inc., Oak Ridge Natl. Lab., "Heavy-Section Steel Technology Program Semiann. Prog. Rep. October 1987–March 1988," pp. 212–230, USNRC Report NUREG/CR-4219, Vol. 5, No. 1 (ORNL/TM-9593/V5&N1), August 1988.†

5. D. E. McCabe, Materials Engineering Associates, Lanham, Md., "Fracture Evaluation for Surface Cracks Embedded in Reactor Vessel Cladding," USNRC Report NUREG/CR-5326 and MEA-2329, March 1989.†

6. D. E. McCabe, Materials Engineering Associates, Lanham, Md., "Fracture Evaluation for Surface Cracks Embedded in Reactor Vessel Cladding-Material Property Evaluations," USNRC Report NUREG/CR-5207 and MEA-2285, September 1988.†

7. J. Keeney-Walker, Martin Marietta Energy Systems, Inc., Oak Ridge Natl. Lab., "Heavy-Section Steel Technology Program Semiann. Prog. Rep. April–September 1990," pp. 82–88, USNRC Report NUREG/CR-4219, Vol. 7, No. 2 (ORNL/TM-9593/V7&N2), September 1991.†

8. J. Keeney-Walker, B. R. Bass, and W. E. Pennell, "Evaluation of the Effects of Irradiated Cladding on the Behavior of Shallow Flaws Subjected to Pressurized-Thermal-Shock Loading," pp. 195–200 in *SMiRT 11 Transactions*, Vol. G, August 1991.*

9. G. Yagawa, "Study on Elastic-Plastic Fracture Mechanics in Inhomogeneous Materials and Structures," CRC-EPI-030, Century Research Corp., Tokyo, Japan, March 1991.*

10. W. E. Pennell, Martin Marietta Energy Systems, Inc., Oak Ridge Natl. Lab., "Heavy-Section Steel Technology Program Semiann. Prog. Rep. April–September 1990, USNRC Report NUREG/CR-4219, Vol. 7, No. 2 (ORNL/TM-9593/V7&N2), September 1991.†

11. J. Keeney-Walker, B. R. Bass, and J. D. Landes, Martin Marietta Energy Systems, Inc., Oak Ridge Natl. Lab., "An Investigation of Crack-Tip Stress-Field Criteria for Predicting Cleavage-Crack Initiation," USNRC Report NUREG/CR-5651 (ORNL/TM-11692), September 1991.†

---

*Available in public technical libraries.
†Available for purchase from the National Technical Information Service, Springfield, VA 22161.

# 8 Pressurized-Thermal-Shock Technology

T. L. Dickson*

## 8.1 Background Information

During a PTS event, thermal streaming beneath the reactor vessel inlet nozzles can occur when cold safety coolant is injected into a stagnant reactor primary coolant loop. Thermal streaming in the reactor vessel downcomer annulus flow generates a nonuniform, asymmetric, circumferential temperature distribution in the reactor vessel wall.

Published results[1–4] from thermal-hydraulic experiments performed in Germany have raised concerns that thermal streaming may represent a significant source of additional thermal stress not currently included in the OCA-P analysis. The OCA-P computer code is used to perform fracture-mechanics analyses of RPVs subjected to PTS loadings.

Current plans, under Task 5, are to enhance, generalize, and validate the OCA-P code and to make it more "user friendly." Current plans are to name the new code FAVOR. Within the HSST Program, the emphasis is on incorporating into FAVOR the ability to model the effects of thermal streaming in PTS analyses.

## 8.2 Analytical Solution to Thermal-Streaming Problem

Some time was devoted to pursuing a general analytical (nonfinite-element) solution to the thermal-streaming problem. The objective was to develop a methodology that can be incorporated into a 1-D, finite-element, probabilistic, fracture mechanics program (FAVOR). The thermal-streaming problem is multidimensional; therefore, an analytical solution was desirable (as opposed to a multidimensional, finite-element solution methodology).

This analytical solution methodology involved solving the nonhomogeneous biharmonic equation of the Airy stress function for the 2-D, hollow-cylinder problem, in which the boundary conditions correspond to the transient, thermoelastic, thermal-streaming problem. A biharmonic equation solver (developed at Stanford University) was obtained; however, attempts to validate the analytical model against previously reported finite-element solutions[5] were not successful.

This activity has now been terminated. Stresses induced by thermal streaming will now be calculated using an approximate solution in which mean temperatures for the vessel wall are first calculated from 1-D radial heat transfer analyses results. These local mean temperatures will then be integrated around the vessel periphery, and this integral will be used to define the vessel mean temperature, $T_{AV}$. Thermal stresses due to thermal streaming at any point in the vessel can then be defined as a function of the local temperature minus $T_{AV}$. This approach is considered sufficiently accurate to calculate thermal-streaming stresses because the distribution of temperature in the thermal-streaming flux is itself not well defined.

## 8.3 Anticipated Activities

The previous finite-element analyses[5] have shown that the additional axial stress component (due to streaming) acting at the inner vessel surface can be approximated with a simple $E \times \alpha \times \Delta T$ calculation, where $\Delta T$ is the plume strength (i.e., the temperature differential between the plume center-line temperature and the well-mixed fluid temperature). Further finite-element analyses will be performed to quantify the axial stress component due to streaming through the vessel wall for a variety of geometries and plume strengths. With this information, the methodology for incorporating thermal streaming into the fracture analysis of circumferential flaws will only require plume strength as a user-specified input parameter.

## References

1. M. Geib, "Verification of OCA-P and VISA II on Behalf of Strains and Stresses Induced During HDR-TEMB Thermal Mixing Tests," Battelle-Institute, Frankfurt, Federal Republic of Germany, 1988.*

2. G. E. Neubrech et al., "Crack Initiation and Crack Growth During Thermal Shock Tests in the Reactor Pressure Vessel of the HDR under Corrosive Medium Conditions," *Int. J. Pres. Ves. Piping* 24, 1–5, 1988.*

*Computing and Telecommunications Division, Martin Marietta Energy Systems, Inc., Oak Ridge, Tenn.

3. L. Wolf et al., pplication of Engineering and Multi-Dimensional Finite Difference Codes to HDT Thermal Mixing Experiments," *Nucl. Eng. Des.* 108, 137-165 (1988).*

4. H. Kordish, "Analysis of Initiation and Growth of a Circumferential Crack in the HDR-RPV Cylinder Under Pressurized Thermal Shock," *10th SMiRT Post Conference*, Number 2, Monterey, Calif., August 1989.*

5. W. E. Pennell, Martin Marietta Energy Systems, Inc., Oak Ridge Natl. Lab., "Heavy-Section Steel Technology Program Semiann. Prog. Rep. October 1989–March 1990," USNRC Report NUREG/CR-4219, Vol. 7, No. 2 (ORNL/TM-9593/V7&N2), September 1991.†

*Available in public technical libraries.

†Available for purchase from the National Technical Information Service, Springfield, VA 22161.

# 9 Analysis Methods Validation

B. R. Bass*

## 9.1 Background Information

During this report period, several subtasks were completed in support of the Project for Fracture Analysis of Large-Scale International Reference Experiment (Project FALSIRE). Work continued on comparing and evaluating the analyses of large-scale experiments performed for the Project FALSIRE Workshop. Results from the comparisons are being used to prepare an interpretive report incorporating results, conclusions, and recommendations of the workshop. Detailed discussions were held with the staff of Gesellshaft für Reaktorsicherheit (GRS), Köln, Germany, concerning (1) completion of the final draft report, (2) development of plans for presenting Project FALSIRE results at an International Atomic Energy Agency (IAEA) Specialists' Meeting in 1992, and (3) consideration of a second phase of international fracture assessments similar to Project FALSIRE. A review was conducted at AEA/Risley, United Kingdom, of the spinning cylinder experiments used in Project FALSIRE. An invited technical paper[1] summarizing results from the Project FALSIRE Workshop was presented at the 11th International SMiRT Conference in August 1991 in Tokyo, Japan. Finally, a letter report on Project FALSIRE was issued to the NRC in September 1991.

## 9.2 CSNI/FAG Final Report on Project FALSIRE Workshop

(B. R. Bass,* J. Keeney-Walker,* C. E. Pugh, C. W. Schwartz,† H. Schulz,‡ and J. Sievers‡)

Project FALSIRE was sponsored by the Fracture Assessment Group (FAG) of Principal Working Group No. 3 (PWG/3) of the Organization for Economic Cooperation and Development (OECD)/Nuclear Energy Agency's (NEA's) Committee on the Safety of Nuclear Installations (CSNI). On behalf of the CSNI/FAG, the HSST Program at ORNL and the GRS, Köln, Germany, were responsible for organization arrangements related to Project FALSIRE. The chairman of the CSNI/FAG is H. Schulz of GRS-Köln. Motivation for the project was derived from recognition by the CSNI/PWG-3 that inconsistencies were being revealed in predictive capabilities of a variety of fracture assessment methods, especially in ductile fracture applications. As a consequence, the CSNI/FAG was formed to evaluate fracture prediction capabilities currently used in safety assessments of nuclear components. Members were from laboratories and research organizations in Western Europe, Japan, and the United States.

The CSNI/FAG planned Project FALSIRE to assess various fracture methodologies through interpretive analyses of selected large-scale fracture experiments. Six reference experiments were eventually selected by CSNI/FAG for detailed analysis and interpretation.[1] The CSNI/FAG established a common format for comprehensive statements of these experiments, including supporting information and available analysis results.

These statements formed the basis for evaluations performed by an international group of analysts using a variety of techniques. At a 3-day workshop in Boston, Massachusetts, in May 1990, all participating analysts examined these evaluations in detail.

Comparative assessments of the solutions presented at the Project FALSIRE Workshop are being carried out by GRS-Köln, ORNL, and other participants in the workshop. A comprehensive report of the findings, conclusions, and recommendations is being prepared based on these assessments as a cooperative effort between GRS-Köln, ORNL, and other members of the CSNI/FAG. In May 1991, a meeting was held at GRS-Köln with Dr. Schulz and members of his staff concerning completion of the draft report on Project FALSIRE. They agreed that an initial draft should be completed by early fall of 1991. The current status of each chapter of the report was reviewed in detail, and the tasks required to complete each of them were identified. Following completion, the draft will be submitted to the individual workshop participants for review and comments. After comments from the participants have been incorporated, the draft will be submitted to members of the CSNI/PWG-3 committee for review. The report will be finalized after comments and approval have been obtained from the CSNI/PWG-3 committee.

*Computing and Telecommunications Division, Martin Marietta Energy Systems, Inc., Oak Ridge, Tenn.
†University of Maryland, College Park, Maryland.
‡GRS, Köln, Federal Republic of Germany.

## 9.3 Joint IAEA and OECD/NEA Meeting on Fracture Mechanics Verification by Large-Scale Testing

The IAEA and the OECD/NEA have agreed to cosponsor a Specialists' Meeting on Fracture Mechanics Verification by Large-Scale Testing in the United States in 1992. The meeting will address the application and validation of all forms of fracture mechanics methodology for evaluating structural integrity. It will include correlations between small and large specimens and components with special emphases on vessels, piping, and closures. Mr. J. Stronsnider of the NEA Nuclear Safety Division and Mr. L. Ianko of the IAEA Division of Nuclear Power have been nominated as coscientific secretaries responsible for organizing the meeting.

The CSNI/PWG-3 has agreed to support the joint IAEA/OECD Specialists' Meeting through the work of the CSNI/FAG and the participants in Project FALSIRE. At the May meeting in Köln, Dr. Schulz proposed that contributions to the Specialists' Meeting focus on the results of the Project FALSIRE Workshop in Boston. There would be one extended presentation for each of the experiments considered in the workshop. These presentations would include discussions of the objectives and results of experiments, comparative analyses from the report on Project FALSIRE, and any ongoing work to update the analyses and interpretations.

Following the Köln meeting, a modified agenda for the CSNI portion of the meeting was prepared at ORNL by C. E. Pugh and the author. (The U.S. member of the IAEA International Working Group for Life Management of Nuclear Power Plants is Dr. C. E. Pugh; he also chairs the technical program for the 1992 Specialists' Meeting.) Briefly, the 1-day agenda proposed by the program chairman calls for an overview talk on Project FALSIRE, followed by two presentations for each experiment used in Project FALSIRE, and, finally, a closure discussion. The first presentation for each experiment, to be given by a representative of the testing organization, would review the results of the experiment and provide an overview of the analysis results presented at the FALSIRE Workshop. A second presentation would focus on recent analysis results compiled since the workshop, with emphasis on applications of more advanced fracture methodologies. This modified agenda was presented to Schulz at a second meeting held concurrently with the 11th SMiRT Conference, in Tokyo, Japan. In Tokyo, Schulz proposed to further modify this agenda to incorporate a panel discussion, with the panel comprising two experimentalists, two analysts, and two materials science researchers. This panel discussion would be positioned to close the CSNI session on Project FALSIRE. The details of the final agenda will be completed early in FY 1992.

## 9.4 CSNI/FAG Phase II Project

At the May meeting in Köln, GRS proposed a tentative plan for a second phase of fracture assessments of large-scale experiments to be carried out as part of the CSNI/FAG project. Problem statements having a format previously used in Project FALSIRE would be distributed to selected organizations that have conducted candidate experiments. These experiments include (but are not limited to) NKS-5 and -6 (MPA), Japanese Step-C wide plate (JAPEIC), PTSE-1 (ORNL), DSR1 clad beam (Electric de France), and spinning cylinders 4–6 (AEA). Emphasis in this phase would be on tests in the transition region and on applications of alternative analysis methods such as the dual parameter approaches. Interest by GRS in these new experiments stems partly from a desire to identify experiments that are more tractable from an analysis viewpoint than some of those considered previously in Project FALSIRE. The completed problem statements would be evaluated to determine which experiments would be useful for the second phase of analyses. Based on the outcome of these evaluations, a proposal for the second phase will be made to the CSNI/PWG-3 committee. Dr. Schulz is requesting that the PWG-3 officially approve a second phase of the CSNI/FAG project and that the approval be included in the minutes of the PWG-3 meeting. This approval would certify that the second phase is considered an important international project and worthy of financial support from research institutions on behalf of interested participants. Assuming that approval is forthcoming from the PWG-3 committee, the new series of problem statements would be distributed to analysts only after a draft version of the final report on Project FALSIRE is available for distribution. The date, location, and format for a meeting to review the results of the second phase of analyses have not been discussed.

## 9.5 Spinning-Cylinder Experiments

At a meeting held in May 1991 at AEA/Risley, UK, discussions were held to review the results of spinning-cylinder tests 1 through 3. These discussions provided an update to

the interpretations of the measured data and the specimen fracture surfaces from the experiments. The spinning-cylinder tests 1 and 2 were two of the large-scale experiments used in the CSNI/FAG Project FALSIRE Workshop. Recent efforts have focused attention on improving the interpretation of the alternating current potential drop (ACPD) data, which provide a history of crack growth in the specimen. According to AEA/Risley, considerable progress has been made in accounting for the effects of temperature variation and for sensitivity to stress/strain variations due to changes in loading conditions. For spinning-cylinder test 2, in which the cylinder was subjected to thermal-only loading, the stress-induced response of the potential drop has been identified and separated from that due to crack growth. This task remains to be done for test 3, which was subjected to combined mechanical and thermal loading. According to the interpretations made at Risley, the fracture resistance of the spinning-cylinder specimens has been shown to be the same for mechanical shock, thermal shock, and combined mechanical/ thermal shock loading. However, a significant elevation remains in upper-shelf fracture toughness, both at initiation and after a small amount of ductile tearing, for the spinning-cylinder specimens (in contained yield) compared with compact specimens (in contained yield and postyield). The letter differences in fracture toughness are being studied further via two approaches supported at Risley: (1) T-stress effects by Prof. M. Goldthorpe at Sheffield University and (2) local approach by staff at Risley with assistance from French researchers. Reports are currently in preparation at Risley on the results of spinning-cylinder experiments 1–3.

Tests of spinning-cylinder specimens 4 and 6 have also been completed at Risley. The only information revealed by Risley concerning these experiments is that the specimens contain surface cracks that were tested in a cleavage mode. The last spinning-cylinder specimen in this series, specimen 5, is scheduled for testing in the fall of 1991. The crack in specimen 5 is located in a weld much like that in the Sizewell B vessel; the loading conditions for specimen 5 are intended to be similar to those of specimen 3. The specimen was subjected to cyclic loading to fatigue-sharpen the crack. Potentially, one or more of these experiments could be candidates for a future phase of international fracture assessments being considered by the CSNI/FAG.

## Reference

1. B. R. Bass et al., "Assessment of Ductile Fracture Methodology Based on Applications to Large-Scale Experiments," pp. 25–36 in *SMiRT 11 Transactions*, Vol. G, August 1991. Available in public technical libraries.

# 10 Fracture Evaluation Tests

T. J. Theiss

## 10.1 Introduction

The purpose of this task is to provide experimental support for all remaining tasks within the HSST Program. Currently, the only testing under way is the shallow-crack fracture-toughness testing. The motivation for the shallow-crack program and the test results and interpretation are detailed in Chap. 6. This chapter describes the details of the testing in support of the shallow-crack fracture-toughness program.

## 10.2 Shallow-Crack Fracture-Toughness Testing Program

### 10.2.1 Specimen Fabrication and Testing

The specimen configuration used for all testing in the shallow-crack project is the SENB specimen with a through-thickness crack (as opposed to the 3-D surface crack). The bend specimen better simulates the varying stress field in a reactor wall under PTS conditions. In addition, previous shallow-crack work has utilized SENB specimens.[1,2] The straight-through notch simulates an infinitely long, axially oriented crack in an RPV. To better simulate the conditions of a shallow flaw in the wall of a reactor vessel, the specimen depth W and thickness B should be as large as practicable. PWR vessel walls are nominally 200 to 280 mm (8 to 11 in.) thick. A beam ~100 mm (4 in.) deep has been selected for use in the HSST shallow-crack project. To maintain consistency with ASTM standards, the beams are being tested in three-point bending. All testing is being conducted on reactor material (A 533 grade B class 1) with the cracks oriented in the L-S orientation.

Instrumentation is attached to the specimens to make possible J-integral and CTOD measurement of fracture toughness. The J-integral is determined from the load-line-displacement using the reference bar technique. CTOD is determined from CMOD using clip gages mounted on the crack mouth of the specimen. Toughness data are expressed in terms of CTOD according to ASTM E1290-89, "Crack-Tip Opening Displacement (CTOD) Fracture Toughness Measurement." ASTM E399, "Plane-Strain Fracture Toughness of Metallic Materials," is used for the deep-crack specimens to determine if the test results can be considered "valid" plane-strain data. ASTM E813, $J_{Ic}$, "A Measure of Fracture Toughness," is not strictly applicable to these tests because all failures to date have been cleavage failures.

### 10.2.2 Thickness Effects on Toughness (Six Additional Beam Tests)

Six additional deep-crack beams were fabricated and tested during the current reporting period. These beams were not originally part of the program plan but were added at the midyear review. The beams were cut from remaining halves from the development beams 100 and 150 mm (4 and 6 in.) thick tested previously (HSST-WP-CE A 533 B material). All of the beams were ≈100 mm (4 in.) deep with a 406-mm (16-in.) span. The purpose of the tests was to further study the influence of varying beam thickness on ...ure toughness for deep-crack specimens.

The three thicknesses used in the development phase (B = 50, 100, and 150 mm) were also used for these tests. All six additional beams were tested at approximately –45°C (–50°F). Table 10.1 gives the test matrix for these tests. Fatigue precracking and failure testing were conducted in accordance with ASTM E1290-89; however, ASTM E399 is being applied to determine if these test results are "valid" plane-strain results. Additional details of the interpretation of the data are given in Sect. 6.4.

Table 10.1 Test matrix for the six additional beams[a]

| Thickness (mm) | Number of beams tested |
|---|---|
| 50 | 2 |
| 100 | 2 |
| 150 | 2 |

[a]All beams were deep crack ($a/W \sim 0.50$). $RT_{NDT}$ = –34°C (–30°F). Temperature = –46°C (–50°F).

### 10.2.3 Shallow-Crack Testing Production Phase

The production phase of the shallow-crack fracture-toughness testing program was begun during this reporting period. Source material for the beams is HSST Plate 13B. Material from HSST Plate 13A, a companion plate to Plate 13B, was used as source material for most of the wide-plate tests and was extensively characterized at the time.[3] The beams were machined from blanks that were flame cut from Plate 13B. In sum, 22 specimens were fabricated, with 18 beams tested this reporting period. HSST Plates 13A and 13B have not been post-weld heat treated. Therefore, to be more prototypic of the conditions in RPV material, the blanks were heat treated at 620°C (1150°F) for 40 h before final machining. A characterization piece was also heat treated and delivered for fabrication into the various characterization specimens and testing. The original characterization of this material was performed in the L-T orientation. This recent characterization supplements the original characterization by providing properties in the L-S orientation through the plate thickness. Material properties through the thickness of the plate are required because some of the production specimens are to be cut from the surface portion of the plate. All shallow-crack testing is in the L-S orientation. Additional information on the shallow-crack material characterization can be found in Chap. 3.

Each beam in the production phase of the shallow-crack program is machined to the same size: 100 × 100 × 610 mm (4 × 4 × 24 in.). The beam size was chosen based on the results of the development phase.[4] The only dimension that varies is the crack depth, a. Crack depths of 50 and 10 mm (2 and 0.4 in.) are being used for the deep and shallow prototypic flaws, respectively. Figure 10.1 shows an instrumented shallow-crack specimen ready for testing. Strain gages on the face of the beam ahead of the crack and the dual clip gages are used to determine the plastic rotation factor (see Sect. 6.1 for more details).

The test matrix for the 18 production beams is given in Table 10.2. A batch of three beams was tested at each temperature and crack depth. Of the 18 beams tested, 12 have been shallow-crack beams and 6 have been deep-crack beams. Beams have been tested at temperatures of –104, –40, –23, and –7°C (–155, –40, –10, and +20°F).

Fatigue precracking has been successful in all of the shallow-crack testing to date, especially the production-phase testing performed during this reporting period. Test techniques developed during the development phase of the program were used to optimize current test procedures. All phases of the fatigue precracking and failure testing have been conducted in accordance with ASTM E1290-89. Generally, sufficient crack growth is obtained in about 50,000 cycles of fatigue using the load limits supplied in ASTM E1290.

**Table 10.2 Test matrix for the production beams tested to date[a]**

| Temperature [°C(°F)] | Crack depth | |
|---|---|---|
| | Deep ~50 mm | Shallow ~10 mm |
| –104 (–155) | 0 | 3 |
| –40 (–40) | 3 | 3 |
| –23 (–10) | 0 | 3 |
| –7 (+20) | 3 | 3 |

[a]All beams were square cross section (~100 × 100 mm). $RT_{NDT}$ = –18°C (0°F).

Crack growth was monitored by means of the change of crack-mouth-opening compliance, using the clip gage data. In the development phase of the shallow-crack testing, crack length and growth were related to beam compliance using the equation in ASTM E813. This equation was developed for only deep-crack beams and does not properly relate compliance and crack length for shallow-crack specimens. However, a change in beam compliance of 10 to 15% generally indicated sufficient crack growth. For the production beams, a new compliance equation relating crack depth to compliance for the shallow-crack beams was used with much greater reliability than the equation in ASTM E813. These equations were derived by Joyce, Hackett, and Roe in a paper presented at the Indianapolis symposium on constraint.* The new equations allow the crack depth to be determined explicitly from the compliance directly for all crack depths.

The sharpened flaws have consistently maintained very flat crack fronts during fatigue growth. Figure 10.2 depicts a representative shallow- and deep-crack fracture surface showing the straight crack front. Table 10.3 gives the

*J. A. Joyce, E. M. Hackett, and C. Roe, "Effects of Crack Depth and Mode of Loading on the J-R Curve Behavior of a High Strength Steel," presented at the Symposium on Constraint Effects in Fracture, ASTM, Indianapolis, Ind., May 8–9, 1991.

ORNL-PHOTO 8410-91

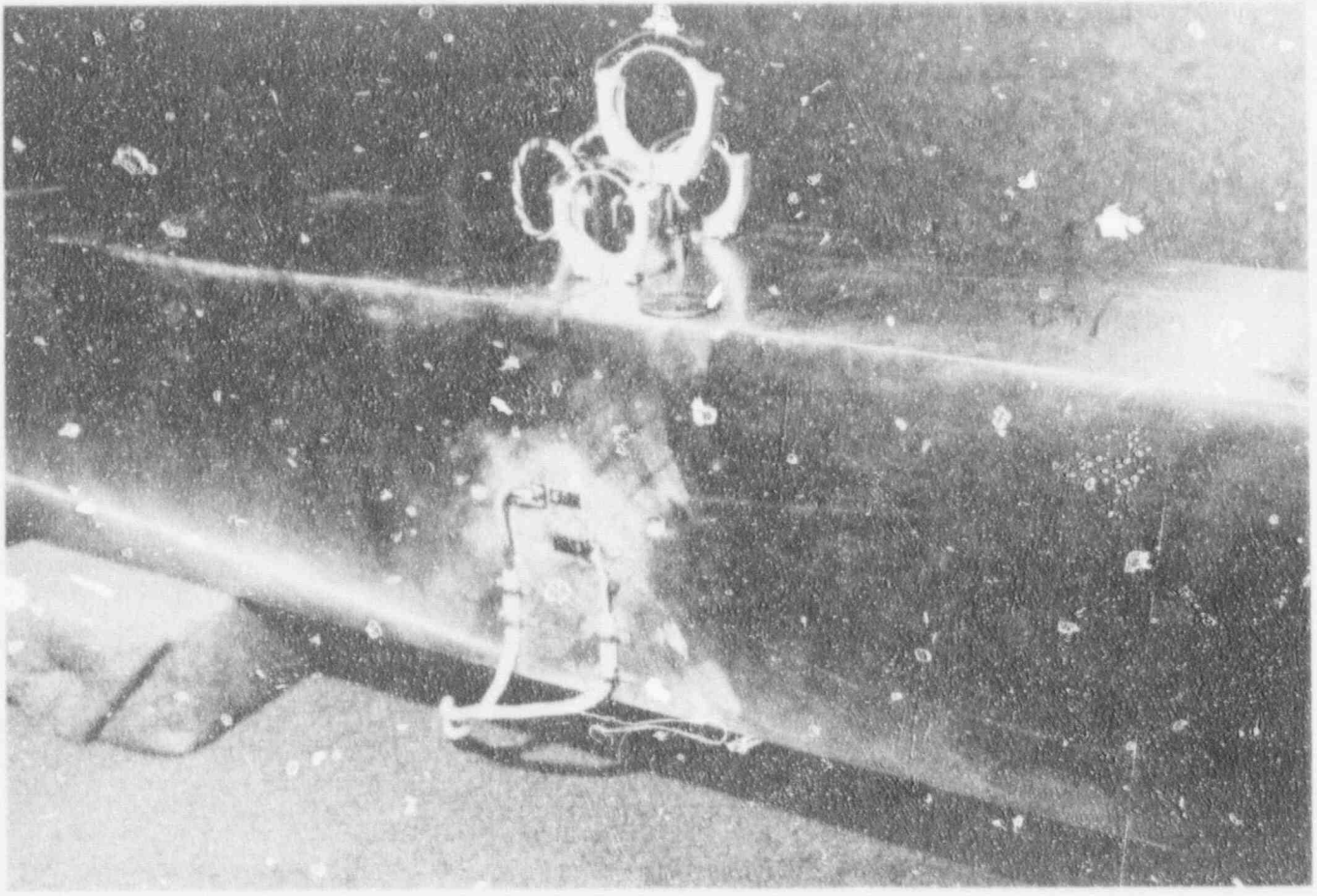

Figure 10.1 Photograph of production beam with instrumentation

ORNL-PHOTO 8408-91

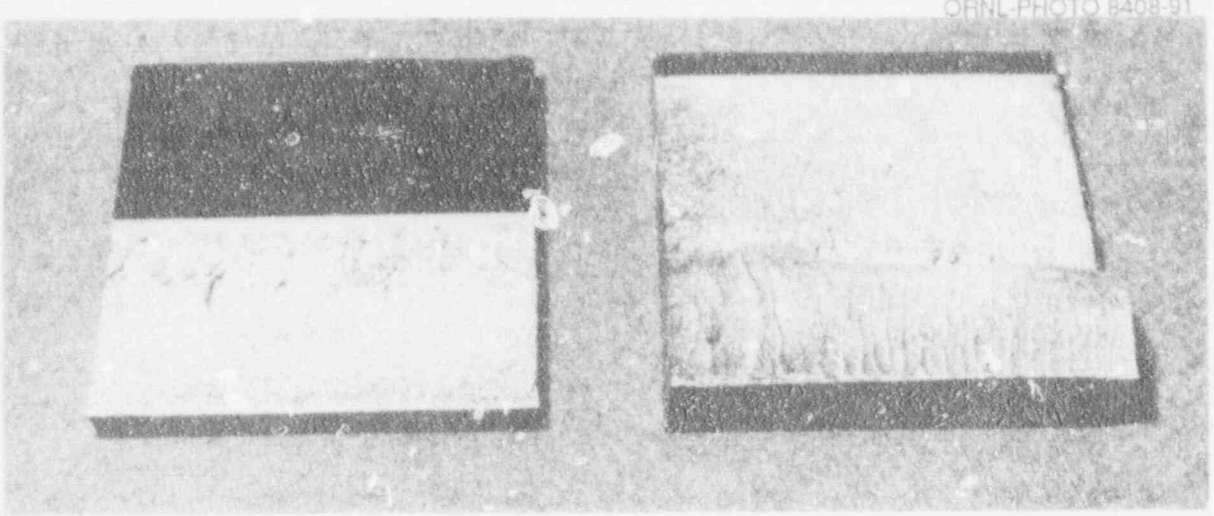

Figure 10.2 Photograph of representative shallow- and deep-crack beam [HSST beams 25 (left) and 26]

Table 10.3 Crack-depth measurements for a representative deep- and shallow-crack beam

| Reading | Crack depth [mm (in.)] |
|---|---|
| *HSST beam 25*[a] | |
| 1 | 50.75 (1.988) |
| 2 | 51.92 (2.044) |
| 3 | 52.22 (2.056) |
| 4 | 52.40 (2.063) |
| 5 | 52.40 (2.063) |
| 6 | 52.32 (2.060) |
| 7 | 52.15 (2.053) |
| 8 | 51.74 (2.037) |
| 9 | 50.55 (0.990) |
| *HSST beam 26*[b] | |
| 1 | 9.96 (0.392) |
| 2 | 11.20 (0.441) |
| 3 | 11.23 (0.442) |
| 4 | 11.18 (0.440) |
| 5 | 11.05 (0.435) |
| 6 | 11.15 (0.439) |
| 7 | 11.23 (0.442) |
| 8 | 11.30 (0.445) |
| 9 | 10.11 (0.398) |

[a]ASTM E1290 crack depth: 51.97 mm (2.046 in.). Maximum difference ≤ 0.02W.
[b]ASTM E1290 crack depth: 11.05 mm (0.435 in.). Maximum difference ≤ 0.02W.

crack-depth measurements using the nine-point method of crack-depth determination as outlined in ASTM E813 or E1290. ASTM E1290 requires that the minimum and maximum crack-depth readings differ by <0.1W and that the seven in... measurements differ by no more than 0.05W. As indicated in Fig. 10.2 and Table 10.3, the variation in the crack front is minimal, easily meeting the ASTM requirements. The reason for the straight crack profiles is believed to be the method of notch preparation. Initial notches were inserted into the specimens using electron discharge machining (EDM). The EDM process produces a very thin notch (≈0.3 mm) with a small notch root radius. In addition, the EDM process itself may produce residual stresses that enhance crack growth. Generally, the crack is only grown about 2.5 mm (0.1 in.), which seems to enhance a flat crack front profile.

A detailed measurement of the crack front irregularity was performed during the current reporting period. The goal of the study was to quantify the local variation in the crack front of a fatigue flaw that has a relatively straight crack front. Measurements were made on HSST beam 25 accurate to 0.0025 mm (0.0001 in.) every 0.13 mm (0.005 in.) apart along the center 12 mm (0.5 in.) of the crack front. The results indicate that the local crack front variation averages about 0.025 mm (0.001 in.), with a maximum variation of approximately 0.11 mm (0.0044 in.). The process zone in a cracked member is about 2–3 × CTOD, which is approximately 0.11 mm (0.0043 in.). In other words, the local crack front variation is on the order of the distance to the process zone from the crack tip. This local crack front variation influences the local stress triaxiality along the crack front, which could influence the global fracture initiation behavior of the material. Precise determination of the influence of the local crack front variation on fracture behavior will be difficult because analytical and experimental investigation of this issue is expensive and time consuming.

The portion of the shallow-flaw fracture-toughness testing matrix assigned to ORNL was completed at the end of the current reporting period. Additional testing will be performed at the David Taylor Research Center.

### 10.2.4 Test Reports

Test reports for the development beam test series were issued during the current reporting period. Each test report is signed and checked for QA purposes and includes information on geometry, material properties, fatigue precracking, and toughness results in terms of CTOD, J, and K. An example test report (HSST-SC-3) is given in Appendix 10.1 (at the end of this chapter).

## 10.3 Full-Thickness, Shallow-Crack, Clad Beam Tests

Shallow-flaw specimens have been shown to exhibit an effective fracture toughness greater than similar deep-flaw specimens in the transition region. These specimens are single-edge-notch, three-point-bend specimens taken from the homogeneous center region of the source plate. However, shallow flaws in an RPV are located near the plate surface where large metallurgical gradients exist. Axial flaws in an RPV are oriented in the L-S material direction rather than the L-T orientation. In addition, the

cladding process may influence material properties near the surface on the RPV. These metallurgical differences may have a significant impact on the resulting fracture toughness. To quantify the fracture toughness of shallow flaws in reactor vessels, several full-thickness, clad beam experiments were planned. Comparison of results from these tests with those from homogeneous shallow-flaw test specimens will provide a quantitative definition of the effect of near-surface conditions on fracture toughness. The effective fracture toughness from these large beams will also be compared with the toughness as determined by current ASME Section XI rules.

The specimens tested will be single-edge-notch, arc-bend specimens with the flaw in the L-S orientation. The source plate of the specimens will be A 533 grade B class 1 steel with stainless steel cladding. This material was taken from a cancelled PWR reactor vessel. The plate material, cladding, and weldment are completely prototypic of a production quality RPV.

Tests are planned to begin in FY 1992. Preliminary discussions were held with the National Institute of Standards and Technology (NIST) about performing this work in FY 1992.

## 10.4 Out-of-Plane Biaxial Loading Fracture-Toughness Tests

Current RPV life assessments are most often limited by PTS accident conditions. These PTS loads (specifically, the hoop stress) create significant positive out-of-plane strains along circumferentially oriented flaws. The fracture resistance for the RPV is based on the ASME $K_{IR}$ fracture-toughness curve developed using specimens with zero out-of-plane strain (i.e., plane-strain conditions). Therefore, the influence of out-of-plane strain along a crack front needs to be properly understood.

The influence of negative out-of-plane strains is very well known. As negative out-of-plane strains are introduced in a specimen, the fracture resistance increases from the plane-strain fracture toughness to the plane-stress fracture toughness. However, the influence of positive out-of-plane strains applicable to the RPV during PTS loading is not known. Previous analytical studies of the influence of out-of-plane loading on the crack have yielded uncertain results.* Therefore, to experimentally determine the influence of positive out-of-plane strain, the HSST Program plans to test a series of out-of-plane biaxial loading fracture toughness tests. The tests will be designed to closely match the conditions in an RPV under PTS loading.

During the current reporting period, a potential test vendor (UKAEA Technology) for the out-of-plane tests has been located, and preliminary discussions have been initiated. Initial specimen designs have been considered based on the primary criterion that the load in the throat not exceed the yield strength of the material. The current specimen design is a square plate with a long semielliptical flaw in the center of the plate, but specimen dimensions have not been determined at this point.

## References

1. W. A. Sorem, R. H. Dodds, Jr., and S. T. Rolfe, "An Analytical Comparison of Short Crack and Deep Crack CTOD Fracture Specimens of an A36 Steel," *WRC Bulletin 351*, Welding Research Council, New York, February 1990.†

2. J. A. Smith and S. T. Rolfe, "The Effect of Crack Depth to Width Ratio on the Elastic-Plastic Fracture Toughness of a High-Strength Low-Strain Hardening Steel," *WRC Bulletin 358*, Welding Research Council, New York, November 1990.†

*W. E. Pennell, Oak Ridge National Laboratory, "Heavy-Section Steel Technology Program: Recent Developments in Crack Initiation and Arrest Research," to be published in *Proceedings from the 19th Water Reactor Safety Meeting*, USNRC Report NUREG-CP-xxxx, March 1992.

3. D. J. Naus et al., Martin Marietta Energy Systems, Inc., Oak Ridge Natl. Lab., "Crack Arrest Behavior in SEN Wide Plates Of Quenched and Tempered A 533 Grade B Steel Tested Under Nonisothermal Conditions," USNRC Report NUREG/CR-4930 (ORNL-6388), August 1987.‡

4. T. J. Theiss, Martin Marietta Energy Systems, Inc., Oak Ridge Natl. Lab., "Cleavage Crack Initiation," pp. 35–43 in *"HSST Program Semiann. Prog. Rep. October 1990–March 1991,"* USNRC Report NUREG/CR-4219, Vol. 8, No. 1 (ORNL/TM-9593/V8&N1), February 1992.‡

---

†Available in public technical libraries.
‡Available for purchase from the National Technical Information Service, Springfield, VA 22161.

# Appendix 10.1

# 1

IMAGE EVALUATION
TEST TARGET (MT-3)

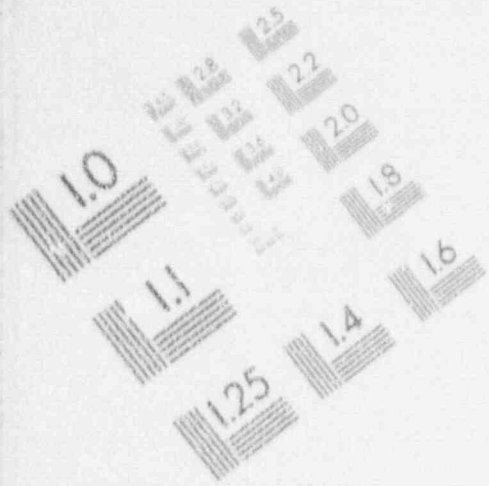


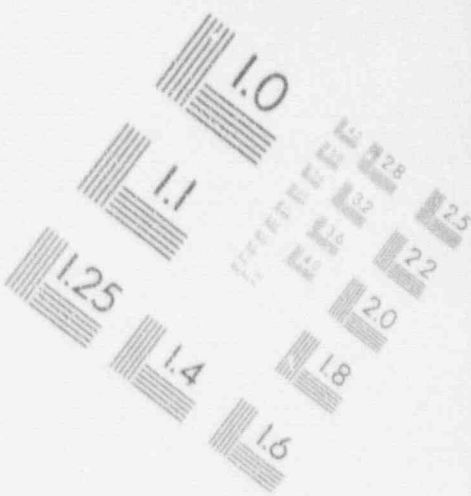



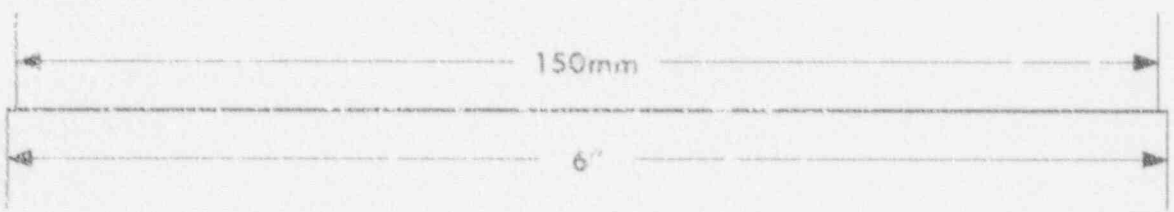



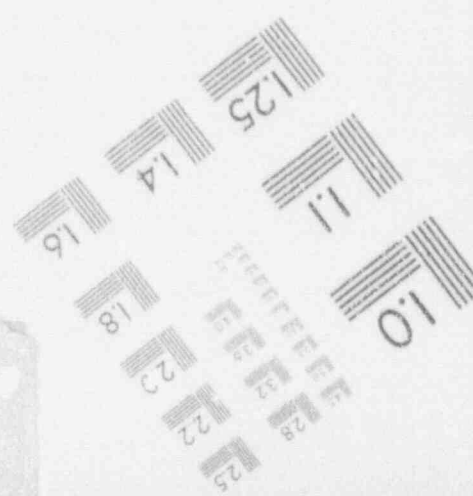

# 1

## IMAGE EVALUATION TEST TARGET (MT-3)

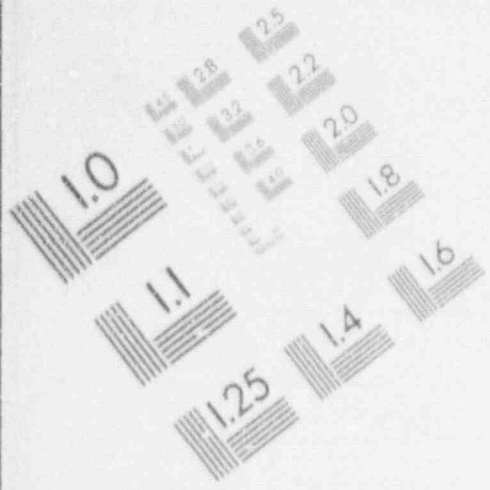


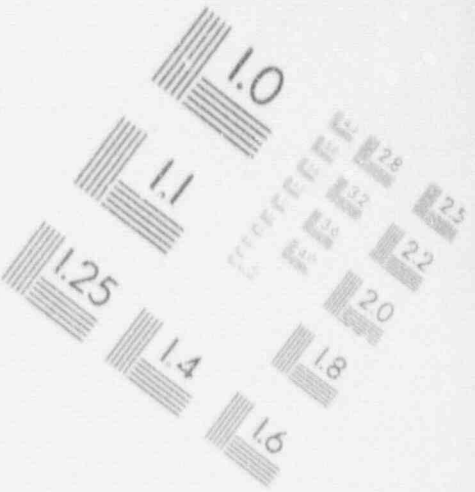



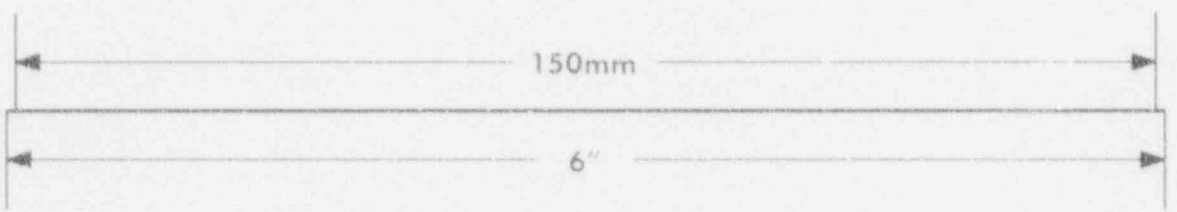



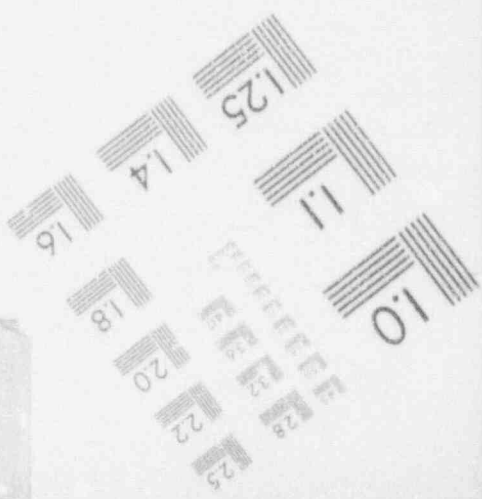


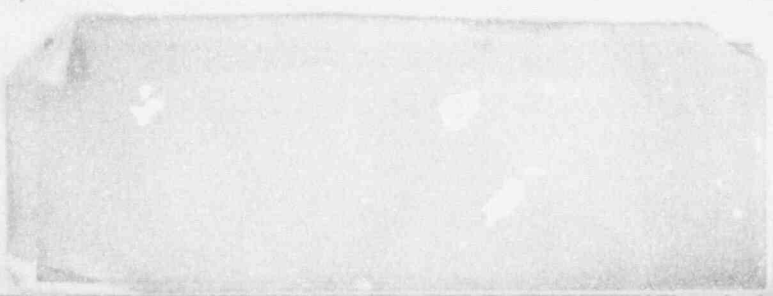

Oak Ridge National Laboratory (ORNL)

Heavy-Section Steel Technology Program (HSST)

# Shallow-Crack Fracture Toughness Testing

## Development Phase

Test Report

for

HSST Shallow-Crack Beam # 3
(HSST-SC-3)

Tested Mar. 12, 1991

Prepared: _____ 9-3-91
HSST Shallow-Crack Task Leader — Date

Checked: _____ 9-3-91

Appendix 10.1

## Test Data for HSST-SC-3

| | | |
|---|---|---|
| 1. | Specimen Configuration: | SE(B) |
| 2. | Crack Plane Orientation: | L-S |
| 3. | Test Temperature (air environment): | -32 °F |
| 4. | Stroke Rate: | 0.076 in/min |
| 5. | Time to Failure: | 109 sec |
| 6. | Material Properties (A533, Grade B, Class 1, CE Plate) | |
| | 6.1 Elastic Modulus, E: | 30,000 ksi |
| | 6.2 Poisson's ratio, $\upsilon$: | 0.3 |
| | 6.3 Yield & Tensile Strength at Room Temperature, $\sigma_{ys}$ & $\sigma_{ult}$: | 57.4 & 80.6 ksi |
| | 6.4 Yield & Tensile Strength at Test Temp. (Note 1): | 64 & 87 ksi |
| 7. | Specimen Geometry | |
| | 7.1 Load Span, S: | 16 in |
| | 7.2 Thickness, B: | 1.993 in |
| | 7.3 Width, W: | 3.925 in |
| | 7.4 Crack Depth, $a_0$ (9-point method): | 0.395 in |
| 8. | Fatigue Precracking Parameters (ASTM E399-83) | |
| | 8.1 Precracking Temperature: | 70 °F |
| | 8.2 Load Ratio ($P_{max}/P_{min}$): | 0.08 |
| | 8.3 Maximum Stress Intensity Factor, $K_{max}$: | 49 ksi$\sqrt{in}$ |
| | 8.4 Final Stress-Intensity Range, $\Delta K$: | 45 ksi$\sqrt{in}$ |
| | 8.5 0.6 ($\sigma_{ys1}/\sigma_{ys2}$) $K_Q$: | 51 ksi$\sqrt{in}$ |
| 9. | Failure Load, $P_c$: | 134.9 kip |
| 10. | Stress-Intensity Factor at $P_c$, K: | 118 ksi$\sqrt{in}$ |
| 11. | CTOD Toughness (ASTM E1290-89): | |
| | 11.1 Elastic Component of CTOD: | 0.0033 in |
| | 11.2 Plastic Component of CMOD, $\upsilon_p$: | 0.0245 in |
| | 11.3 Plastic Rotation Factor, $r_p$: | 0.50 |
| | 11.4 Clip Gage Elevation, z: | 0.025 in |
| | 11.5 Critical CTOD, $\delta_c$: | 0.023 in |
| 12. | J-Integral Toughness (Note 2): | |
| | 12.1 Elastic Component of J: | 0.42 ksi-in |
| | 12.2 Plastic Area under P-$\Delta$: | 6652 in-lb |
| | 12.3 Plastic $\eta$-factor: | 1.13 |
| | 12.4 Critical J-integral, $J_c$: | 1.49 ksi-in |

## Test Data for HSST-SC-3

13. LEFM Toughness (ASTM E399-83):

| | | |
|---|---|---|
| 13.1 | Provisional LEFM Toughness, $K_Q$ : | 96 ksi$\sqrt{in}$ |
| 13.2 | $P_o/P_Q$: | 1.23 |
| 13.3 | Validity Criterion, 2.5 $(K_Q/\sigma_{ys})^2$: | 5.6 in |
| 13.3.1 | Sufficient thickness, B ? | No |
| 13.3.2 | Sufficient Crack Depth, a ? | No |
| 13.4 | Valid $K_{Ic}$ value? | No |

Notes:

1. Tensile and Yield Strength Values Estimated from room temperature values.
2. ASTM E813 not applicable because crack growth did not occur. J integral toughness calculated according to $J_c = J_{el} + J_{pl}$, where $J_{pl} = \eta_{pl} / (B(W-a)) \cdot \int (P \cdot \Delta)_{pl}$.

## Additional Information

Test data are available in electronic spreadsheet format in either Lotus for the IBM-PC or Excel for the Apple Macintosh. Test data or additional information on any shallow crack test can be obtained by the Task Leader at the address below. Shallow-crack tests conducted by HSST are distinguished by the program, SC (for shallow-crack) and beam number (e.g. HSST-SC-1). A total of 14 beams were tested in the development phase of the shallow-crack program, numbered HSST-SC-3 through HSST-SC-16.

T. J. Theiss
Martin Marietta Energy Systems, Inc.
P.O. Box 2009
MS-8056; Bldg. 9204-1
Oak Ridge, TN 37831-8056
(615) 574-0755

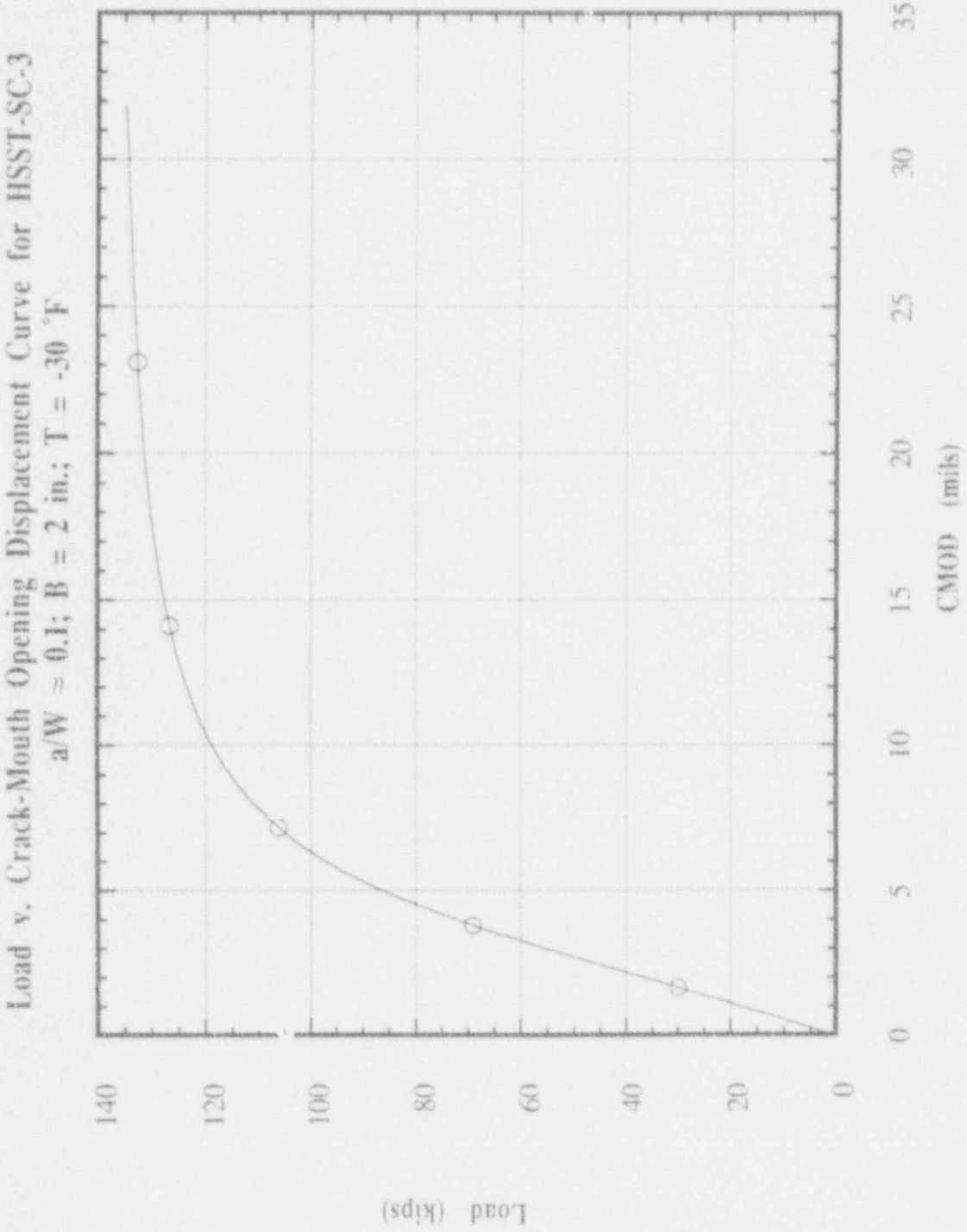
Load v. Crack-Mouth Opening Displacement Curve for HSST-SC-3
a/W = 0.1; B = 2 in.; T = -30 °F
Load (kips)
0
20
40
60
80
100
120
140
CMOD (mils)
0
5
10
15
20
25
30
35

## CONVERSION FACTORS[a]

| SI unit | English unit | Factor |
|---|---|---|
| mm | in. | 0.0393701 |
| cm | in. | 0.393701 |
| m | ft | 3.28084 |
| m/s | ft/s | 3.28084 |
| kN | $lb_f$ | 224.809 |
| kPa | psi | 0.145038 |
| MPa | ksi | 0.145038 |
| $MPa \cdot \sqrt{m}$ | $ksi \cdot \sqrt{in.}$ | 0.910048 |
| J | ft·lb | 0.737562 |
| K | °F or °R | 1.8 |
| $kJ/m^2$ | $in.\text{-}lb/in.^2$ | 5.71015 |
| $W \cdot n^{-3} \cdot K^{-1}$ | $Btu/h\text{-}ft^2 \cdot °F$ | 0.176110 |
| kg | lb | 2.20462 |
| $kg/m^3$ | $lb/in.^3$ | $3.61273 \times 10^{-5}$ |
| mm/N | $in./lb_f$ | 0.175127 |
| T(°F) = 1.8(°C) + 32 | | |

[a]Multiply SI quantity by given factor to obtain English quantity.

# Prior Heavy-Section Steel Technology Reports

The work reported here was performed at Oak Ridge National Laboratory under the Heavy-Section Steel Technology (HSST) Program, W. E. Pennell, Program Manager. The program is sponsored by the Office of Nuclear Regulatory Research of the U.S. Nuclear Regulatory Commission (NRC). The technical monitor for NRC is S. N. M. Malik.

This report is designated HSST Report NUREG/CR-4219, Vol. 8, No. 2 (ORNL/TM-9593/V8&N2). Prior and future reports in this series are listed below.

1. S. Yukawa, General Electric Company, Schenectady, N.Y., *Evaluation of Periodic Proof Testing and Warm Prestressing Procedures for Nuclear Reactor Vessels*, HSSTP-TR-1, July 1, 1969.

2. L. W. Loechel, Martin Marietta Corporation, Denver, Colo., *The Effect of Testing Variables on the Transition Temperature in Steel*, MCR-69-189, November 20, 1969.

3. P. N. Randall, TRW Systems Group, Redondo Beach, Calif., *Gross Strain Measure of Fracture Toughness of Steels*, HSSTP-TR-3, November 1, 1969.

4. C. Visser, S. E. Gabrielse, and W. VanBuren, Westinghouse Electric Corporation, PWR Systems Division, Pittsburgh, Pa., *A Two-Dimensional Elastic-Plastic Analysis of Fracture Test Specimens*, WCAP-7368, October 1969.

5. T. R. Mager and F. O. Thomas, Westinghouse Electric Corporation, PWR Systems Division, Pittsburgh, Pa., *Evaluation by Linear Elastic Fracture Mechanics of Radiation Damage to Pressure Vessel Steels*, WCAP-7328 (Rev.), October 1969.

6. W. O. Shabbits, W. H. Pryle, and E. T. Wessel, Westinghouse Electric Corporation, PWR Systems Division, Pittsburgh, Pa., *Heavy-Section Fracture Toughness Properties of A533 Grade B Class 1 Steel Plate and Submerged Arc Weldment*, WCAP-7414, December 1969.

7. F. J. Loss, Naval Research Laboratory, Washington, D.C., *Dynamic Tear Test Investigations of the Fracture Toughness of Thick-Section Steel*, NRL-7056, May 14, 1970.

8. P. B. Crosley and E. J. Ripling, Materials Research Laboratory, Inc., Glenwood, Ill., *Crack Arrest Fracture Toughness of A533 Grade B Class 1 Pressure Vessel Steel*, HSSTP-TR-8, March 1970.

9. T. R. Mager, Westinghouse Electric Corporation, PWR Systems Division, Pittsburgh, Pa., *Post-Irradiation Testing of 2T Compact Tension Specimens*, WCAP-7561, August 1970.

10. T. R. Mager, Westinghouse Electric Corporation, PWR Systems Division, Pittsburgh, Pa., *Fracture Toughness Characterization Study of A533 Grade B, Class 1 Steel*, WCAP-7578, October 1970.

11. T. R. Mager, Westinghouse Electric Corporation, PWR Systems Division, Pittsburgh, Pa., *Notch Preparation in Compact Tension Specimens*, WCAP 7579, November 1970.

12. N. Levy and P. V. Marcal, Brown University, Providence, R.I., *Three-Dimensional Elastic-Plastic Stress and Strain Analysis for Fracture Mechanics, Phase I: Simple Flawed Specimens*, HSSTP-TR-12, December 1970.

13. W. O. Shabbits, Westinghouse Electric Corporation, PWR Systems Division, Pittsburgh, Pa., *Dynamic Fracture Toughness Properties of Heavy Section A533 Grade B Class 1 Steel Plate*, WCAP-7623, December 1970.

14. P. N. Randall, TRW Systems Group, Redondo Beach, Calif., *Gross Strain Crack Tolerance of A 533-B Steel* HSSTP-TR-14, May 1, 1971.

15. H. T. Corten and R. H. Sailors, University of Illinois, Urbana, Ill., *Relationship Between Material Fracture Toughness Using Fracture Mechanics and Transition Temperature Tests*, T&AM Report 346, August 1, 1971.

16. T. R. Mager and V. J. McLaughlin, Westinghouse Electric Corporation, PWR Systems Division, Pittsburgh, Pa., *The Effect of an Environment of High Temperature Primary Grade Nuclear Reactor Water on the Fatigue Crack Growth Characteristics of A533 Grade B Class 1 Plate and Weldment Material*, WCAP-7776, October 1971.

17. N. Levy and P. V. Marcal, Brown University, Providence, R.I., *Three-Dimensional Elastic-Plastic Stress and Strain Analysis for Fracture Mechanics, Phase II: Improved Modelling*, HSSTP-TR-17, November 1971.

18. S. C. Grigory, Southwest Research Institute, San Antonio, Tex., *Tests of 6-in.-Thick Flawed Tensile Specimens. First Technical Summary Report*,

*Longitudinal Specimens Numbers 1 through 7*, HSSTP-TR-18, June 1972.

19. P. N. Randall, TRW Systems Group, Redondo Beach, Calif., *Effects of Strain Gradients on the Gross Strain Crack Tolerance of A533-B Steel*, HSSTP-TR-19, June 15, 1972.

20. S. C. Grigory, Southwest Research Institute, San Antonio, Tex., *Tests of 6-Inch-Thick Flawed Tensile Specimens, Second Technical Summary Report, Transverse Specimens Numbers 8 through 10, Welded Specimens Numbers 11 through 13*, HSSTP-TR-20, June 1972.

21. L. A. James and J. A. Williams, Hanford Engineering Development Laboratory, Richland, Wash., Heavy Section Steel Technology Program Technical Report No. 21, *The Effect of Temperature and Neutron Irradiation Upon the Fatigue-Crack Propagation Behavior of ASTM A533 Grade B, Class 1 Steel*, HEDL-TME 72-132, September 1972.

22. S. C. Grigory, Southwest Research Institute, San Antonio, Tex., *Tests of 6-Inch-Thick Flawed Tensile Specimens, Third Technical Summary Report, Longitudinal Specimens Numbers 14 through 16, Unflawed Specimen Number 17*, HSSTP-TR-22, October 1972.

23. S. C. Grigory, Southwest Research Institute, San Antonio, Tex., *Tests of 6-Inch-Thick Tensile Specimens, Fourth Technical Summary Report, Tests of 1-Inch-Thick Flawed Tensile Specimens for Size Effect Evaluation*, HSSTP-TR-23, June 1973.

24. S. P. Ying and S. C. Grigory, Southwest Research Institute, San Antonio, Tex., *Tests of 6-Inch-Thick Tensile Specimens, Fifth Technical Summary Report, Acoustic Emission Monitoring of One-Inch and Six-Inch-Thick Tensile Specimens*, HSSTP-TR-24, November 1972.

25. R. W. Derby, J. G. Merkle, G. C. Robinson, G. D. Whitman, and F. J. Witt, Oak Ridge Natl. Lab., Oak Ridge, Tenn., *Test of 6-Inch-Thick Pressure Vessels, Series 1: Intermediate Test Vessels V-1 and V-2*, ORNL-4895, February 1974.

26. W. J. Stelzman and R. G. Berggren, Oak Ridge Natl. Lab., Oak Ridge, Tenn., *Radiation Strengthening and Embrittlement in Heavy Section Steel Plates and Welds*, ORNL-4871, June 1973.

27. P. B. Crosley and E. J. Ripling, Materials Research Laboratory, Inc., Glenwood, Ill., *Crack Arrest in an Increasing K-Field*, HSSTP-TR-27, January 1973.

28. P. V. Marcal, P. M. Stuart, and R. S. Bettes, Brown University, Providence, R.I., *Elastic Plastic Behavior of a Longitudinal Semi-Elliptic Crack in a Thick Pressure Vessel*, HSSTP-TR-28, June 1973.

29. W. J. Stelzman, R. G. Berggren, and T. N. Jones, Oak Ridge Natl. Lab., Oak Ridge, Tenn., *ORNL Characterization of Heavy-Section Steel Technology Program Plates 01, 02 and 03*, USNRC Report NUREG/CR-4092 (ORNL/TM-9491), April 1985.

30. Canceled.

31. J. A. Williams, Hanford Engineering Development Laboratory, Richland, Wash., *The Irradiation and Temperature Dependence of Tensile and Fracture Properties of ASTM A533, Grade B, Class 1 Steel Plate and Weldment*, HEDL-TME 73-75, August 1973.

32. J. M. Steichen and J. A. Williams, Hanford Engineering Development Laboratory, Richland, Wash., *High Strain Rate Tensile Properties of Irradiated ASTM A533 Grade B Class 1 Pressure Vessel Steel*, July 1973.

33. P. C. Riccardella and J. L. Swedlow, Westinghouse Electric Corporation, Pittsburgh, Pa., *A Combined Analytical-Experimental Fracture Study of the Two Leading Theories of Elastic-Plastic Fracture (J-Integral and Equivalent Energy)*, WCAP-8224, October 1973.

34. R. J. Podlasek and R. J. Eiber, Battelle Columbus Laboratories, Columbus, Ohio, *Final Report on Investigation of Mode III Crack Extension in Reactor Piping*, December 14, 1973.

35. T. R. Mager, J. D. Landes, D. M. Moon, and V. J. McLaughlin, Westinghouse Electric Corporation, Pittsburgh, Pa., *Interim Report on the Effect of Low Frequencies on the Fatigue Crack Growth Characteristics of A533 Grade B Class 1 Plate in an Environment of High-Temperature Primary Grade Nuclear Reactor Water*, WCAP-8256, December 1973.

36. J. A. Williams, Hanford Engineering Development Laboratory, Richland, Wash., *The Irradiated Fracture Toughness of ASTM A533, Grade B, Class 1 Steel*

*Measured with a Four-Inch-Thick Compact Tension Specimen*, HEDL-TME 75-10, January 1975.

37. R. H. Bryan, J. G. Merkle, M. N. Raftenberg, G. C. Robinson, and J. E. Smith, Oak Ridge Natl. Lab., Oak Ridge, Tenn., *Test of 6-Inch-Thick Pressure Vessels. Series 2: Intermediate Test Vessels V-3, V-4, and V-6*, ORNL-5059, November 1975.

38. T. R. Mager, S. E. Yanichko, and L. R. Singer, Westinghouse Electric Corporation, Pittsburgh, Pa., *Fracture Toughness Characterization of HSST Intermediate Pressure Vessel Material*, WCAP-8456, December 1974.

39. J. G. Merkle, G. D. Whitman, and R. H. Bryan, Oak Ridge Natl. Lab., Oak Ridge, Tenn., *An Evaluation of the HSST Program Intermediate Pressure Vessel Tests in Terms of Light-Water-Reactor Pressure Vessel Safety*, ORNL/TM-5090, November 1975.

40. J. C. Merkle, G. C. Robinson, P. P. Holz, J. E. Smith, and R. H. Bryan, Oak Ridge Natl. Lab., Oak Ridge, Tenn., *Test of 6-In.-Thick Pressure Vessels. Series 3: Intermediate Test Vessel V-7*, USNRC Report ORNL/NUREG-1, August 1976.

41. J. A. Davidson, L. J. Ceschini, R. P. Shogan, and G. V. Rao, Westinghouse Electric Corporation, Pittsburgh, Pa., *The Irradiated Dynamic Fracture Toughness of ASTM A533, Grade B, Class 1 Steel Plate and Submerged Arc Weldment*, WCAP-8775, October 1976.

42. R. D. Cheverton, Oak Ridge Natl. Lab., Oak Ridge, Tenn., *Pressure Vessel Fracture Studies Pertaining to a PWR LOCA-ECC Thermal Shock: Experiments TSE-1 and TSE-2*, USNRC Report ORNL/NUREG/TM-31, September 1976.

43. J. G. Merkle, G. C. Robinson, P. P. Holz, and J. E. Smith, Oak Ridge Natl. Lab., Oak Ridge, Tenn., *Test of 6-in.-Thick Pressure Vessels. Series 4: Intermediate Test Vessels V-5 and V-9 with Inside Nozzle Corner Cracks*, USNRC Report ORNL/NUREG-7, August 1977.

44. J. A. Williams, Hanford Engineering Development Laboratory, Richland, Wash., *The Ductile Fracture Toughness of Heavy Section Steel Plate*, USNRC Report NUREG/CR-0859, September 1979.

45. R. H. Bryan, T. M. Cate, P. P. Holz, T. A. King, J. G. Merkle, G. C. Robinson, G. C. Smith, J. E. Smith, and G. D. Whitman, Oak Ridge Natl. Lab., Oak Ridge, Tenn., *Test of 6-in.-Thick Pressure Vessels. Series 3: Intermediate Test Vessel V-7A Under Sustained Loading*, USNRC Report ORNL/NUREG-9, February 1978.

46. R. D. Cheverton and S. E. Bolt, Oak Ridge Natl. Lab., Oak Ridge, Tenn., *Pressure Vessel Fracture Studies Pertaining to a PWR LOCA-ECC Thermal Shock: Experiments TSE-3 and TSE-4 and Update of TSE-1 and TSE-2 Analysis*, USNRC Report ORNL/NUREG-22, December 1977.

47. D. A. Canonico, Oak Ridge Natl. Lab., Oak Ridge, Tenn., *Significance of Reheat Cracks to the Integrity of Pressure Vessels for Light-Water Reactors*, USNRC Report ORNL/NUREG-15, July 1977.

48. G. C. Smith and P. P. Holz, Oak Ridge Natl. Lab., Oak Ridge, Tenn., *Repair Weld Induced Residual Stresses in Thick-Walled Steel Pressure Vessels*, USNRC Report NUREG/CR-0093 (ORNL/NUREG/TM-153), June 1978.

49. P. P. Holz and S. W. Wismer, Oak Ridge Natl. Lab., Oak Ridge, Tenn., *Half-Bead (Temper) Repair Welding for HSST Vessels*, USNRC Report NUREG/CR-0113 (ORNL/NUREG/TM-177), June 1978.

50. G. C. Smith, P. P. Holz, and W. J. Stelzman, Oak Ridge Natl. Lab., Oak Ridge, Tenn., *Crack Extension and Arrest Tests of Axially Flawed Steel Model Pressure Vessels*, USNRC Report NUREG/CR-0126 (ORNL/NUREG/TM-196), October 1978.

51. R. H. Bryan, P. P. Holz, J. G. Merkle, G. C. Smith, J. E. Smith, and W. J. Stelzman, Oak Ridge Natl. Lab., Oak Ridge, Tenn., *Test of 6-in.-Thick Pressure Vessels. Series 3: Intermediate Test Vessel V-7B*, USNRC Report NUREG/CR-0309 (ORNL/NUREG-38), October 1978.

52. R. D. Cheverton, S. K. Iskander, and S. E. Bolt, Oak Ridge Natl. Lab., Oak Ridge, Tenn., *Applicability of LEFM to the Analysis of PWR Vessels Under LOCA-ECC Thermal Shock Conditions*, USNRC Report NUREG/CR-0107 (ORNL/NUREG-40), October 1978.

53. R. H. Bryan, D. A. Canonico, P. P. Holz, S. K. Iskander, J. G. Merkle, J. E. Smith, and W. J. Stelzman, Oak Ridge Natl. Lab., Oak Ridge, Tenn., *Test of 6-in.-Thick Pressure Vessels, Series 3: Intermediate Test Vessel V-7*, USNRC Report NUREG/CR-0675 (ORNL/NUREG-58), December 1979.

54. R. D. Cheverton and S. K. Iskander, Oak Ridge Natl. Lab., Oak Ridge, Tenn., *Application of Static and Dynamic Crack Arrest Theory to TSE-4*, USNRC Report NUREG/CR-0767 (ORNL/NUREG-57), June 1979.

55. J. A. Williams, Hanford Engineering Development Laboratory, Richland, Wash., *Tensile Properties of Irradiated and Unirradiated Welds of A533 Steel Plate and A508 Forgings*, USNRC Report NUREG/CR-1158 (ORNL/Sub/79-50917/2), July 1979.

56. K. W. Carlson and J. A. Williams, Hanford Engineering Development Laboratory, Richland, Wash., *The Effect of Crack Length and Side Grooves on the Ductile Fracture Toughness Properties of ASTM A533 Steel*, USNRC Report NUREG/CR-1171 (ORNL/Sub/79-50917/3), October 1979.

57. P. P. Holz, Oak Ridge Natl. Lab., Oak Ridge, Tenn., *Flaw Preparations for HSST Program Vessel Fracture Mechanics Testing; Mechanical-Cyclic Pumping and Electron-Beam Weld-Hydrogen Charge Cracking Schemes*, USNRC Report NUREG/CR-1274 (ORNL/NUREG/TM-369), May 1980.

58. S. K. Iskander, Computer Sciences Div., Union Carbide Corp. Nuclear Div., Oak Ridge, Tenn., *Two Finite Element Techniques for Computing Mode I Stress Intensity Factors in Two- or Three-Dimensional Problems*, USNRC Report NUREG/CR-1499 (ORNL/NUREG/CSD/TM-14), February 1981.

59. P. B. Crosley and E. J. Ripling, Materials Research Laboratory, Glenwood, Ill., *Development of a Standard Test for Measuring $K_{Ia}$ with a Modified Compact Specimen*, USNRC Report NUREG/CR-2294 (ORNL/Sub/81-7755/1), August 1981.

60. S. N. Atluri, B. R. Bass, J. W. Bryson, and K. Kathiresan, Computer Sciences Div., Oak Ridge Gaseous Diffusion Plant, Oak Ridge, Tenn., *NOZ-FLAW: A Finite Element Program for Direct Evaluation of Stress Intensity Factors for Pressure Vessel Nozzle-Corner Flaws*, USNRC Report NUREG/CR-1843 (ORNL/NUREG/CSD/TM-18), March 1981.

61. A. Shukla, W. L. Fourney, and G. R. Irwin, University of Maryland, College Park, Md., *Study of Energy Loss and Its Mechanisms in Homalite 100 During Crack Propagation and Arrest*, USNRC Report NUREG/CR-2150 (ORNL/Sub/79-7778/1), August 1981.

62. S. K. Iskander, R. D. Cheverton, and D. G. Ball, Oak Ridge Natl. Lab., Oak Ridge, Tenn., *OCA-I, A Code for Calculating the Behavior of Flaws on the Inner Surface of a Pressure Vessel Subjected to Temperature and Pressure Transients*, USNRC Report NUREG/CR-2113 (ORNL/NUREG-84), August 1981.

63. R. J. Sanford, R. Chona, W. L. Fourney, and G. R. Irwin, University of Maryland, College Park, Md., *A Photoelastic Study of the Influence of Non-Singular Stresses in Fracture Test Specimens*, USNRC Report NUREG/CR-2179 (ORNL/Sub/79-7778/2), August 1981.

64. B. R. Bass, S. N. Atluri, J. W. Bryson, and K. Kathiresan, Oak Ridge Natl. Lab., Oak Ridge, Tenn., *OR-FLAW: A Finite Element Program for Direct Evaluation of K-Factors for User-Defined Flaws in Plate, Cylinders, and Pressure-Vessel Nozzle Corners*, USNRC Report NUREG/CR-2494 (ORNL/CSD/TM-165), April 1982.

65. B. R. Bass and J. W. Bryson, Oak Ridge Natl. Lab., Oak Ridge Tenn., *ORMGEN 3D: A Finite Element Mesh Generator for 3-Dimensional Crack Geometries*, USNRC Report NUREG/CR-2997, Vol. 1 (ORNL/TM-8527/V1), December 1982.

66. B. R. Bass and J. W. Bryson, Oak Ridge Natl. Lab., Oak Ridge, Tenn., *ORVIRT: A Finite Element Program for Energy Release Rate Calculations for 2-Dimensional and 3-Dimensional Crack Models*, USNRC Report NUREG/CR-2997, Vol. 2 (ORNL/TM-8527/V2), February 1983.

67. R. D. Cheverton, S. K. Iskander, and D. G. Ball, Oak Ridge Natl. Lab. Oak Ridge, Tenn., *PWR Pressure Vessel Integrity During Overcooling Accidents: A Parametric Analysis*, USNRC Report NUREG/CR-2895 (ORNL/TM-7931), February 1983.

68. D. G. Ball, R. D. Cheverton, J. B. Drake, and S. K. Iskander, Oak Ridge Natl. Lab., Oak Ridge, Tenn., *OCA-II, A Code for Calculating Behavior of 2-D and 3-D Surface Flaws in a Pressure Vessel Subjected to Temperature and Pressure Transients*, USNRC Report NUREG/ CR-3491 (ORNL-5934), February 1984.

69. A. Sauter, R. D. Cheverton, and S. K. Iskander, Oak Ridge Natl. Lab., Oak Ridge, Tenn., *Modification of OCA-I for Application to a Reactor Pressure Vessel*

*with Cladding on the Inner Surface*, USNRC Report NUREG/CR-3155 (ORNL/TM-8649), May 1983.

70. R. D. Cheverton and D. G. Ball, Martin Marietta Energy Systems, Inc., Oak Ridge Natl. Lab., Oak Ridge, Tenn., *OCA-P, A Deterministic and Probabilistic Fracture-Mechanics Code for Application to Pressure Vessels*, USNRC Report NUREG/CR-3618 (ORNL-5991), May 1984.

71. J. G. Merkle, Martin Marietta Energy Systems, Inc., Oak Ridge Natl. Lab., Oak Ridge, Tenn., *An Examination of the Size Effects and Data Scatter Observed in Small Specimen Cleavage Fracture Toughness Testing*, USNRC Report NUREG/CR-3672 (ORNL/TM-9088), April 1984.

72. C. E. Pugh et al., Martin Marietta Energy Systems, Inc., Oak Ridge Natl. Lab., Oak Ridge, Tenn., *Heavy-Section Steel Technology Program—Five-Year Plan FY 1983–1987*, USNRC Report NUREG/CR-3595 (ORNL/TM-9008), April 1984.

73. D. G. Ball, B. R. Bass, J. W. Bryson, R. D. Cheverton, and J. B. Drake, Martin Marietta Energy Systems, Inc., Oak Ridge Natl. Lab., Oak Ridge, Tenn., *Stress Intensity Factor Influence Coefficients for Surface Flaws in Pressure Vessels*, USNRC Report NUREG/CR-3723 (ORNL/CSD/TM-216), February 1985.

74. W. R. Corwin, R. G. Berggren, and R. K. Nanstad, Martin Marietta Energy Systems, Inc., Oak Ridge Natl. Lab., Oak Ridge, Tenn., *Charpy Toughness and Tensile Properties of Neutron Irradiated Stainless Steel Submerged-Arc Weld Cladding Overlay*, USNRC Report NUREG/CR-3927 (ORNL/TM-9309), September 1984.

75. C. W. Schwartz, R. Chona, W. L. Fourney, and G. R. Irwin, University of Maryland, College Park, Md., *SAMCR: A Two-Dimensional Dynamic Finite Element Code for the Stress Analysis of Moving CRacks*, USNRC Report NUREG/CR-3891 (ORNL/Sub/79-7778/3), November 1984.

76. W. R. Corwin, G. C. Robinson, R. K. Nanstad, J. G. Merkle, R. G. Berggren, G. M. Goodwin, R. L. Swain, and T. D. Owings, Martin Marietta Energy Systems, Inc., Oak Ridge Natl. Lab., Oak Ridge, Tenn., *Effects of Stainless Steel Weld Overlay Cladding on the Structural Integrity of Flawed Steel Plates in Bending, Series 1*, USNRC Report NUREG/CR-4015 (ORNL/TM-9390), April 1985.

77. R. H. Bryan, B. R. Bass, S. E. Bolt, J. W. Bryson, D. P. Edmonds, R. W. McCulloch, J. G. Merkle, R. K. Nanstad, G. C. Robinson, K. R. Thoms, and G. D. Whitman, Martin Marietta Energy Systems, Inc., Oak Ridge Natl. Lab., Oak Ridge, Tenn., *Pressurized-Thermal-Shock Test of 6-in.-Thick Pressure Vessels. PTSE-1: Investigation of Warm Prestressing and Upper-Shelf Arrest*, USNRC Report NUREG/CR-4106 (ORNL-6135), April 1985.

78. R. D. Cheverton, D. G. Ball, S. E. Bolt, S. K. Iskander, and R. K. Nanstad, Martin Marietta Energy Systems, Inc., Oak Ridge Natl. Lab., Oak Ridge, Tenn., *Pressure Vessel Fracture Studies Pertaining to the PWR Thermal-Shock Issue: Experiments TSE-5, TSE-5A, and TSE-6*, USNRC Report NUREG/CR-4249 (ORNL-6163), June 1985.

79. R. D. Cheverton, D. G. Ball, S. E. Bolt, S. K. Iskander, and R. K. Nanstad, Martin Marietta Energy Systems, Inc., Oak Ridge Natl. Lab., Oak Ridge, Tenn., *Pressure Vessel Fracture Studies Pertaining to the PWR Thermal-Shock Issue: Experiment TSE-7*, USNRC Report NUREG/CR-4304 (ORNL-6177), August 1985.

80. R. H. Bryan, B. R. Bass, S. E. Bolt, J. W. Bryson, J. G. Merkle, R. K. Nanstad, and G. C. Robinson, Martin Marietta Energy Systems, Inc., Oak Ridge Natl. Lab., Oak Ridge, Tenn., *Test of 6-in.-Thick Pressure Vessels. Series 3: Intermediate Test Vessel V-8A—Tearing Behavior of Low Upper-Shelf Material*, USNRC Report NUREG/CR-4760 (ORNL-6187), May 1987.

81. R. D. Cheverton and D. G. Ball, Martin Marietta Energy Systems, Inc., Oak Ridge Natl. Lab., Oak Ridge, Tenn., *A Parametric Study of PWR Pressure Vessel Integrity During Overcooling Accidents, Considering Both 2-D and 3-D Flaws*, USNRC Report NUREG/CR-4325 (ORNL/TM-9682), August 1985.

82. E. C. Rodabaugh, E. C. Rodabaugh Associates, Inc., Hilliard, Ohio, *Comments on the Leak-Before-Break Concept for Nuclear Power Plant Piping Systems*, USNRC Report NUREG/CR-4305 (ORNL/Sub/82-22252/3), August 1985.

83. J. W. Bryson, Martin Marietta Energy Systems, Inc., Oak Ridge Natl. Lab., Oak Ridge, Tenn., *ORVIRT.PC: A 2-D Finite Element Fracture Analysis Program for a Microcomputer*, USNRC Report NUREG/CR-4367 (ORNL-6208), October 1985.

84. D. G. Ball and R. D. Cheverton, Martin Marietta Energy Systems, Inc., Oak Ridge Natl. Lab., Oak Ridge, Tenn., *Adaptation of OCA-P, A Probabilistic Fracture-Mechanics Code, to a Personal Computer*, USNRC Report NUREG/CR-4468 (ORNL/CSD/TM-233), January 1986.

85. J. W. Bryson and B. R. Bass, Martin Marietta Energy Systems, Inc., Oak Ridge Natl. Lab., Oak Ridge, Tenn., *ORMGEN.PC: A Microcomputer Program for Automatic Mesh Generation of 2-D Crack Geometries*, USNRC Report NUREG/CR-4475 (ORNL-6250), March 1986.

86. G. D. Whitman, Martin Marietta Energy Systems, Inc., Oak Ridge Natl. Lab., Oak Ridge, Tenn., *Historical Summary of the Heavy-Section Steel Technology Program and Some Related Activities in Light-Water Reactor Pressure Vessel Safety Research*, USNRC Report NUREG/CR-4489 (ORNL-6259), March 1986.

87. C. Inversini and J. W. Bryson, Martin Marietta Energy Systems, Inc., Oak Ridge Natl. Lab., Oak Ridge, Tenn., *ORPLOT PC: A Graphic Utility for ORMGEN.PC and ORVIRT.PC*, USNRC Report NUREG/CR-4633 (ORNL-6291), June 1986.

88. T. J. McGowan, R. K. Nanstad, and K. R. Thoms, Martin Marietta Energy Systems, Inc., Oak Ridge Natl. Lab., Oak Ridge, Tenn., *Characterization of Irradiated Current-Practice Welds and A533 Grade B Class 1 Plate for Nuclear Pressure Vessel Service*, USNRC Report NUREG/CR-4880 (ORNL/TM-10387), July 1988.

89. K. V. Cook and R. W. McClung, Martin Marietta Energy Systems, Inc., Oak Ridge Natl. Lab., Oak Ridge, Tenn., *Flaw Density Examinations of a Clad Boiling Water Reactor Pressure Vessel Segment*, USNRC Report NUREG/CR-4860 (ORNL/TM-10364), April 1987.

90. D. J. Naus, B. R. Bass, C. E. Pugh, R. K. Nanstad, J. G. Merkle, W. R. Corwin, and G. C. Robinson, Martin Marietta Energy Systems, Inc., Oak Ridge Natl. Lab., Oak Ridge, Tenn., *Crack-Arrest Behavior in SEN Wide Plates of Quenched and Tempered A 533 Grade B Steel Tested Under Nonisothermal Conditions*, USNRC Report NUREG/CR-4930 (ORNL-6388), August 1987.

91. D. B. Barker, R. Chona, W. L. Fourney, and G. R. Irwin, University of Maryland, College Park, Md., *A Report on the Round Robin Program Conducted to Evaluate the Proposed ASTM Standard Test Method for Determining the Plane Strain Crack Arrest Fracture Toughness, $K_{Ia}$, of Ferritic Materials*, USNRC Report NUREG/CR-4966 (ORNL/Sub/79-7778/4), January 1988.

92. W. H. Bamford, Westinghouse Electric Corporation, Pittsburgh, Pa., *A Summary of Environmentally Assisted Crack-Growth Studies Performed at Westinghouse Electric Corporation Under Funding from the Heavy-Section Steel Technology Program*, USNRC Report NUREG/CR-5020 (ORNL/Sub/82-21598/1), May 1988.

93. R. H. Bryan, B. R. Bass, S. E. Bolt, J. W. Bryson, W. R. Corwin, J. G. Merkle, R. K. Nanstad, and G. C. Robinson, Martin Marietta Energy Systems, Inc., Oak Ridge Natl. Lab., Oak Ridge, Tenn., *Pressurized-Thermal-Shock Test of 6-in.-Thick Pressure Vessels. PTSE-2: Investigation of Low Tearing Resistance and Warm Prestressing*, USNRC Report NUREG/CR-4888 (ORNL-6377), December 1987.

94. J. H. Giovanola and R. W. Klopp, SRI International, Menlo Park, Calif., *Viscoplastic Stress-Strain Characterization of A533B Class 1 Steel*, USNRC Report NUREG/CR-5066 (ORNL/Sub/87-SA193/1), September 1989.

95. L. F. Miller et al., Martin Marietta Energy Systems, Inc., Oak Ridge Natl. Lab., Oak Ridge, Tenn., *Neutron Exposure Parameters for the Metallurgical Test Specimens in the Fifth Heavy-Section Steel Technology Irradiation Series Capsules*, USNRC Report NUREG/ CR-5019 (ORNL/TM-10582), March 1988.

96. Canceled.

97. D. J. Naus, J. Keeney-Walker, and B. R. Bass, Martin Marietta Energy Systems, Inc., Oak Ridge Natl. Lab., Oak Ridge, Tenn., *High-Temperature Crack-Arrest Behavior in 152-mm-Thick SEN Wide Plates of Quenched and Tempered A 533 Grade B Steel*, USNRC Report NUREG/CR-5330 (ORNL/TM-11083), April 1989.

98. K. V. Cook, R. A. Cunningham, Sr., and R. W. McClung, Martin Marietta Energy Systems, Inc., Oak Ridge Natl. Lab., Oak Ridge, Tenn., *Detection and Characterization of Inaications in Segments of Reactor Pressure Vessels*, USNRC Report NUREG/CR-5322 (ORNL/TM-11072), August 1989.

99. R. D. Cheverton, W. E. Pennell, G. C. Robinson, and R. K. Nanstad, Martin Marietta Energy Systems, Inc., Oak Ridge Natl. Lab., Oak Ridge, Tenn., *Impact of Radiation Embrittlement on Integrity of Pressure Vessel Supports for Two PWR Plants*, NUREG/CR-5320 (ORNL/TM-10966), February 1989.

100. D. J. Naus, J. Keeney-Walker, B. R. Bass, S. K. Iskander, R. J. Fields, R. deWitt, and S. R. Low III, Martin Marietta Energy Systems, Inc., Oak Ridge Natl. Lab., Oak Ridge, Tenn., *SEN Wide-Plate Crack-Arrest Tests* Utilizing *A 533 Grade B Class 1 Material: WP-CE Test Series*, USNRC Report NUREG/CR-5408 (ORNL/TM-11269), November 1989.

101. D. J. Naus, J. Keeney-Walker, B. R. Bass, S. K. Iskander, R. J. Fields, R. deWitt, and S. R. Low III, Martin Marietta Energy Systems, Inc., Oak Ridge Natl. Lab., Oak Ridge, Tenn., *High Temperature Crack-Arrest Tests Using 152-mm-Thick SEN Wide Plates of Low Upper-Shelf Base Material: Tests WP-2.2 and WP-2.6*, USNRC Report NUREG/CR-5450 (ORNL/TM-11352), February 1990.

102. Canceled.

103. D. J. Naus, J. Keeney-Walker, B. R. Bass, G. C. Robinson, S. K. Iskander, D. J. Alexander, R. J. Fields, R. deWitt, S. R. Low, C. W. Schwartz, and L.-B. Johansson, Martin Marietta Energy Systems, Inc., Oak Ridge Natl. Lab., Oak Ridge, Tenn., *Crack-Arrest Behavior in SEN Wide Plates of Low Upper-Shelf Base Metal Tested Under Nonisothermal Conditions: WP-2 Series*, USNRC Report NUREG/CR-5451 (ORNL-6584), August 1990.

104. T. L. Dickson, R. D. Cheverton, and D. K. Shum, Martin Marietta Energy Systems, Inc., Oak Ridge Natl. Lab., Oak Ridge, Tenn., *Inclusion of Unstable Ductile Tearing and Extrapolated Crack-Arrest Toughness Data in PWR Vessel Integrity Assessment*, USNRC Report NUREG/CR-5473 (ORNL/TM-11450), May 1990.

105. T. J. Theiss, Martin Marietta Energy Systems, Inc., Oak Ridge Natl. Lab., Oak Ridge, Tenn., *Recommendations for the Shallow-Crack Fracture Toughness Testing Task Within the HSST Program*, USNRC Report NUREG/CR-5554 (ORNL/TM-11509), September 1990.

106. J. G. Merkle, Martin Marietta Energy Systems, Inc., Oak Ridge Natl. Lab., Oak Ridge, Tenn., *An Overview of the Low Upper Shelf Toughness Safety Margin Issue*, USNRC Report NUREG/CR-5552 (ORNL/TM-11314), August 6, 1990.

107. D. K. M. Shum, J. G. Merkle, J. Keeney-Walker, and B. R. Bass, Martin Marietta Energy Systems, Inc., Oak Ridge Natl. Lab., Oak Ridge, Tenn., *Analytical Studies of Transverse Strain Effects on Fracture Toughness for Circumferentially Oriented Cracks*, USNRC Report NUREG/CR-5592 (ORNL/TM-11581), April 1991.

108. J. D. Landes, *Extrapolation of the J-R Curve for Predicting Reactor Vessel Integrity*, USNRC Report NUREG/CR-5650 (ORNL/Sub/89-99732/1), January 1992.

109. J. Keeney-Walker, B. R. Bass, and J. D. Landes, Martin Marietta Energy Systems, Inc., Oak Ridge Natl. Lab., Oak Ridge, Tenn., *An Investigation of Crack-Tip Stress-Field Criteria for Predicting Cleavage-Crack Initiation*, USNRC Report NUREG/CR-5651 (ORNL/TM-11692) September 1991.

110. G. R. Irwin, University of Maryland, *Use of Thickness Reduction to Estimate Values of K*, USNRC Report NUREG/CR-5697 (ORNL/Sub/79-7778/5), prepared at University of Maryland for Martin Marietta Energy Systems, Inc., Oak Ridge Natl. Lab., Oak Ridge, Tenn., November 1991.

111. Pedro Albrecht, University of Maryland, *Limit Pressure Analysis of PTSE-2 Vessel*, USNRC Report NUREG/CR-5698 (ORNL/Sub/79-7778/6), prepared at University of Maryland for Martin Marietta Energy Systems, Inc., Oak Ridge Natl. Lab., Oak Ridge, Tenn. (to be published).

112. J. W. Dally, W. L. Fourney, and G. R. Irwin, University of Maryland, *Lower-Bound Initiation Toughness with a Modified-Charpy Specimen*, USNRC Report NUREG/CR-5703 (ORNL/ Sub/79-7778/7), prepared at Univeristy of Maryland for Martin Marietta Energy Systems, Inc., Oak Ridge Natl. Lab., Oak Ridge, Tenn. November 1991.

113. S. K. Iskander, G. C. Robinson, W. R. Corwin, B. C. Oland, D. J. Alexander, and K. V. Cook, Martin Marietta Energy Systems, Inc., Oak Ridge Natl. Lab., Oak Ridge, Tenn., *Experimental Results of Tests to Investigate Flaw Behavior of Mechanically Loaded Stainless Steel Clad Plates*, USNRC Report NUREG/CR-xxxx (to be published).

114. S. T. Rolfe, University of Kansas, *Interpretive Report on the Application of Shallow-Flaw CTOD Test Data to the Structural Margin Assessment of Reactor Pressure Vessels with Flaws*, USNRC Report NUREG/CR-5767 (ORNL/Sub/90-SH640/1), November 1991.

115. D. E. McCabe, Martin Marietta Energy Systems, Inc., Oak Ridge Natl. Lab., *Comparison of Weibull and $\beta_{1c}$ Analysis of Transition Range Fracture Toughness Data*, USNRC Report NUREG/CR-5788 (ORNL/TM-11959), January 1992.

116. R. D. Cheverton et al., Martin Marietta Energy Systems, Inc., Oak Ridge Natl. Lab., Oak Ridge, Tenn., "Oak Ridge National Laboratory/Nuclear Regulatory Commission, ORNL/NRC Review of Reactor Pressure Vessel Evaluation Report for Yankee Nuclear Power Station (YAEC No. 1735)," USNRC Report NUREG/CR-5799 (ORNL/TM-11982), March 1992.

117. T. L. Dickson, R. D. Cheverton, and J. W. Bryson, Martin Marietta Energy Systems, Inc., Oak Ridge Natl. Lab., Oak Ridge, Tenn., "Pressurized-Thermal-Shock Probabilistic Fracture Mechanics Sensitivity Analyses for Yankee Rowe Reactor Pressure Vessel," USNRC Report NUREG/CR-5782 (ORNL/TM-11945) (to be published).

118. D. K. M. Shum, C. W. Schwartz, J. Kenney-Walker, and B. R. Bass, Martin Marietta Energy Systems, Inc., Oak Ridge Natl. Lab., Oak Ridge, Tenn., "Analytical Studies of Transverse Strain Effects on Fracture Toughness for Circumferentially Oriented Cracks (Part II)," USNRC Report NUREG/CR-xxxx (ORNL/TM- ) (to be published).

119. J. W. Dally, G. R. Irwin, Xian-Jie Zhang, and R. J. Bonenberger, University of Maryland for Martin Marietta Energy Systems, Inc., Oak Ridge Natl. Lab., Oak Ridge, Tenn., "The Influence of Precompression on the Lower-Bound Initiation Toughness of A 533 B Reactor Grade Steel," USNRC Report NUREG/CR-xxxx (ORNL/Sub/79-7778/8) (to be published).

120. J. D. Landes, University of Tennessee for Martin Marietta Energy Systems, Inc., Oak Ridge Natl. Lab., Oak Ridge, Tenn., "Study of the Effect of Cladding on Reactor Vessel Integrity," USNRC Report NUREG/CR-5733 (ORNL/Sub/89-99732/2) (to be published).

NUREG/CR-4219
Vol. 8, No. 2
ORNL/TM-9593/V8&N2
Dist. Category RF

## Internal Distribution

1. D. J. Alexander
2. B. R. Bass
3. J. W. Bryson
4. E. W. Carver
5–7. R. D. Cheverton
8. J. M. Corum
9. W. R. Corwin
10. T. L. Dickson
11. F. M. Haggag
12. J. J. Henry
13. W. F. Jackson
14. J. E. Jones Jr.
15. S. K. Iskander
16. J. Keeney-Walker
17. W. J. McAfee
18. D. E. McCabe
19. E. T. Manneschmidt
20. J. G. Merkle
21–22. F. K. Nanstad
23. D. J. Naus
24. C. B. Oland
25–30. W. E. Pennell
31. C. E. Pugh
32. G. C. Robinson
33. D. K. M. Shum
34. R. L. Swain
35. T. J. Theiss
36. E. W. Whitfield
37. ORNL Patent Section
38. Central Research Library
39. Document Reference Section
40–41. Laboratory Records Department
42. Laboratory Records (RC)

## External Distribution

43. L. C. Shao, Director, Division of Engineering, U.S. Nuclear Regulatory Commission, Washington, DC 20555
44. C. Z. Serpan, Jr., Division of Engineering, U.S. Nuclear Regulatory Commission, Washington, DC 20555
45–46. S. N. M. Malik, Division of Engineering, U.S. Nuclear Regulatory Commission, Washington, DC 20555
47. M. E. Mayfield, Division of Engineering, U.S. Nuclear Regulatory Commission, Washington, DC 20555
48. A. Taboada, Division of Engineering, U.S. Nuclear Regulatory Commission, Washington, DC 20555
49. E. D. Hackett, Division of Engineering, U.S. Nuclear Regulatory Commission, Washington, DC 20555
50. A. L. Hiser, Division of Engineering, U.S. Nuclear Regulatory Commission, Washington, DC 20555
51. W. L. Fourney, Department of Mechanical Engineering, University of Maryland, College Park, MD 20742
52. J. D. Landes, The University of Tennessee, Knoxville, TN 37996-2030
53. S. T. Rolfe, The University of Kansas, Lawrence, KS 66045-2235
54. A. R. Rosenfield, Battelle Columbus Division, Columbus, OH 43201
55. C. W. Schwartz, Department of Civil Engineering, University of Maryland, College Park, MD 20742
56. E. T. Wessel, 312 Wolverine, Haines City, FL 33844
57. R. G. Hoppe, Bettis Atomic Power Laboratory, P.O. Box 79, West Mifflin, PA 15122

58. Office of Assistant Manager for Energy Research and Development, DOE–OR, Oak Ridge, TN 37831
59–60. Office of Scientific and Technical Information, P. O. Box 62, Oak Ridge, TN 37831
61–310 Given distribution as shown in category RF (NTIS-10)

NRC FORM 335 (2-89) NRCM 1102, 3201, 3202

U.S. NUCLEAR REGULATORY COMMISSION

# BIBLIOGRAPHIC DATA SHEET

(See instructions on the reverse)

1. REPORT NUMBER (Assigned by NRC, Add Vol., Supp., Rev., and Addendum Numbers, if any.)
NUREG/CR-4219
ORNL/TM-9593/V8&N2
Vol. 8, No. 2

2. TITLE AND SUBTITLE
Heavy-Section Steel Technology Program
Semiannual Progress Report for April-September 1991

3. DATE REPORT PUBLISHED
MONTH: April
YEAR: 1992

FIN OR GRANT NUMBER
B0119

5. AUTHOR(S)
W. E. Pennell

6. TYPE OF REPORT
Semiannual

7. PERIOD COVERED (Inclusive Dates)
April-September 1991

8. PERFORMING ORGANIZATION – NAME AND ADDRESS (If NRC, provide Division, Office or Region, U.S. Nuclear Regulatory Commission, and mailing address; if contractor, provide name and mailing address.)

Oak Ridge National Laboratory
Oak Ridge, TN 37831-6285

9. SPONSORING ORGANIZATION – NAME AND ADDRESS (If NRC, type "Same as above"; if contractor, provide NRC Division, Office or Region, U.S. Nuclear Regulatory Commission, and mailing address.)

Division of Engineering
Office of Nuclear Regulatory Research
U. S. Nuclear Regulatory Commission
Washington, DC 20555

10. SUPPLEMENTARY NOTES

11. ABSTRACT (200 words or less)

The Heavy-Section Steel Technology (HSST) Program is conducted for the Nuclear Regulatory Commission (NRC) by Oak Ridge National Laboratory (ORNL). The program focus is on the development and validation of technology for the assessment of fracture-prevention margins in commercial nuclear reactor pressure vessels. The HSST Program is organized in 11 tasks: (1) program management, (2) fracture methodology and analysis, (3) material characterization and properties, (4) special technical assistance, (5) fracture analysis computer programs, (6) cleavage-crack initiation, (7) cladding evaluations, (8) pressurized-thermal-shock technology, (9) analysis methods validation, and (10) fracture evalution tests. The program tasks have been structured to place emphasis on the resolution of fracture issues with near-term licensing significance. Resources to execute the research tasks are drawn from ORNL with subcontract support from universities and other research laboratories. Close contact is maintained with related research programs both in the United States and abroad.

12. KEY WORDS/DESCRIPTORS (List words or phrases that will assist researchers in locating the report.)

Pressure vessels, cleavage-crack initiation, compact specimens, finite-element analysis, fracture correlation parameters, hydrostatic constraint, and shallow-flaw fracture toughness data

13. AVAILABILITY STATEMENT
Unlimited

14. SECURITY CLASSIFICATION
(This Page)
Unclassified
(This Report)
Unclassified

15. NUMBER OF PAGES

16. PRICE

NRC FORM 335 (2-89)

UNITED STATES
NUCLEAR REGULATORY COMMISSION
WASHINGTON, D.C. 20555

OFFICIAL BUSINESS
PENALTY FOR PRIVATE USE, $300

SPECIAL FOURTH-CLASS RATE
POSTAGE AND FEES PAID
USNRC
PERMIT NO. G-67